VILNIUS TECH
Vilniaus Gedimino technikos universitetas

Kamyab MOHAMMADI

RESEARCH AND APPLICATION OF BIOFILTRATION MATERIALS IN THE PURIFICATION OF BIOGAS FROM HYDROGEN SULFIDE

DOCTORAL DISSERTATION

TECHNOLOGICAL SCIENCES
ENVIRONMENTAL ENGINEERING (T 004)

Vilnius, 2026

2026-014-M

VILNIUS GEDIMINAS TECHNICAL UNIVERSITY

Kamyab MOHAMMADI

RESEARCH AND APPLICATION OF BIOFILTRATION MATERIALS IN THE PURIFICATION OF BIOGAS FROM HYDROGEN SULFIDE

DOCTORAL DISSERTATION

TECHNOLOGICAL SCIENCES
ENVIRONMENTAL ENGINEERING (T 004)

Vilnius, 2026

The doctoral dissertation was prepared at Vilnius Gediminas Technical University in 2022–2026.

Supervisor

Assoc. Prof. Dr Rasa VAIŠKŪNAITĖ (Vilnius Gediminas Technical University, Environmental Engineering – T 004).

The Dissertation Defense Council of the Scientific Field of Environmental Engineering of Vilnius Gediminas Technical University:

Chairman

Prof. Dr Saulius VASAREVIČIUS (Vilnius Gediminas Technical University, Environmental Engineering – T 004).

Members:

Dr Steigvilė BYČENKIENĖ (State Research Institute Center for Physical Sciences and Technology, Physics – N 002),

Dr Bahareh FEIZI MOHAZZAB (Johannes Gutenberg University Mainz, Germany, Chemistry – N 003),

Assoc. Prof. Dr Eglė MARČIULAITIENĖ (Vilnius Gediminas Technical University, Environmental Engineering – T 004),

Prof. Dr Jaunius URBONAVIČIUS (Vilnius Gediminas Technical University, Environmental Engineering – T 004).

The dissertation will be defended at the public meeting of the Dissertation Defense Council of the Scientific Field of Environmental Engineering in the *Aula Doctoralis* Meeting Hall of Vilnius Gediminas Technical University at **10 a.m. on 15 June 2026**.

Address: Saulėtekio al. 11, LT-10223 Vilnius, Lithuania.
Tel.: +370 5 274 4956; fax +370 5 270 0112; e-mail: *doktor@vilniustech.lt*

A notification on the intended defense of the dissertation was sent on 14 May 2026. A copy of the doctoral dissertation is available for review at the Vilnius Gediminas Technical University repository https://etalpykla.vilniustech.lt and the Library of Vilnius Gediminas Technical University (Saulėtekio al. 14, LT-10223 Vilnius, Lithuania).

Vilnius Gediminas Technical University book No 2026-014-M

https://doi.org/:10.20334/2026-014-M

VILNIAUS GEDIMINO TECHNIKOS UNIVERSITETAS

Kamyab MOHAMMADI

BIOFILTRACIJOS MEDŽIAGŲ TYRIMAI IR TAIKYMAS ŠALINANT IŠ BIODUJŲ SIEROS VANDENILĮ

DAKTARO DISERTACIJA

TECHNOLOGIJOS MOKSLAI,
APLINKOS INŽINERIJA (T 004)

Vilnius, 2026

Disertacija rengta 2022–2026 metais Vilniaus Gedimino technikos universitete.

Vadovas

doc. dr. Rasa VAIŠKŪNAITĖ (Vilniaus Gedimino technikos universitetas, Aplinkos inžinerija – T 004).

Vilniaus Gedimino technikos universiteto Aplinkos inžinerijos mokslo krypties disertacijos gynimo taryba:

Pirmininkas

prof. dr. Saulius VASAREVIČIUS (Vilniaus Gedimino technikos universitetas, Aplinkos inžinerija – T 004).

Nariai:

dr. Steigvilė BYČENKIENĖ (Valstybinis mokslinių tyrimų institutas Fizinių ir technologijos mokslų centras, Fizika – N 002),

dr. Bahareh FEIZI MOHAZZAB (Mainco Johano Gutenbergo universitetas, Vokietija, Chemija – N 003),

doc. dr. Eglė MARČIULAITIENĖ (Vilniaus Gedimino technikos universitetas, Aplinkos inžinerija – T 004),

prof. dr. Jaunius URBONAVIČIUS (Vilniaus Gedimino technikos universitetas, Aplinkos inžinerija – T 004).

Disertacija bus ginama viešame Aplinkos inžinerijos mokslo krypties disertacijos gynimo tarybos posėdyje **2026 m. birželio 15 d. 10 val.** Vilniaus Gedimino technikos universiteto *Aula Doctoralis* posėdžių salėje.

Adresas: Saulėtekio al. 11, LT-10223 Vilnius, Lietuva.
Tel.: (0 5) 274 4956; faksas (0 5) 270 0112; el. paštas *doktor@vilniustech.lt*

Pranešimai apie numatomą ginti disertaciją išsiųsti 2026 m. gegužės 14 d. Disertaciją galima peržiūrėti Vilniaus Gedimino technikos universiteto talpykloje https://etalpykla.vilniustech.lt ir Vilniaus Gedimino technikos universiteto bibliotekoje (Saulėtekio al. 14, LT-10223 Vilnius, Lietuva).

Abstract

This dissertation analyzes the removal of hydrogen sulfide (H_2S) from biogas via biofiltration. The study addresses one of the major challenges in biogas utilization, effective H_2S removal, since this compound is toxic and corrosive, and significantly reduces the operational efficiency and service life of biogas energy systems. The main object of the research is biofiltration materials intended for hydrogen sulfide removal from biogas: biochar produced from sewage sludge, cellular lightweight concrete (CLC) waste, and polyurethane foam (PUF). The doctoral dissertation aims to increase the efficiency of hydrogen sulfide removal from biogas and to enhance the operational stability of the biofilter by applying physically and chemically modified as well as unmodified waste-derived materials within the biofiltration process.

The dissertation consists of an introduction, a literature review, chapters on methodology and results, general conclusions and recommendations, and lists of references and the author's publications related to the dissertation topic.

The Introduction presents the research problem and its relevance, describes the research object, formulates the aim and objectives, outlines the research methodology, scientific novelty, and practical significance of the results, and states the defended propositions.

The First Chapter reviews biotechnologies for hydrogen sulfide removal from biogas, with particular emphasis on biofiltration mechanisms, the properties of biofilter packing materials, and the key factors determining process efficiency. The Second Chapter describes the experimental methodologies used to select biofiltration materials, determine their physicochemical and adsorption properties, inoculate and cultivate microorganisms, evaluate hydrogen sulfide removal efficiency, and the mathematically model the biofiltration process. The Third Chapter presents the results of theoretical and experimental investigations of innovative filtration materials, revealing the relationship between their properties and modification with microbial establishment, biofilm formation, and filter performance in hydrogen sulfide removal, and compares experimental results with mathematical modeling outcomes.

Eight scientific papers related to the dissertation topic have been published: two in Web of Science-indexed journals with an impact factor, one in a Web of Science-indexed journal without an impact factor, four in other internationally indexed journals, and one in a conference proceedings volume indexed in the Scopus database. Seven presentations on the dissertation topic were given at national and international scientific conferences.

Reziumė

Disertacijoje analizuojamas sieros vandenilio (H_2S) pašalinimas iš biodujų, taikant biofiltracijos metodą. Darbe sprendžiama viena pagrindinių biodujų panaudojimo problemų – efektyvus H_2S šalinimas, kadangi ši medžiaga yra toksiška, korozinė ir reikšmingai mažina biodujų energetinių sistemų eksploatacinį efektyvumą bei jų tarnavimo laiką. Pagrindinis tyrimo objektas – sieros vandeniliui šalinti iš biodujų skirtos biofiltracijos medžiagos: iš nuotekų dumblo pagamintos bioanglys, akytojo lengvojo betono (CLC) atliekos ir putų poliuretanas (PUF). Pagrindinis disertacijos tikslas – didinti sieros vandenilio šalinimo iš biodujų efektyvumą ir biofiltro veikimo stabilumą, biofiltracijos procese taikant fiziškai ir chemiškai modifikuotas bei nemodifikuotas atliekų kilmės medžiagas.

Darbą sudaro įvadas, literatūros apžvalga, metodikos ir rezultatų skyriai, bendrosios išvados ir rekomendacijos, naudotos literatūros ir autoriaus publikacijų disertacijos tema sąrašai. Įvadiniame skyriuje pateikiama tiriamoji darbo problema, aktualumas, aprašomas tyrimų objektas, formuluojamas tikslas ir uždaviniai, aprašoma tyrimų metodika, darbo mokslinis naujumas, rezultatų praktinė reikšmė, ginamieji teiginiai.

Pirmajame skyriuje apžvelgiamos sieros vandenilio šalinimo iš biodujų biotechnologijos, daugiausia dėmesio skiriant biofiltracijos mechanizmams, biofiltrų užpildų savybėms ir pagrindiniams proceso efektyvumą lemiantiems veiksniams. Antrajame skyriuje aprašomos eksperimentinių tyrimų metodikos, skirtos biofiltracijos medžiagoms parinkti, jų fizikinėms ir cheminėms savybėms, adsorbcinėms charakteristikoms nustatyti, mikroorganizmų inokuliacijai ir auginimui, taip pat sieros vandenilio šalinimo efektyvumui vertinti ir biofiltracijos procesui matematiškai modeliuoti. Trečiajame skyriuje pateikiami inovatyvių filtravimo medžiagų teorinių ir eksperimentinių tyrimų rezultatai, atskleidžiantys šių medžiagų savybių ir modifikacijos ryšį su mikroorganizmų įsitvirtinimu, bioplėvelės formavimusi ir filtro efektyvumu šalinant sieros vandenilį, taip pat palyginami eksperimentiniai duomenys su matematinio modeliavimo rezultatais.

Disertacijos tema yra atspausdinti 8 moksliniai straipsniai: du – *Web of Science* duomenų bazės leidiniuose, turinčiuose citavimo rodiklį, vienas – *Web of Science* duomenų bazės leidinyje, neturinčiame citavimo rodiklio, keturi – kitose tarptautinėse duomenų bazėse referuojamuose leidiniuose, vienas tik *Scopus* duomenų bazėje referuojamame konferencijų darbų leidinyje. Disertacijos tema perskaityti 7 pranešimai Lietuvos ir kitų šalių konferencijose.

Notations

Symbols

C_{in} – concentration of H_2S in inlet gas, $g \cdot m^{-3}$ (liet. *H_2S koncentracija įleidžiamose dujose*);

C_{out} – concentration of H_2S in outlet gas, $g \cdot m^{-3}$ (liet. *H_2S koncentracija išleidžiamose dujose*);

k – constant kinetics (liet. *kinetinė konstanta*);

k_{max} – maximum constant kinetics (liet. *didžiausia kinetinė konstanta*);

K – immersion steady, $g \cdot m^{-3}$ (%) (liet. *sugerties (prisotinimo) pastovioji*);

K_I – hindrance consistent, $g.m^{-3}$ (liet. *slopinimo koeficientas*);

Ks – saturation constant, ppm (liet. *prisotinimo konstanta*);

K'_s – immersion steady, $g \cdot m^{-3}$ (liet. *sugerties (prisotinimo) pastovioji*);

m – gas-liquid partition coefficient, (C/CL) (liet. *dujų ir skysčio pasiskirstymo koeficientas*);

Q – gas flow rate, $L \cdot d^{-1}$ (liet. *dujų debitas*);

V – gas volume, L (liet. *dujų tūris*);

X – length of boundary condition, cm (liet. *ribinio intervalo ilgis*);

δ – biofilm thickness, cm (liet. *bioplėvelės storis*);

$Ø$ – Thiele modulus (liet. *Thiele modulis*);

σ – biofilm dimensionless length coordinate = X/δ (liet. *bedimensė bioplėvelės ilgio koordinatė*);

λ – active thickness of biofilm (less than δ), cm (liet. *aktyvus bioplėvelės storis*);

α_{lump} – variable = A√((K.D)/(2 m)) (liet. *modelio kintamasis, apibrėžtas kaip* $\alpha_{lump} = A\sqrt{((K \cdot D)/(2m))}$).

Abbreviations

AD – anaerobic digestion (liet. *anaerobinis pūdymas*);

AC – activated carbon (liet. *aktyvintosios anglys*);

BET – Brunauer–Emmett–Teller (liet. *Brunauer, Emmett ir Teller*);

BD – bulk density (liet. *tūrinis tankis – medžiagos masė, tenkanti vienetiniam tūriui, įskaitant porėtumą*);

CLC – cellular lightweight concrete (liet. *akytojo lengvojo betono (CLC) atliekos*);

CFU – colony-forming units (liet. *koloniją formuojantys vienetai*);

COMSOL – Multiphysics® simulation software (liet. *Multiphysics® modeliavimo programinė įranga*);

CAA – Clean Air Act (liet. *Švaraus oro įstatymas*);

DO – dissolved oxygen (liet. *ištirpęs deguonis*);

DAPI – 4′,6-diamidino-2-phenylindole (liet. *4′,6-diamidino-2-fenilindolis – fluorescencinis dažiklis, naudojamas mikroorganizmų DNR vizualizacijai*);

EPS – extracellular polymeric substance (liet. *tarpląstelinės polimerinės medžiagos – tai mikroorganizmų išskiriami polimerai, formuojantys bioplėvelės struktūrą*);

EBRT – empty bed retention time, sec. (liet. *biodujų buvimo trukmė biofiltre*);

EC – elimination capacity (liet. *teršalo šalinimo geba*);

EC* – electrical conductivity (liet. *elektrinis laidumas*);

EC_{max} – elimination capacity, $g \cdot m^{-3} \cdot h^{-1}$ (liet. *didžiausia teršalo šalinimo geba*);

GDA – gas data analyzer (liet. *dujų analizatorius*);

GA – generic algorithm (liet. *genetinis algoritmas*);

HSD – honest significant difference (liet. *statistiškai reikšmingas skirtumas – tai kriterijus, taikomas skirtumų tarp duomenų grupių patikimumui įvertinti*);

ILR – inlet loading rate (liet. *įleidžiamų teršalų tūrinė koncentracija*);

LCA – life-cycle assessment (liet. *gyvavimo ciklo vertinimas – tai aplinkosauginio poveikio analizė nuo žaliavų gavybos iki utilizavimo*);

MSW – municipal solid waste (liet. *komunalinės kietosios atliekos*);

NSPS – new source performance standard (liet. *naujų taršos šaltinių veiklos standartas – tai reglamentuojami naujai įrengtų taršos šaltinių reikalavimai*);

OSHA – occupational safety and health administration (liet. *darbuotojų saugos ir sveikatos administracija – institucija, nustatanti darbuotojų saugos ir sveikatos reikalavimus*);

ODE – ordinary differential equations (liet. *paprastosios diferencialinės lygtys*);

PPM – parts per minute (liet. *santykinis koncentracijos matavimo vienetas*);

PUF – polyurethane foam (liet. *putų poliuretanas*);

POTW – publicly owned treatment works (liet. *savivaldybės nuotekų valymo įrenginiai*);

RE – removal efficiency (liet. *valymo efektyvumas*);

RPM – rotation per minute (liet. *apsisukimai per minutę*);

SOB – sulfur-oxidizing bacteria (liet. *sierą oksiduojančios bakterijos*);

SEM – scanning electron microscopy (liet. *skenuojančioji elektroninė mikroskopija*);

SYPRO – SYPRO® protein fluorescent stain (liet. *baltymų fluorescenciniai dažai SYPRO®*);

SVM – support vector machines (liet. *atraminių vektorių mašinos*);

TDR – time domain reflectometry (liet. *laiko srities reflektometrija – metodas, taikomas terpės fizinėms savybėms nustatyti*);

TDS – transport of diluted species (liet. *praskiestų medžiagų pernaša*);

WIFI – wireless fidelity (liet. *belaidis duomenų perdavimas*);

WWTP – wastewater treatment plant (liet. *nuotekų valymo įrenginiai – įrenginiai, skirti nuotekų teršalams pašalinti*);

XRF – x-ray fluorescence (liet. *rentgeno fluorescencija*).

Contents

INTRODUCTION 1
Problem formulation 1
Relevance of the dissertation 2
Research object 3
Aim of the dissertation 3
Tasks of the dissertation 3
Research methodology 4
Scientific novelty of the dissertation 4
Practical value of the research findings 5
Defended statements 5
Approval of the research findings 6
Structure of the dissertation 6
Acknowledgments 6

1. LITERATURE REVIEW OF BIOTECHNOLOGIES FOR H_2S REMOVAL FROM BIOGAS 9
1.1. Introduction to biofiltration for H_2S removal 10
1.1.1. Overview of biogas purification 10
1.1.2. Importance of H_2S removal in biogas systems 11
1.1.3. Assessment of biogas purification methods and technologies from H_2S 14

1.2. Biofilters for H_2S removal: key concepts and mechanisms 16
1.2.1. Fundamentals of biofiltration 16
1.2.2. Types of biofilter materials and their roles 17
1.3. Impact of biofilter material properties on H_2S removal 23
1.4. Microbial communities in biofilters 24
1.4.1. Sulfur oxidation pathways in biofilters 25
1.4.2. Key sulfur-oxidizing microorganisms 26
1.4.3. Factors influencing microbial colonization and biofilm formation 26
1.4.4. Fluorescence microscopy for biofilm visualization 26
1.5. Environmental and operational factors affecting biological H_2S removal in biofilters 27
1.5.1. pH 27
1.5.2. Sulfur accumulation (clogging) 28
1.5.3. EBRT (Empty Bed Retention Time) 28
1.5.4. Temperature 28
1.5.5. Water retention (humidity) 29
1.6. Numerical validation of experimental results 29
1.6.1. Mathematical modeling by MATLAB 29
1.6.2. Simulation by COMSOL 30
1.7. Conclusions of the First Chapter and formulation of the dissertation tasks ... 32

2. METHODOLOGIES FOR DETERMINING THE PHYSICOCHEMICAL PROPERTIES AND ADSORPTION CHARACTERISTICS OF MATERIALS AND THEIR APPLICATION IN H_2S REMOVAL FROM BIOGAS 35
2.1. Experimental system setup 36
2.1.1. Biofilter construction and materials 36
2.1.2. Operational conditions and flow regulations 38
2.2. Concept for the selection of biofilter packing materials 39
2.2.1. Functional criteria for the selection of biofilter packing materials 40
2.2.2. Rationale for the selection of organic-origin packing materials 40
2.2.3. Rationale for the selection of inorganic-origin packing materials 42
2.2.4. Rationale for the selection of synthetic-origin packing materials 43
2.2.5. Concept of a combined biofilter packing system 43
2.3. Physicochemical characteristics of selected biofilter packing materials 45
2.3.1. Bulk density 45
2.3.2. pH 45
2.3.3. Electrical conductivity 45
2.3.4. Porosity 46
2.3.5. Specific surface area 46
2.3.6. Chemical composition 47
2.4. Inoculation and cultivation of microorganisms 47
2.5. Hydrogen sulfide removal efficiency (H_2S RE) 53
2.5.1. Gas sampling ports and analytical procedure 54
2.5.2. Experimental conditions and monitoring 54
2.5.3. Calculation of H_2S removal efficiency 55

2.6. Data analysis and mathematical modeling 55
2.6.1. Mathematical modeling of sulfur-oxidizing bacterial growth 56
2.6.2. Graphical representation and kinetic modeling of biofiltration using COMSOL 58
2.7. Conclusions of the Second Chapter 61

3. RESULTS OF THEORETICAL AND EXPERIMENTAL STUDIES OF BIOFILTRATION MATERIALS 63
3.1. Impact of packing material properties on biofiltration efficiency 64
3.1.1. Bulk density 64
3.1.2. Porosity 65
3.1.3. Specific surface area 66
3.1.4. pH 68
3.1.5. Electrical conductivity 69
3.1.6. Chemical composition 69
3.2. Modification of physicochemical properties of packing materials 73
3.3. Microbial colonization and biofilm formation on biofiltration materials 76
3.3.1. Microscopic analysis of microbial activity and material effects 77
3.3.2. Biofilm distribution across biofilter layers and its relationship with H_2S removal 82
3.4. Investigation of biofilter performance in H_2S removal 90
3.4.1. Performance comparison of biofilters with single-component packing material 91
3.4.2. Performance comparison of biofilters with multi-component packing material 96
3.5. Comparison of mathematical modeling and experimental results 106
3.6. Modeling of H_2S removal efficiency from biogas using COMSOL 6.1 111
3.7. Comparative analysis and scientific discussion of biofilter performance based on experimental, statistical, and simulation results 118
3.8. Conclusions of the Third Chapter 121

GENERAL CONCLUSIONS 123

RECOMMENDATIONS 125

REFERENCES 127

LIST OF SCIENTIFIC PUBLICATIONS BY THE AUTHOR ON THE TOPIC OF THE DISSERTATION 143

SUMMARY IN LITHUANIAN 145

Introduction

Problem formulation

Biogas, primarily composed of methane (CH_4) and carbon dioxide (CO_2), is a promising renewable energy source produced through anaerobic digestion of organic waste. However, its efficient utilization is limited by the presence of hydrogen sulfide (H_2S), a highly toxic and corrosive compound that threatens human health, reduces system reliability, and shortens equipment lifetime (Torres et al., 2020; Wang, 2020b). When H_2S concentrations exceed ~100 ppm, severe corrosion of pipelines, engines, and turbines occurs, increasing maintenance costs and reducing equipment durability, as well as the calorific value and combustion efficiency of biogas (Zhang et al., 2022; Khan et al., 2021; Pabby & Sastre, 2013).

Various physical, chemical, and biological methods have been developed for H_2S removal. Although physical adsorption and chemical absorption provide high efficiency, they often involve high operational and energy costs, chemical reagent consumption, and secondary waste management issues, limiting their environmental sustainability (Perez et al., 2020; Gao et al., 2022). Therefore, biological filtration based on sulfur-oxidizing microorganisms has attracted increasing attention as a cost-effective and environmentally friendly alternative (Vikrant et al., 2018; Muthulakshmi & Sundrarajan, 2020).

Nevertheless, the performance of biofiltration systems remains limited by insufficient optimization of biofilter packing materials, limited control of microbiological processes, and the lack of reliable mathematical models that predict biofilter performance under varying operating conditions (Haosagul et al., 2020; Yuan et al., 2018). In particular, the potential of waste-derived materials as sustainable and cost-effective biofilter packing media remains underexplored (Xia et al., 2019; Ying et al., 2020).

Relevance of the dissertation

As biogas production and its application in energy and environmental sectors increase, the demand for scientifically grounded technologies for hydrogen sulfide removal is growing (Torres et al., 2020; Rivard et al., 2018). Biological filtration is considered a promising approach due to its effectiveness in hydrogen sulfide removal and the flexibility of its technological solutions (Vikrant et al., 2018; Ying et al., 2020).

The efficiency and stability of biofiltration systems largely depend on the physical, chemical, and structural properties of biofilter packing materials, which influence hydrogen sulfide transport, microbial activity, and overall process performance (Haosagul et al., 2020; Zhang et al., 2021). Therefore, the modification and optimization of biofiltration materials have become an important research direction, enabling the transition from laboratory studies to scientifically based biofilter design and practical application.

The relevance of this research also relates to the integration of waste-derived materials into biofiltration systems. In the European Union, about 7–15 million tonnes of sewage sludge (dry matter) are generated annually, while in Lithuania, about 60–70 thousand tonnes are generated per year. Construction and demolition waste accounts for approximately 30–35% of total waste, and polymer waste represents a continuously growing waste stream with still limited environmental applications (Eurostat, 2020; Eurostat, 2021; European Commission, 2020). Converting these wastes into functional biofiltration materials supports circular economy principles and the development of innovative biogas purification solutions.

This dissertation focuses on the development and application of biofiltration materials for hydrogen sulfide removal from biogas. The research evaluates physically and chemically modified and unmodified waste-derived materials, including sewage sludge biochar, autoclaved cellular concrete (CLC) waste, and polyurethane foam (PUF). By integrating experimental research, microbiological analysis, statistical evaluation, and mathematical modeling, the study establishes a scientific basis for biofiltration material selection and modification, contributing

to both fundamental and applied research (Haosagul et al., 2020; Zhanga et al., 2020; Kalinska et al., 2019).

Research object

The research object is biofiltration materials intended for the removal of hydrogen sulfide from biogas: biochar produced from sewage sludge, CLC waste, and PUF.

Aim of the dissertation

The doctoral dissertation aims to assess methods to increase the efficiency of hydrogen sulfide removal from biogas and to enhance the operational stability of the biofilter by applying physically and chemically modified as well as unmodified waste-derived materials within the biofiltration process.

Tasks of the dissertation

The following tasks are set to achieve the aims of the dissertation:

1. To analyze the scientific literature and identify existing research gaps related to technologies for biogas purification from hydrogen sulfide, biofiltration materials, and microbiological processes.
2. To select and characterize waste-derived biofiltration materials**,** including biochar, CLC waste, and PUF, and to evaluate the effects of physical and chemical modification on their physicochemical properties relevant to H_2S removal.
3. To experimentally evaluate the performance of modified and unmodified biofiltration materials in the removal of hydrogen sulfide from biogas under controlled laboratory-scale conditions.
4. To investigate the formation and development of biofilms on the surfaces of different biofiltration materials and to determine the influence of material properties and their modification on microbial activity and distribution.
5. To determine statistical relationships between the physicochemical properties of biofiltration materials, microbiological indicators, and hydrogen sulfide removal efficiency in biofiltration systems.

6. To develop a mathematical model of the biofiltration process describing hydrogen sulfide removal and microbial activity, and to evaluate its agreement with experimental results.
7. To perform numerical modeling of biofiltration systems and to substantiate the experimental results by analyzing hydrogen sulfide concentration and reaction rate distributions within the biofilter under different biofiltration material configurations.

Research methodology

Biological filtration technology was applied to remove hydrogen sulfide (H_2S) from biogas using physically and chemically modified biochar, CLC waste, and PUF. During the study, the physicochemical properties of biofiltration materials were determined, and H_2S removal efficiency, microbial activity, and biofilter operational stability were evaluated. The experimental results were further analyzed using mathematical modeling and numerical calculations.

Scientific novelty of the dissertation

The following results, new to environmental engineering science, were obtained during the preparation of the dissertation:

1. A biofiltration material concept for biogas purification from hydrogen sulfide (H_2S) was developed and experimentally validated, demonstrating the effective application of physically and chemically modified waste-derived materials-KOH-modified biochar and $FeCO_3$-modified CLC waste, which enabled the achievement of H_2S removal efficiencies of up to 90–95%.
2. The role of biofiltration material modification in regulating microbial activity and ensuring biofiltration process stability was revealed by establishing quantitative relationships between the physicochemical properties of modified packing materials – porosity (~65–75%) and specific surface area (180–320 $m^2 \cdot g^{-1}$) – the activity of sulfur-oxidizing microorganisms, the intensity of biofilm formation, and hydrogen sulfide removal efficiency.
3. A mathematical and numerical model of the biofiltration process was developed and validated using experimental data, enabling the prediction of hydrogen sulfide removal efficiency with deviations of less than 10% and providing a basis for optimizing biofiltration systems.

Practical value of the research findings

The results of this dissertation have practical relevance for biogas production, environmental protection, and waste management by providing a material-oriented biofiltration solution for removing hydrogen sulfide from biogas. The application of physically and chemically modified waste-derived biofiltration materials enables stable biological desulfurization, reduces H_2S-induced corrosion of energy system components, and improves the energetic quality of biogas.

The demonstrated use of sewage sludge-derived biochar and construction waste-based CLC, in combination with PUF as a mechanically and hydraulically stable support material, offers a sustainable alternative to commercial biofilter packings. The obtained results can be applied in agricultural biogas plants, wastewater treatment facilities, and other biogas utilization systems, supporting the implementation of environmentally friendly, circular-economy-based biogas purification technologies.

Defended statements

1. Sewage sludge-derived biochar modified with KOH exhibits a specific BET surface area increased from 24.66 $m^2 \cdot g^{-1}$ to 471.54 $m^2 \cdot g^{-1}$, along with a higher specific micro- and mesopore volume; this leads to an increase in hydrogen sulfide (H_2S) removal efficiency in the biofiltration system from approximately 80% to 92%.
2. The combination of KOH-modified biochar and $FeCO_3$-impregnated cellular lightweight concrete (CLC) waste in biofilters creates a synergistic adsorption–biocatalytic effect, resulting in a relative increase of H_2S removal efficiency by 10–15% compared to unmodified or single-component packing materials, while ensuring more stable process operation.
3. In biofiltration systems, the hydrogen sulfide (H_2S) removal process is governed by the interaction between sulfur-oxidizing bacteria (*Acidithiobacillus* spp.) and biofilm-forming microorganisms (*Pseudomonas* spp.), which promotes more intensive biofilm formation and enhanced synthesis of extracellular polymeric substances (EPS) on the surface of modified packing materials, thereby enabling H_2S removal efficiencies exceeding 90%.

Approval of the research findings

The research results of the dissertation are presented in eight scientific publications: two articles published in journals indexed in the Web of Science database with an Impact Factor (Mohammadi et al., 2024a; Mohammadi et al., 2025a), one article published in a journal indexed in the Web of Science Emerging Sources Citation Index (ESCI) and Scopus databases (Mohammadi et al., 2024b), four articles published in other peer-reviewed international journals indexed in international databases (Mohammadi 2022; Mohammadi et al., 2023a; Mohammadi et al., 2024; Mohammadi et al., 2025), and one article published in Scopus-indexed international conference proceedings (Mohammadi et al., 2023c). A patent application entitled "Application of modified biofilter media derived from sewage sludge and concrete waste for the removal of hydrogen sulfide (H_2S) from biogas" (Mohammadi et al., 2024e) has been submitted to obtain a patent of the Republic of Lithuania (Application number: 2025 018; Date of submission: 10-10-2025).

The results of the research were presented at seven national and international scientific conferences in Lithuania and abroad:

- at four thematic conferences of young Lithuanian scientists "Science – Future of Lithuania: Environmental Protection Engineering", held in 2022–2025, Vilnius, Lithuania;
- at the 13th International Conference "Environmental Engineering", held in 2023, Vilnius, Lithuania;
- at two international Conferences of Environmental and Climate Technologies (CONECT 2024 and CONECT 2025), held in 2024 and 2025 in Riga, Latvia.

Structure of the dissertation

The dissertation consists of an introduction, three chapters, general conclusions, and recommendations.

The entire dissertation consists of 137 pages. It contains 36 numbered formulas, 49 figures, and 27 tables. A total of 158 literature sources were used in writing the dissertation.

Acknowledgments

I sincerely thank the staff of the Department of Environmental Protection and Water Engineering at Vilnius Gediminas Technical University for providing tech-

nical support, research infrastructure, and resources. I express my special gratitude to my supervisor, Assoc. Prof. Dr Rasa Vaiškūnaitė, for her scientific guidance, valuable comments, and continuous support during the preparation of this dissertation. I also thank Dr Sc. Ing. Linda Mežule (Riga Technical University) for consultations on biofiltration and microbiological research, and Assoc. Prof. Dr Teresė Leonavičienė from the Department of Mathematical Modelling at VILNIUS TECH for her assistance with mathematical and numerical modeling. I am grateful to the staff of the Civil Engineering Laboratory at the University of Tehran and the Chemical Analysis Laboratory at Ferdowsi University for their assistance with structural and chemical analyses, and to Tomas Žemaitis for his support in conducting laboratory experiments and analyzing the obtained data.

1

Literature review of biotechnologies for H_2S removal from biogas

The First Chapter presents a comprehensive literature review of biotechnologies for hydrogen sulfide (H_2S) removal from biogas, with particular emphasis on biological filtration processes. The Chapter analyzes the composition of biogas and the environmental, technical, and economic importance of H_2S removal, evaluates physical, chemical, and biological desulfurization methods, and discusses the mechanisms of biofiltration, including sulfur oxidation pathways, microbial communities, and the influence of biofilter packing material properties on process efficiency. Special attention is given to waste-derived materials as sustainable biofilter media and to the integration of experimental and modeling approaches for performance optimization. The results of this review, presented in this Chapter, were published in Mohammadi and Vaiškūnaitė (2023a) and Mohammadi and Vaiškūnaitė (2023b).

1.1. Introduction to biofiltration for H_2S removal

Biogas produced through anaerobic digestion is an important renewable energy source; however, its practical utilization is significantly constrained by the presence of hydrogen sulfide. Depending on feedstock composition and process conditions, H_2S concentrations in raw biogas typically range from 100 to 20,000 ppm, posing serious risks due to toxicity, corrosion, and reduced equipment lifetime (Huan et al., 2020; Jia et al., 2022). Consequently, effective H_2S removal is a prerequisite for upgrading biogas to biomethane that complies with technical, environmental, and safety standards.

Biofiltration has emerged as a sustainable alternative to conventional physical and chemical desulfurization methods, particularly for small- and medium-scale biogas facilities. This technology relies on Sulfur-Oxidizing Bacteria (SOBs) immobilized on porous packing materials and enables H_2S conversion to elemental sulfur or sulfate with comparatively low energy demand and environmental impact.

1.1.1. Overview of biogas purification

Biogas produced via Anaerobic Digestion (AD) of organic waste is a key renewable energy source with significant potential for electricity generation, heat production, and transport fuel applications. However, its overall quality and applicability depend strongly on the effective removal of undesirable components, among which hydrogen sulfide is particularly problematic due to its high toxicity and corrosivity (Taheriyoun et al., 2019). Recent studies emphasize that efficient H_2S removal not only improves operational safety but also enhances the calorific value and market competitiveness of biomethane (Taheriyoun et al., 2019; Dada, 2025).

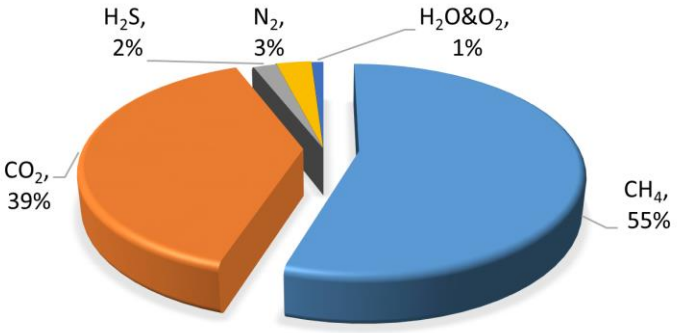

Fig. 1.1. Composition of raw biogas in percentage (approximate data) (Das et al., 2022a)

Raw biogas mainly consists of methane (40–70%) and carbon dioxide (20–45%), together with minor components such as water vapor, nitrogen, oxygen, and hydrogen sulfide. Even relatively low H_2S concentrations (<100 ppm) can cause severe corrosion, pitting, and an increased risk of cracking in engines, turbines, and pipelines, leading to significantly higher maintenance costs and increased downtime (Das et al., 2022a; Torres et al., 2020; Kulawong et al., 2022). A general overview of the typical composition of raw biogas is presented in Figure 1.1.

These considerations clearly highlight the necessity for integrated biogas purification strategies that are both technically robust and economically viable. Contemporary review studies increasingly emphasize the importance of integrating physical, chemical, and biological treatment principles to develop advanced biogas purification systems that can meet diverse operational and regulatory requirements. Hybrid purification systems integrating physical adsorption with biological oxidation have demonstrated improved overall removal efficiency while maintaining economic and environmental sustainability (Alayande et al., 2024). These approaches provide the conceptual foundation for biofiltration-based systems investigated in this dissertation.

1.1.2. Importance of H_2S removal in biogas systems

Environmental regulations strictly limit allowable hydrogen sulfide concentrations in biogas and derived transportation fuels due to its toxicity, corrosivity, and adverse impacts on energy-conversion equipment. Even trace amounts of H_2S and ammonia (NH_3) in raw biogas can significantly restrict its end-use applications by accelerating corrosion in engines, turbines, pipelines, and heat exchangers (Kulawong et al., 2022; Das et al., 2019). Environmental and occupational regulations limit allowable H_2S concentrations due to its toxicity and corrosivity. Exposure limits below 20 ppm are commonly enforced, while concentrations above 100 ppm pose severe health risks (Liu & Zhou, 2023). From an environmental perspective, the combustion of H_2S produces sulfur oxides, which contribute to acid rain and air pollution (Nowicki et al., 2014). Consequently, effective H_2S removal is a prerequisite for safe, reliable, and economically viable biogas utilization.

Occupational exposure limits further highlight the need for H_2S control. According to occupational health guidelines referenced in recent studies, short-term exposure limits for H_2S are typically set at 10–20 ppm, while concentrations exceeding 50–100 ppm pose serious risks to human health, including respiratory irritation, neurological effects, and, at higher levels, fatal outcomes (Prasertcharoensuk et al., 2022; Dada, 2025). In addition to health concerns, H_2S contributes to biogenic corrosion by oxidizing to sulfuric acid (H_2SO_4), particularly in

moist environments, leading to material degradation and increased maintenance costs (Ghimire et al., 2021; Haosagul et al., 2020).

Table 1.1. Transmission of the amount of consumed biogas in Lithuania (every possible sector) from 2021 to 2024 (1 TJ (terajoules) = 0.278 GW/h) (European biogas association, 2024)

		Fuel commodities balances, TJ			
		2021	**2022**	**2023**	**2024**
Landfill biogas	Gross consumption	231	190	160	135
	Statistical differences	–	–	–	–
	Transformation in plants	224	185	155	130
	Consumption in the energy sector	–	–	–	–
	Non-energy use	–	–	–	–
	Final consumption	7	5	4	3
Sludge biogas	Gross consumption	340	365	390	420
	Statistical differences	–	–	–	–
	Transformation in plants	106	115	120	125
	Consumption in the energy sector	–	–	–	–
	Non-energy use	–	–	–	–
	Final consumption	234	250	270	295
Another biogas	Gross consumption	1.111	1.180	1.250	1.320
	Statistical differences	–	–	–	–
	Transformation in plants	924	985	1,045	1,110
	Consumption in the energy sector	–	–	–	–
	Non-energy use	–	–	–	–
	Final consumption	187	195	205	210

From an environmental perspective, the combustion of H_2S-containing biogas emits sulfur oxides (SO_x), which contribute to acid rain formation and atmospheric pollution. These impacts reinforce the need for upstream desulfurization to ensure compliance with environmental regulations and to minimize the overall environmental footprint of biogas-based energy systems (Vaiskunaite, 2020; Dada, 2025).

The economic implications of insufficient H_2S removal are equally significant. Elevated H_2S concentrations reduce the efficiency and lifespan of energy conversion equipment, increase downtime, and necessitate costly post-combustion gas treatment. In contrast, purified biogas – often upgraded to biomethane – has a higher calorific value, improved market competitiveness, and broader applicability in energy grids and the transportation sector (Zhang et al., 2024; Alayande et al., 2024; Cui et al., 2022).

Regional trends in biogas production further underscore the relevance of H_2S removal. In Lithuania, biogas-derived energy production declined from 34.1 ktoe in 2017 to 14.7 ktoe by 2020, reflecting structural changes in the sector (Cortés et al., 2021). At the European scale, total biogas production reached approximately 71 billion m^3 in 2023 and is projected to increase substantially in the coming years, driven by renewable energy policies and circular economy objectives (Cano et al., 2021; European Biogas Association, 2024).

Analysis of Lithuanian biogas statistics reveals a growing contribution of sludge-derived biogas, which typically contains elevated sulfur concentrations. As shown in Table 1.1, the structure of biogas consumption in Lithuania between 2021 and 2024 reveals a clear shift toward sludge-derived biogas. While landfill biogas consumption decreased steadily, sludge biogas utilization increased from 340 TJ in 2021 to 420 TJ in 2024, corresponding to an approximate 24% increase over four years (European Biogas Association, 2024). This trend is particularly significant for desulfurization technologies, as biogas produced from sewage sludge typically contains higher sulfur concentrations compared to agricultural or landfill feedstocks.

Given that H_2S can account for up to ~3% of raw biogas volume, the growing reliance on sludge-based biogas implies an increased potential release of sulfur compounds if adequate purification is not implemented. Previous estimates suggest that several hundred tons of H_2S could be associated with biogas production in Lithuania alone, underscoring the need for robust, sustainable H_2S removal solutions prior to energy recovery or grid injection.

Overall, the data presented in Table 1.1 directly support the scientific and practical relevance of this dissertation. The increasing role of sludge-derived biogas in Lithuania strengthens the need for efficient, low-cost, and environmentally

sustainable H_2S removal technologies, particularly those suitable for variable operating conditions and high sulfur loads. Addressing these challenges is essential for ensuring the long-term viability of biogas as a renewable energy source.

1.1.3. Assessment of biogas purification methods and technologies from H_2S

Physical and chemical H_2S removal methods achieve high removal efficiencies but are often associated with high operational costs, chemical consumption, and secondary waste generation. In contrast, biological filtration offers superior sustainability and cost-effectiveness, albeit with slower reaction kinetics and higher sensitivity to operational conditions.

Physical adsorption (dry technologies) involves the attachment of sulfide compounds onto the surface of solid adsorbents, thereby reducing H_2S concentration in the gas phase. Commonly applied adsorbents include activated carbon, metal oxides, and natural or synthetic zeolites (Gao et al., 2022). These technologies are characterized by relatively simple system designs, mild operating conditions, and the absence of wastewater generation, making them attractive for decentralized applications (Ma et al., 2018). The efficiency of physical adsorption is strongly influenced by the adsorbent's specific surface area, pore structure, and surface chemistry (Jiao et al., 2022; Zhang et al., 2021).

Chemical absorption (wet technologies) involves transferring H_2S into the liquid phase, where it reacts with chemical reagents such as alkanolamines, alkaline solutions, or oxidizing agents (Gao et al., 2022). These systems generally achieve high removal efficiencies and rapid reaction rates; however, they require significant chemical consumption, complex process control, and the generation of secondary waste streams. As a result, their large-scale implementation is often associated with high operational and environmental costs.

Biological filtration (biofiltration) represents an alternative approach in which H_2S is biologically oxidized by SOBs immobilized on a porous packing material within a biofilter (Scarlat et al., 2018; Vikrant et al., 2018). Depending on oxygen availability and microbial community composition, SOBs can convert H_2S into elemental sulfur or sulfate. These microorganisms are susceptible to environmental and operational conditions, particularly temperature, pH, moisture content, and nutrient availability (Wang et al., 2022; Haosagul et al., 2020). Therefore, selecting and modifying suitable packing materials is critical to ensuring stable microbial activity and efficient biological desulfurization.

A structured overview of the most common physical and chemical H_2S removal technologies is presented in Table 1.2, highlighting their classification and principal operating mechanisms.

The principal sulfur oxidation pathways involved in biological H_2S removal are described by the reactions presented in Equations (1.1) and (1.2).

$$2S + 3O_2 + 2H_2O \rightarrow 2H_2SO_4; \quad (1.1)$$

$$CO_2 + 2H_2S \rightarrow CH_2O + H_2O + 2S. \quad (1.2)$$

Table 1.2. Dry and wet technologies to purify H_2S from biogas

Physical adsorption	Electrochemical oxidation
	Adsorption by zeolite
	Adsorption on nanoparticles
	Adsorption on metal oxides
	Adsorption on modified carbon
	Pressure swing adsorption
Chemical absorption	Metal sulfide precipitation
	Water scrubbing
	Membrane separation
	Organic solvents (amine)

Each H_2S removal method exhibits specific strengths and weaknesses. Biological filtration is generally associated with low operational costs and minimal environmental impact, but is limited by slower reaction kinetics and sensitivity to process disturbances. In contrast, physical and chemical methods provide faster and often higher removal efficiencies, albeit at the expense of higher costs, greater operational complexity, and increased environmental burden.

A quantitative comparison of biological, physical, and chemical H_2S removal technologies, including typical removal efficiencies, reaction rates, operational costs, and environmental impacts, is summarized in Table 1.3 (Perez et al., 2020; Torres et al., 2020).

Table 1.3. Comparison of main parameters of H_2S removal technologies (Perez et al., 2020; Torres et al., 2020)

Parameter	Biological filtration	Physical adsorption	Chemical absorption
Typical H_2S RE,%	70–95	80–98	95–>99
Reaction speed	Slow	Immediate	Fast
Operational cost	Low	Medium to high	High
Sensitivity to conditions	High (Temp/pH sensitive)	Low	Medium

End of Table 1.3

Parameter	Biological filtration	Physical adsorption	Chemical absorption
Environmental impact	Low	Medium	High
Maintenance requirement	Low to moderate	Moderate	High
Waste generation	Low	Medium (spent adsorbent)	High (chemical waste)
Scalability	Moderate	Moderate	High
Typical EBRT, s	30–120	5–30	5–20

As shown in Table 1.3, chemical absorption achieves the highest H_2S removal efficiency and fastest reaction rates, whereas biological filtration offers superior sustainability and cost-effectiveness. Consequently, improving the performance of biofiltration systems – particularly by optimizing packing materials and operating conditions – represents a promising strategy to overcome the inherent limitations of biological processes. This approach forms the scientific basis for the experimental investigations presented in the subsequent chapters of this dissertation.

1.2. Biofilters for H_2S removal: key concepts and mechanisms

Biofilters are widely recognized as a sustainable, cost-effective technology for removing hydrogen sulfide from biogas. Their operation is based on the synergistic interaction of physical adsorption and biological oxidation, enabling high H_2S removal efficiency (RE) with comparatively low operational costs and environmental impact. Recent studies confirm that biofilters packed with waste-derived materials, such as biochar and CLC waste, can achieve stable RE values exceeding 90% across a broad range of operating conditions, highlighting their suitability for sustainable biogas purification systems (Mohammadi & Vaiškūnaitė, 2025; Aukstinaitis & Vaiškūnaitė, 2012).

1.2.1. Fundamentals of biofiltration

Biofiltration is a gas treatment process in which a contaminated gas stream is passed through a packed bed colonized by sulfur-oxidizing bacteria (SOBs). In biofilter systems designed for H_2S removal, the process proceeds through two

coupled mechanisms: (i) physical adsorption of H_2S onto the packing material surface and (ii) biological oxidation within the microbial biofilm.

Physical adsorption represents the initial removal step, during which H_2S molecules are retained on the surface of the packing material. The efficiency of this process is primarily governed by the physicochemical properties of the packing media, including specific surface area, porosity, surface chemistry, and moisture content. These properties not only influence adsorption capacity but also determine the material's suitability for microbial colonization.

Subsequently, biological oxidation becomes the dominant removal mechanism. SOBs oxidize H_2S to elemental sulfur (S^0) or sulfate (SO_4^{2-}), depending on oxygen availability, according to the reactions presented in Equations (1.1) and (1.2). These reactions occur within the biofilm on the surface of the packing material, which provides a stable microenvironment for microbial metabolism.

Variations in inlet H_2S concentration and Empty-Bed Residence Time (EBRT) directly affect the outlet concentration and overall RE. As illustrated in Figure 1.2, sudden operational disturbances (e.g., shock loads or changes in flow rate) can temporarily reduce biofilter performance, highlighting the importance of stable operating conditions for sustained desulfurization efficiency.

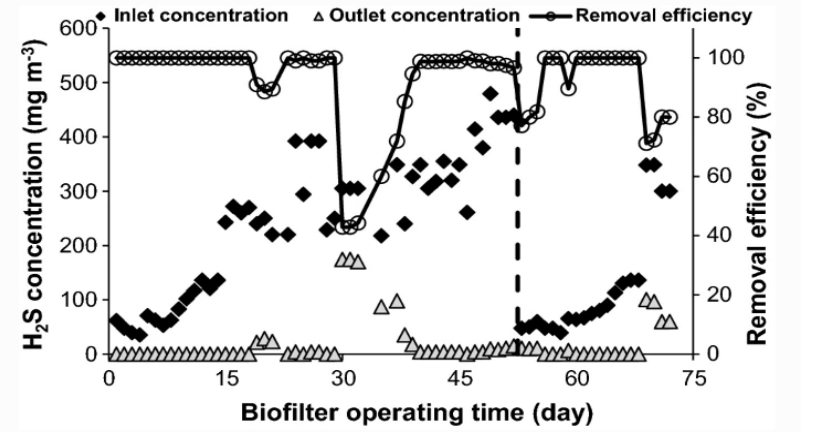

Fig. 1.2. Comparing the removal efficiency of H_2S during 75 days (Khalil et al., 2019)

1.2.2. Types of biofilter materials and their roles

The performance, efficiency, and operational stability of biofilters for hydrogen sulfide removal under laboratory conditions are strongly dependent on the selection of packing materials. Packing materials play a dual role in biofilter systems: they act as a physical support for SOBs and simultaneously participate in H_2S adsorption, mass transfer, and transformation processes (Guo et al., 2023; Das

et al., 2022b). Their physicochemical properties directly influence gas–solid contact efficiency, microbial attachment, pressure drop, moisture retention, and biofilm development, thereby determining overall biofilter performance.

Packing materials used in biofilter systems are commonly classified into three main categories: inorganic, carbon-based, and polymeric. Inorganic materials, particularly CLC waste, have gained increasing attention as biofilter packing media due to their low cost, high porosity, and compatibility with circular economy principles (Xu et al., 2022; Zhang et al., 2021). CLC waste provides a large specific surface area that supports both H_2S adsorption and microbial colonization. When chemically modified or impregnated with iron-containing compounds such as iron carbonate ($FeCO_3$), CLC waste exhibits enhanced catalytic activity, accelerating the oxidation of H_2S to elemental sulfur or sulfate (Ying et al., 2020; Cuimei et al., 2018).

Reported elimination capacity (EC) values for CLC-based packing materials reach up to 32 $g \cdot m^{-3} \cdot h^{-1}$ under laboratory-scale conditions (Wu et al., 2021). The underlying mechanism involves physicochemical interactions between H_2S and calcium- and iron-containing phases of CLC, including calcium silicate hydrates ($CaO \cdot SiO_2 \cdot nH_2O$), calcium carbonate ($CaCO_3$), and iron oxides, resulting in the formation of gypsum ($CaSO_4 \cdot 2H_2O$) and elemental sulfur (Ibrahim et al., 2021; Ying et al., 2020; Cano et al., 2019). These reactions are schematically illustrated in Figure 1.3, while visual changes in CLC structure before and after desulfurization are shown in Figure 1.4.

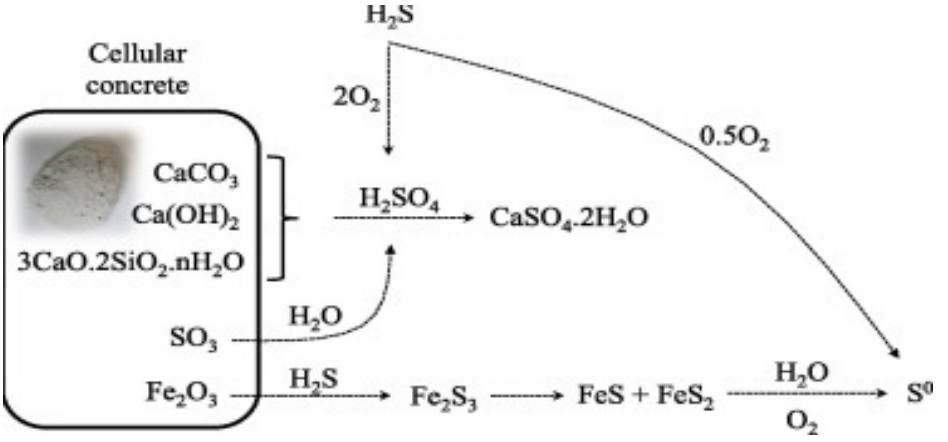

Fig. 1.3. Principal reactions in wet conditions between H_2S and the components of CLC (Wu et al., 2021)

Representative experimental results obtained using CLC waste as biofilter packing material, including reported RE, EBRT, and Elimination Capacity (EC) values, are summarized in Table 1.4. These studies demonstrate that CLC waste is particularly well-suited for applications that prioritize low-cost, sustainable materials.

Table 1.4. Function of the CLC waste sample to be used as packing material in the biofilter

Packing Bed	**H_2S, ppm**	**Time, day**	**EBRT, s**	**RE, %**	**EC_{max}, $g \cdot m^{-3} h^{-1}$**	**Experiment properties**	**Reference**
CLC waste	100	N/A	63	97	5.6	Lab-scale biofilter was topped with a layer of CLC	(Pudi et al., 2022)

Carbon-based materials, especially biochar, are among the most extensively investigated biofilter packing media due to their high specific surface area, well-developed micro- and mesoporous structure, and favorable surface chemistry (Strohmaier et al., 2019; Wu et al., 2021). Biochar supports both effective H_2S adsorption and robust biofilm formation, resulting in high RE and elimination capacity. Chemical activation, such as KOH modification, further enhances biochar adsorption capacity, pore development, alkalinity, and moisture retention, improving biofilter performance under dynamic operating conditions (Lin et al., 2021; Das et al., 2019).

a) b)

Fig. 1.4. CLC waste (a) after desulfurization, (b) before desulfurization (Wu et al., 2021)

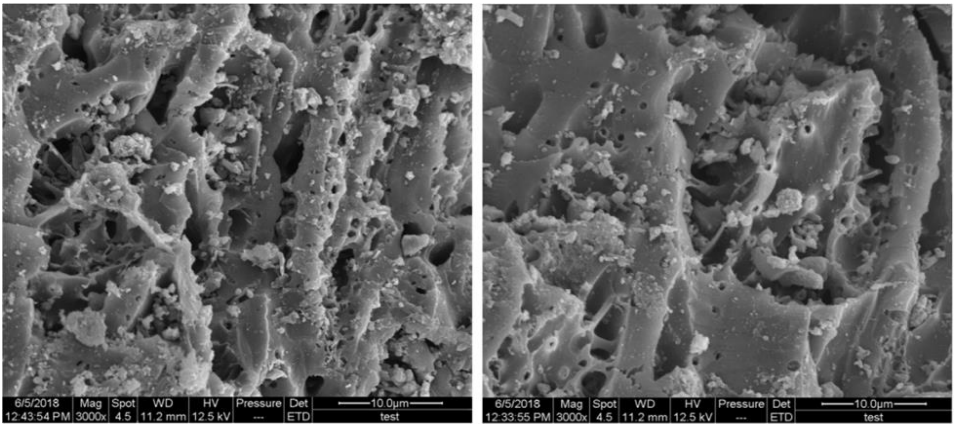

a) b)

Fig. 1.5. Scanning Electron Microscopy (SEM) picture of the biochar before (a) and after (b) the adsorption of H_2S (Lin et al., 2021)

SEM images presented in Figure 1.5 illustrate pore-filling and surface-morphology changes in biochar after prolonged H_2S adsorption, indicating potential clogging effects that may influence long-term biofilter operation. Experimental applications of biochar-packed biofilters, including RE, EBRT, and EC values, are summarized in Table 1.5.

Table 1.5. Function of biochar samples used as packing material in different bioreactors (Bahraminia et al., 2020)

Packing Bed	**H_2S, ppm**	**Time, day**	**EBRT, s**	**RE,%**	**EC_{max}, $g \cdot m^{-3} h^{-1}$**	**Experiment properties**	**Reference**
Biochar	105-1020	20	80	98	94	Bench-scale biofilter packed with MSW	(Wu et al., 2021)
Biochar	110-1065	110	80	70	90	Lab-scale, Michaelis-Menten model	(Pudi et al., 2022)

In addition to adsorption capacity, biochar improves biofilter stability under fluctuating inlet loading rates. The influence of Inlet Loading Rate (ILR) and EBRT on H_2S removal efficiency in biochar-based biofilters is illustrated in Figure 1.6, which demonstrates higher tolerance to loading shocks and more stable

RE than in compost-only systems (Das et al., 2019). These findings confirm the suitability of biochar as a multifunctional biofilter packing material.

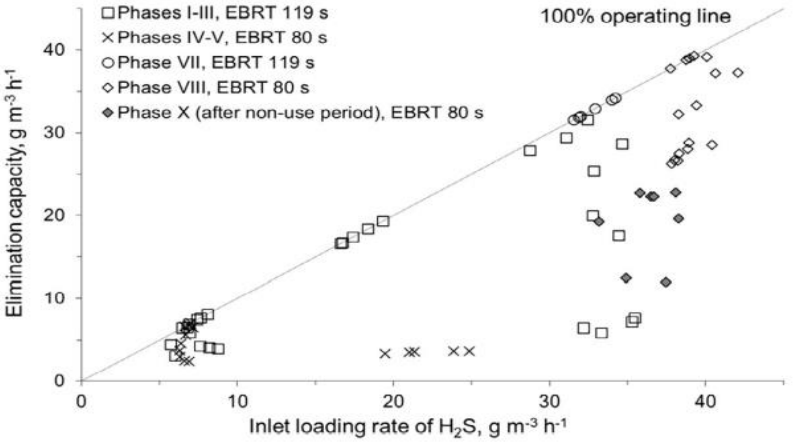

Fig. 1.6. Impact of the inlet loading rate (ILR) on the biofilter's ability to remove H_2S (Das et al. 2019)

Polymeric materials, such as PUF, are primarily applied in biofilter systems due to their mechanical stability, high porosity, low density, and resistance to biodegradation (Juntranapaporn et al., 2019; Das et al., 2022b). Although PUF exhibits limited intrinsic adsorption capacity for H_2S, it provides a practical structural framework for microbial attachment, uniform gas distribution, and stable hydrodynamic conditions

Table 1.6. PUF samples are used as packing material in various bioreactors

Packing bed	H_2S, ppm	Time, day	EBRT, s	RE, %	Experiment properties	Reference
PUF+polypropylene	8000	270	3.5	>94	*Pseudomonas* spp., temperature 25–27 ◦C; sludge from WWTP	(Das et al., 2022)
PUF	66	N/A	45–129	> 98	*Acidithiobacillus* spp., pH 0.44–7.30	(Juntranapaporn et al., 2019)
Open-pore PUF	20–157	N/A	>16	98	*Acidithiobacillus* spp., pH 6.9–8.6	(Juntranapaporn et al., 2019)

End of Table 1.6

Packing bed	H_2S, ppm	Time, day	EBRT, s	RE, %	Experiment properties	Reference
Open-pore PUF	5000	33	N/A	N/A	*Pseudomonas* spp., pH 6–8, temperature 23–27 °C, WWTP	(Zeng et al., 2019)
Open-pore PUF	4100–7900	119	N/A	99	*Acidithiobacillus* spp., pH 6.8–7.4, WWTP	(Zeng et al., 2019)
Open-pore PUF	1400–14600	N/A	N/A	99	*Acidithiobacillus* spp., pH 7.4–7.5, temperature 28–30°C	(Zeng et al., 2019)
Open-pore PUF	96	78	40	98	*Pseudomonas* spp., gathered from the soils and sediments of a lake	(Das et al., 2022)
PUF rings	2000	365	60	98	*Acidithiobacillus* spp., WWTP	(Das et al., 2022)
PUF	4000	189	180	97	*Pseudomonas* spp.	(Aryal et al., 2022)
PUF cubes	450	138	210	99	*Acidithiobacillus* spp., temperature 24°C; N/S ratios of 1.2–1.7 mol	(Das et al., 2022)
PUF	5–35	>365	1.6–2.3	>97 %	*Pseudomonas* spp., pH 1.5–2, nutrient-rich water was used	(Pudi et al., 2022)
PUF	45–129	N/A	60	100	*Pseudomonas* spp.	(Huan et al., 2020)

PUF is frequently employed in hybrid biofilter configurations, combined with adsorptive or catalytic materials, to compensate for its low sorption capacity while benefiting from its structural advantages. Experimental studies employing PUF as biofilter packing material under various operational conditions, including different SOB strains, pH ranges, temperatures, and EBRT values, are summarized in Table 1.6. These studies report H_2S removal efficiencies exceeding 90–99%, highlighting the importance of PUF as a mechanically and hydraulically stable support medium.

Comparative analysis of biofilter packing materials indicates that hybrid configurations, combining inorganic (CLC waste), carbon-based (biochar), and PUF, effectively mitigate the limitations of single-material systems. Such hybrid biofilters enhance H_2S removal efficiency, operational stability, resistance to clogging, and long-term performance, making them particularly suitable for scalable and industrial biogas purification applications.

1.3. Impact of biofilter material properties on H_2S removal

Recent studies consistently demonstrate that hybrid and chemically modified packing materials enhance adsorption, microbial stability, and long-term biofilter performance (Zhang et al., 2024; Bora et al., 2024). These interactions determine hydrogen sulfide mass transfer, adsorption kinetics, and SOB activity under variable operational conditions.

Bulk density plays a critical role in controlling gas distribution, pressure drop, and long-term hydraulic performance of biofilters. Low-density materials, such as biochar, enhance the void fraction and gas permeability, thereby improving gas–solid mass transfer; however, excessive reduction in bulk density may lead to bed compaction and mechanical instability during prolonged operation (Li et al., 2020).

Specific surface area remains one of the most influential parameters for H_2S adsorption and microbial attachment. Recent comparative studies demonstrate that activated and chemically modified biochars with surface areas exceeding 300 $m^2 \cdot g^{-1}$ consistently achieve higher elimination capacity (EC) values than conventional organic media (Zhang et al., 2020a; Dada, 2025). Nevertheless, high surface area alone is insufficient if pore accessibility and moisture distribution are not optimized.

Porosity and pore size distribution govern internal diffusion resistance and biofilm development. Microporous structures favor adsorption but are susceptible to pore blockage by elemental sulfur, whereas meso- and macro-porous materials improve operational robustness by facilitating sulfur removal and preventing excessive pressure drop (Bora et al., 2024). This trade-off underscores the need to balance adsorption capacity with long-term operational stability.

Surface chemistry strongly influences the affinity of biofilter materials toward H_2S and their interaction with SOBs. Functional groups, such as hydroxyl (–OH), carboxyl (–COOH), and carbonyl (>C=O), enhance chemical adsorption and promote redox reactions involved in sulfur oxidation (Zhou et al., 2021a). Recent spectroscopic studies confirm that chemically activated biochar exhibits increased density of oxygen-containing functional groups, leading to improved H_2S uptake and biofilm adhesion (Li et al., 2020).

Catalyst incorporation has emerged as a key strategy to enhance biofilter performance. Iron-based additives, including $FeCO_3$ and Fe_2O_3, significantly accelerate H_2S oxidation and reduce reliance on purely biological conversion pathways. Recent laboratory-scale investigations report up to 20–30% improvement in removal efficiency when catalytic and biological processes are coupled within hybrid packing materials (Bora et al., 2024; Zhang et al., 2024).

Electrical conductivity (EC*), expressed in $\mu S \cdot cm^{-1}$, has gained attention as an indirect indicator of ionic strength and nutrient availability for microbial communities. Elevated EC* values observed in modified biochar and mineral-based media correlate with enhanced microbial activity and more stable sulfur oxidation under fluctuating inlet H_2S concentrations (Dada 2025).

Recent literature confirms that chemical modification of packing materials is a practical approach to overcoming the inherent limitations of unmodified media. KOH activation of biochar significantly increases porosity, surface area, and hydrophilicity, thereby improving moisture retention and sustaining microbial activity. Removal efficiencies exceeding 90% have been reported under controlled laboratory conditions, particularly at moderate EBRT values (Zhang et al., 2021; Li et al., 2021).

Similarly, $FeCO_3$-modified CLC waste exhibits synergistic catalytic–biological behavior, enabling rapid initial H_2S oxidation followed by biological stabilization. This dual mechanism enhances tolerance to high inlet loading rates and reduces biofilter start-up time, which is a critical factor for practical implementation (Bora et al., 2024).

Overall, recent studies confirm that optimal biofilter performance is achieved by integrating high surface area, tailored pore structure, favorable surface chemistry, and sufficient electrical conductivity. Hybrid and modified materials outperform single-function media by enhancing adsorption kinetics, microbial resilience, and long-term operational stability. These findings provide a strong scientific basis for selecting and modifying biofilter packing materials investigated in this dissertation.

1.4. Microbial communities in biofilters

Microbial communities play a critical role in the efficiency and stability of biofilters used for hydrogen sulfide removal from biogas. The biological desulfurization process is primarily driven by SOBs, chemolithoautotrophic microorganisms that can use reduced sulfur compounds as electron donors and convert them into less harmful sulfur species, such as elemental sulfur (S^0) or sulfate (SO_4^{2-}) (Vikrant et al., 2018; Binti, 2019; Dada, 2025).

In biofiltration systems, SOBs colonize surfaces of packing materials and form biofilms, providing a stable microenvironment for microbial growth and metabolic activity. The structure, composition, and activity of these microbial communities strongly influence H_2S RE, EC, and the long-term operational stability of biofilters (Haosagul et al., 2020; Jedynak et al., 2024).

1.4.1. Sulfur oxidation pathways in biofilters

Anaerobic phototrophic sulfur oxidation. Under anaerobic and light-dependent conditions, phototrophic SOBs utilize H_2S as an electron donor and CO_2 as both an electron acceptor and carbon source. Green and purple sulfur bacteria can oxidize sulfide extracellularly, forming elemental sulfur or sulfate depending on environmental conditions (Fan et al., 2021; Huang et al., 2022a):

$$2H_2S + CO_2 \rightarrow 2S^0 + CH_2O + H_2O; \quad (1.3)$$

$$2H_2S + 2CO_2 + 2H_2O \rightarrow SO_4^{2-} + 2H^+ + 2CH_2O. \quad (1.4)$$

These pathways are less relevant for engineered biogas biofilters due to light requirements, but they provide a theoretical foundation for understanding sulfur cycling.

Aerobic sulfur oxidation. Aerobic SOBs dominate most practical biofiltration systems because they use molecular oxygen as the terminal electron acceptor. Under aerobic conditions, H_2S oxidation proceeds via either partial oxidation to elemental sulfur or complete oxidation to sulfate (Gonzalez et al., 2020; Dada, 2025):

$$H_2S \rightleftharpoons HS^- + H^+; \quad (1.5)$$

$$H_2S + \tfrac{1}{2}O_2 \rightarrow S^0 + H_2O; \quad (1.6)$$

$$H_2S + 2O_2 \rightarrow SO_4^{2-} + 2H^+. \quad (1.7)$$

The relative dominance of reactions (1.6) and (1.7) depends on oxygen availability, pH, and microbial community composition. Partial oxidation is often preferred in biofilters to limit acidification and sulfate accumulation.

Anoxic (nitrate-dependent) sulfur oxidation. In oxygen-limited systems, nitrate can act as an alternative electron acceptor. Nitrate-reducing sulfur-oxidizing bacteria (NR-SOBs) oxidize H_2S via sequential pathways, with the final product controlled by the nitrate-to-sulfide (N/S) molar ratio (Juntranapaporn et al., 2019; Watsuntorn et al., 2020):

$$5H_2S + 2NO_3^- \rightarrow 5S^0 + N_2 + 4H_2O + 2OH^-; \quad (1.8)$$

$$5H_2S + 8NO_3^- \rightarrow 5SO_4^{2-} + 4N_2 + 4H_2O + 2H^+; \quad (1.9)$$

$$H_2S + CO_2 + NO_3^- \rightarrow \text{Biomass} + SO_4^{2-} + N + H_2O. \quad (1.10)$$

Anoxic biofilters offer advantages, such as improved safety (no CH_4/O_2 explosive mixtures) and stable operation under high H_2S loads, although they require external nitrate addition, increasing operational costs (Clotas et al., 2020; Severi et al., 2025).

1.4.2. Key sulfur-oxidizing microorganisms

Among SOBs, *Thiobacillus* spp. are the most extensively studied in biofilter applications. These obligate or facultative chemolithoautotrophs oxidize H_2S and sulfur intermediates using oxygen or nitrate as electron acceptors. Under oxygen-limited conditions, *Thiobacillus* spp. Primarily from elemental sulfur:

$$2H_2S + O_2 \rightarrow 2S^0 + 2H_2O. \quad (1.11)$$

Under oxygen-rich conditions, elemental sulfur is further oxidized to sulfate:

$$S^0 + 2H_2O + O_2 \rightarrow SO_4^{2-} + 4H^+. \quad (1.12)$$

In addition to *Thiobacillus* spp., *Acidithiobacillus* spp. are commonly observed in acidic biofilters, while *Pseudomonas* spp. contribute to biofilm formation and EPS production, enhancing microbial attachment and process stability (Wang, 2020a; Vaiskunaite, 2022).

1.4.3. Factors influencing microbial colonization and biofilm formation

The long-term efficiency of biofilters depends on stable biofilm development. Key influencing factors include:

- pH: Optimal SOB activity typically occurs between pH 6.5 and 8.0; excessive sulfate formation can reduce pH and inhibit microbial metabolism.
- Temperature: Most SOBs are mesophilic, with optimal growth at 25–35 °C.
- Moisture content: Adequate water availability ensures nutrient transport and enzymatic activity.
- Packing material properties: High surface area, porosity, and suitable surface chemistry (e.g., KOH-modified biochar, $FeCO_3$-impregnated CLC waste) enhance microbial attachment and stability.

Mixed microbial cultures derived from wastewater sludge are frequently used due to their resilience and lower cost compared to pure cultures, despite the need for more extended acclimation periods (Watsuntorn et al., 2020; Jedynak et al., 2024).

1.4.4. Fluorescence microscopy for biofilm visualization

Fluorescence microscopy is widely applied to investigate microbial colonization and biofilm structure on biofilter packing materials. DAPI staining enables visualization of total microbial biomass by binding to DNA, while protein-specific

stains, such as SYPRO Red, highlight EPS distribution within the biofilm matrix (Zhang et al., 2020b; Zhou et al., 2021a).

It can be used to assess microbial development on biochar and CLC waste. Results showed dense, EPS-rich biofilms formed by *Pseudomonas* spp., while *Acidithiobacillus* spp. formed thinner but metabolically active biofilms. These complementary microbial roles support stable and efficient H_2S removal and validate the integration of microscopy with chemical and performance analyses. (Zhang et al., 2020b; Zhou et al., 2021a).

1.5. Environmental and operational factors affecting biological H_2S removal in biofilters

The performance and operational stability of biofilters for hydrogen sulfide removal under laboratory conditions depend on a range of environmental and operational factors that directly affect microbial activity, mass transfer, and physicochemical processes within the packing bed. Key parameters include pH, sulfur accumulation (clogging), EBRT, temperature, and moisture content. Each factor interacts with the properties of specific packing materials (organic, inorganic, or synthetic) and must be controlled to maintain high H_2S RE and process stability (Mohammadi et al., 2025; Jedynak et al., 2023).

Environmental and operational factors, such as pH, sulfur accumulation, EBRT, temperature, and moisture content, are interconnected parameters that collectively determine the efficiency and resilience of biological H_2S removal in biofilters. Careful optimization and real-time control of these factors, particularly when applying modified waste-derived packing materials, can significantly enhance RE and process stability.

1.5.1. pH

pH significantly influences the biological removal of H_2S by affecting microbial metabolism, H_2S solubility, and biofilm development. The oxidation of H_2S to sulfate releases hydrogen ions, leading to acidification of the packing bed if not buffered (Nhut et al., 2020). Without sufficient buffering, pH can decline sharply, inhibiting sulfur-oxidizing bacteria (SOB) and reducing RE – a trend observed experimentally in various biofilter systems.

Most SOBs exhibit optimal activity between pH 6.5 and 8.0; deviations outside this range can lead to enzyme inactivation and reduced microbial performance (Jedynak et al., 2024). Buffering materials, such as calcium carbonate ($CaCO_3$), NaOH, and phosphate salts, are commonly added to maintain a near-

neutral pH. In some systems, specialized operating conditions with potent buffering agents allow operation at lower pH values without loss of function, but this is material- and culture-specific.

1.5.2. Sulfur accumulation (clogging)

Elemental sulfur and sulfate can accumulate within the biofilter packing bed under high ILRs, leading to pore blockage, increased pressure drop, and reduced H_2S mass transfer, ultimately lowering RE (Farghali et al., 2022; Jiang et al., 2020).

Clogging propensity is influenced by airflow velocity, particle size, packing media shape, and moisture content. Optimizing these parameters and implementing periodic backwashing or media replacement helps mitigate clogging. Materials with high porosity, such as biochar or modified CLC waste, may delay clogging but require validation under continuous operation for long-term application.

1.5.3. EBRT (Empty Bed Retention Time)

EBRT defines the theoretical time that a gas stream remains within the biofilter bed in the absence of packing material. It is calculated as:

$$ERBT = V/Q, \tag{1.13}$$

where V is the empty bed volume (m^3), and Q is the gas volumetric flow rate ($m^3 \cdot s^{-1}$). Longer *EBRTs* typically enhance H_2S contact with microbial biofilms, improving RE, but can reduce throughput and operational efficiency. Optimal *EBRT* values reported for H_2S removal under typical conditions range from 30 to 120 seconds, depending on inlet concentrations and packing media properties (Mohammadi et al., 2025; Morgado et al., 2018).

1.5.4. Temperature

Temperature directly affects microbial metabolism, enzymatic activity, and biofilm stability. Most SOB consortia in biodesulfurization operate optimally at mesophilic temperatures (25–35 °C), with diminished performance below ~20 °C and potential biofilm disruption above ~40 °C (Arıman, 2022; Mohammadi et al., 2025).

Maintaining stable temperatures within this range supports consistent H_2S removal and reduces the risk of temperature-induced stress on microbial communities. Thermotolerant strains or insulated biofilter designs may be required under variable environmental conditions.

1.5.5. Water retention (humidity)

Moisture is a critical physical factor for microbial survival, nutrient transport, and H_2S dissolution in biofilters. Adequate moisture enhances biofilm viability and facilitates both biological oxidation and physicochemical sorption processes. Packing materials that retain moisture (e.g., CLC waste, modified biochar) create favorable microenvironments for SOBs and improve RE (Fang, 2022; Zarei et al., 2025).

However, excessive moisture can cause compaction, anaerobic zones, and increased pressure drop, negatively affecting gas flow and microbial performance. Moisture control strategies include inlet gas humidification and periodic irrigation of the packing bed.

1.6. Numerical validation of experimental results

1.6.1. Mathematical modeling by MATLAB

MATLAB is a high-level numerical computing environment commonly employed in environmental engineering research for rigorous mathematical modeling of coupled biological, transport, and kinetic phenomena. Its matrix-oriented structure and built-in solvers for ordinary and partial differential equations facilitate simulation of complex systems such as biofilters, where nonlinear kinetics, transient dynamics, and parameter sensitivity must be quantified (Zhang et al., 2022; Li et al., 2020).

In studies of biogas desulfurization, MATLAB modeling has been used to describe microbial growth kinetics, substrate utilization, and pollutant degradation mechanisms, often in conjunction with classical kinetic frameworks, such as Monod, Haldane, and modified Michaelis–Menten models, to represent SOB behavior under varying environmental conditions (Gao et al., 2021). These models provide insight into how parameters such as substrate concentration, inhibition, and diffusion limitations influence H_2S removal efficiency and can be integrated with optimization algorithms to estimate kinetic constants from experimental data.

Recent advances address limitations of classical formulations by combining MATLAB with machine learning and advanced regression techniques, such as Support Vector Machines (SVMs) and Genetic Algorithms (GAs), to accurately predict H_2S removal under varied operational conditions (e.g., moisture content, EBRT, and inlet concentration) without requiring extensive mechanistic assumptions. Such hybrid approaches have demonstrated high predictive accuracy ($R^2 > 0.97$), highlighting their applicability for rapid screening of operational scenarios and parameter optimization in biofilter design (Clotas et al., 2020).

Table 1.7. Conceptual framework of MATLAB-based modeling of sulfur-oxidizing bacterial growth on biofilter packing materials

Modeling component	**Considerable items**
Modeled process	Growth of SOBs attached to packing materials
Biological focus	Biomass growth and activity of *Acidithiobacillus* spp. and *Pseudomonas* spp. within biofilms
Packing materials considered	Biochar, CLC waste, and PUF
Independent variables	Inlet H_2S concentration and EBRT
Dependent variables	Bacterial growth rate, H_2S RE
Kinetic framework	Monod-type and modified Michaelis–Menten kinetics describing microbial growth
Mathematical formulation	Ordinary differential equations describing biomass growth and H_2S RE over time
Role in the dissertation	Interpretation of microbial activity on different packing materials and estimation of kinetic parameters governing biological H_2S removal

MATLAB's graphical capabilities further support visualization of growth curves, velocity profiles, and sensitivity analyses, enabling effective comparison of modeled predictions and experimental results using statistical indicators and correlation coefficients. By enabling systematic interpretation of experimental data and characterization of model uncertainty, MATLAB modeling strengthens the mechanistic understanding of biofiltration processes and supports scalable design and control strategies (Zarei et al., 2025).

1.6.2. Simulation by COMSOL

COMSOL Multiphysics is a finite-element simulation platform that enables the comprehensive numerical modeling of multiphysics systems, including coupled mass transport, fluid flow, and biochemical reaction processes. In environmental biotechnology, COMSOL is frequently used to simulate biofilters and packed-bed reactors, where concentration gradients and biofilm development significantly affect process performance (Alonso et al. 2022).

Recent studies have applied COMSOL to simulate H_2S removal in biofilters packed with various materials, combining experimental and numerical results to evaluate the performance under different operational conditions. For example, laboratory-scale biofilters packed with biochar, CLC waste, or PUF have been modeled using COMSOL to predict spatial concentration profiles, RE, and EC across the reactor. Model predictions have shown material-dependent performance trends, with biochar achieving high RE (> 92%) and EC values. At the same time,

CLC and PUF exhibited moderate performance, illustrating the influence of residence time and microbial activity on H_2S removal (Mohammadi et al., 2025; Abbasabadi et al., 2020).

COMSOL's multiphysics environment facilitates coupling reaction kinetics with convection–diffusion transport and flow fields, enabling detailed spatial resolution of species profiles and sensitivity analysis of design parameters such as bed geometry, flow regime, and diffusion coefficients. However, numerical simulation accuracy depends on the reliable specification of kinetic and transport parameters, making validation against experimental data essential (Alonso et al., 2022).

Table 1.8. Conceptual framework of COMSOL-based simulation for layer-wise analysis of biofilter performance

Simulation aspect	**Considerable items**
Modeled system	Multi-layer biofilter packed with biochar, CLC waste, and PUF
Spatial domain	Axial sections representing different biofilter layers
Transport processes	Transport of biogas and hydrogen sulfide
Key monitored parameters	H_2S concentration, air pressure, biogas velocity, biogas distribution
Reaction mechanism	Biological oxidation of H_2S within the biofilm
Numerical outputs	Layer-wise H_2S concentrations, pressure drop, velocity distribution
Model validation approach	Comparison of simulated outlet concentration trends with experimental measurements
Role in the dissertation	Identification of limiting biofilter layers, assessment of material performance, and support for biofilter design and scale-up

In this dissertation, COMSOL modeling is implemented to simulate hydrogen sulfide transport and biological oxidation in biofilters packed with modified biochar, CLC waste, and PUF. By comparing simulation outcomes with experimental measurements, the numerical framework supports the identification of dominant limiting mechanisms, guides the selection of packing media, and informs design and scaling strategies for efficient biofiltration systems.

1.7. Conclusions of the First Chapter and formulation of the dissertation tasks

1. Hydrogen sulfide removal is a critical prerequisite for biogas utilization, as H_2S significantly limits its energetic, environmental, and technical applicability. Biofiltration provides a sustainable alternative to conventional physical and chemical methods, offering lower operational costs and reduced environmental impact when appropriately designed and controlled.
2. Packing material properties determine biofilter performance, as their high surface area, adequate porosity, moisture retention, and surface reactivity are decisive factors for H_2S removal efficiency. KOH-modified biochar and $FeCO_3$-impregnated CLC waste exhibit enhanced adsorption capacity and catalytic activity, thereby improving removal efficiency and elimination capacity.
3. Microbial material interactions make biological desulfurization, such as SOBs (*Acidithiobacillus* spp., and *Pseudomonas* spp.), essential for sustained H_2S oxidation. Their colonization intensity and biofilm stability strongly depend on the physicochemical properties of the packing materials, particularly surface chemistry and porosity.
4. Hybrid biofilter configurations outperform single-material systems. Therefore, combining inorganic, carbon-based, and polymeric materials enables synergistic coupling of adsorption, catalytic oxidation, and microbial activity, improving biofilter stability and resistance to clogging during long-term operation.
5. Operational conditions critically influence biofilter stability, as pH, EBRT, temperature, moisture content, and sulfur accumulation directly affect H_2S removal efficiency and biofilter longevity. Maintaining a near-neutral pH of approximately 6.5–7.5, EBRT in the range of 30–120 s, operating temperature of 20–35 °C, moisture content of the packing material at about 40–70%, and controlled sulfur washout to prevent excessive sulfur accumulation is essential for stable performance and sustained H_2S removal efficiency.
6. Existing knowledge gaps in long-term material behavior, microbial dynamics, and process scalability justify the use of combined experimental, microbiological, and computational modeling approaches, which are addressed in the subsequent chapters of this dissertation.

The literature review revealed that, despite significant progress in biofiltration-based H_2S removal, several scientific gaps remain. Insufficient attention has

been paid to the systematic evaluation of modified waste-derived packing materials, their interactions with sulfur-oxidizing microorganisms, the operational stability of hybrid biofilter configurations under laboratory conditions, and the integration of experimental results with mathematical and numerical modeling. Based on these identified research gaps, the following research tasks were formulated:

1. To evaluate the physicochemical properties of modified biofilter packing materials and determine their effect on hydrogen sulfide removal efficiency.
2. To investigate microbial colonization and biofilm formation on different biofilter packing materials and their relationship with biological H_2S removal.
3. To experimentally assess the performance of a laboratory-scale biofilter using single-component and hybrid packing materials.
4. To determine the influence of key operational parameters on biofilter stability and H_2S removal efficiency.
5. To identify statistical relationships between microbiological indicators, packing material properties, and H_2S removal efficiency.
6. To develop and apply a mathematical and numerical model of the biofiltration process for biofilter performance analysis and prediction under varying operating conditions.

2

Methodologies for determining the physicochemical properties and adsorption characteristics of materials and their application in H_2S removal from biogas

This Chapter presents the methodological framework for investigating the performance of biofilters for removing hydrogen sulfide from biogas. Based on a recent review of the scientific literature, three representative packing materials were selected: sewage sludge-derived biochar, CLC waste, and PUF, representing organic, inorganic, and synthetic media, respectively. Both individual materials and their combined configurations were examined to evaluate the influence of material properties and their interactions on H_2S removal efficiency. The applied methodology focuses on assessing key physicochemical characteristics of the packing materials, including specific surface area, porosity, chemical composition, surface reactivity, buffering capacity, and adsorption performance, and is supported by statistical analysis in MATLAB to identify significant structure–performance relationships.

A central aspect of the methodology is the integrated evaluation of material properties, microbial colonization, and biofiltration performance. Microbiological analysis, material surface characterization, and numerical modeling were combined to assess biofilm formation, sulfur-oxidizing bacterial activity, and their contribution to H_2S removal under controlled conditions. Experimental investigations were conducted using harmonized protocols across multiple laboratories, while mathematical modeling (MATLAB) and numerical simulations (COMSOL Multiphysics) were used to reproduce biofiltration processes and analyze reaction-zone development within the biofilter. The integration of experimental, microbiological, and computational approaches provides a robust methodological basis for interpreting biofilter performance and supports further optimization and scalability assessment of biogas desulfurization technologies. The results obtained in this Chapter have been published in Vaiškūnaitė et al. (2024), Mohammadi et al. (2024), and Mohammadi and Vaiškūnaitė (2024).

2.1. Experimental system setup

The experimental system was designed to evaluate the performance of biofilter systems for hydrogen sulfide removal from biogas under controlled and reproducible laboratory conditions. The setup enabled systematic investigation of the effects of packing material type, operational parameters, and microbial activity on H_2S RE. Particular emphasis was placed on ensuring experimental repeatability, stable operating conditions, and controlled variation of key parameters.

2.1.1. Biofilter construction and materials

The biofilter used in this study was a custom-designed laboratory-scale vertical column intended to simulate key features of practical biogas purification systems. The column was constructed from transparent acrylic (organic glass) with an internal diameter of 14 cm and a total height of 1 m, enabling visual inspection of the distribution of packing material and gas flow behavior.

The column was sealed at both ends and equipped with five equidistant vertical gas sampling ports to enable periodic collection of packing material for microbiological and physicochemical analyses. Gas sampling ports were installed at the inlet, intermediate sections, and outlet to monitor H_2S concentrations along the biofilter height. A perforated distribution plate was installed at the base of the column to ensure uniform gas distribution through the packing bed.

Three packing configurations were investigated:

a) Single-material configurations, where biochar, CLC waste, or PUF was used individually;

b) Hybrid configurations, combining biochar and CLC waste to evaluate potential synergistic effects between adsorption and biological oxidation;
c) Layered configurations, in which materials were arranged in alternating layers to optimize the spatial distribution of adsorption capacity, catalytic activity, and microbial colonization.

Packing materials were sieved to obtain uniform particle-size distributions, promoting consistent gas–solid contact, microbial attachment, and moisture retention. Alternating layers of biochar and CLC waste were used in hybrid configurations to enhance the biofilter's overall functionality.

Synthetic biogas containing 200 ppm H_2S was supplied from a high-pressure gas cylinder and introduced into the biofilter via an air blower. Gas flow was regulated using a calibrated rotameter, ensuring stable and reproducible inlet conditions.

An automated irrigation system was installed to supply a mineral nutrient solution to the packing bed. Moisture levels were monitored using a Time Domain Reflectometry (TDR)-based digital sensor (VH400, ±3% accuracy) placed at mid-depth of the bed. Irrigation was controlled by a solenoid pump connected to a Wi-Fi-enabled controller, maintaining moisture content within the optimal range of 45–60% for microbial H_2S degradation. Remote monitoring and manual override were enabled via a mobile interface.

(a) (b)

Fig. 2.1. Modified vertical biofilter system used for microbial colonization and H_2S purification experiments (a), measuring the chemical composition of injected biogas into the biofilter packed with biochar (b)

The biofilter operated under anaerobic conditions, achieved by controlling gas composition and excluding oxygen during operation. Continuous nutrient supply, stable gas exposure, and controlled moisture conditions created a reproducible environment for microbial colonization, biofilm development, and evaluation of material-microbe interactions (Fig. 2.1).

Although the primary focus of this dissertation is experimental, sustainability considerations were addressed qualitatively using low-cost, waste-derived packing materials (sewage sludge-derived biochar and recycled CLC waste). These aspects informed material selection and system design, but were not quantitatively assessed in this Chapter.

2.1.2. Operational conditions and flow regulations

The total volume of biochar used in the biofilter was approximately 0.0055 m^3, divided into five layers of ~0.0011 m^3 each, containing biochar produced at the same pyrolysis temperature. The biochar bed height was 10 cm. A mineral nutrient solution composed of K_2HPO_4 (0.02 g), $(NH_4)_2SO_4$ (0.08 g), and Na_2CO_3 (0.39 g) per liter of deionized water was continuously recirculated through the packing bed to support microbial activity.

Biogas entered the biofilter at the bottom and exited at the top of the column. Inlet H_2S concentrations were controlled within the range of 20–25 ppm for baseline experiments, while ILR varied between 0.16 and 0.22 m^3. Gas flow rates were adjusted between 0.2 and 1.0 $L \cdot min^{-1}$ to simulate typical operational conditions and evaluate biofilter performance under different residence times.

The temperature inside the biofilter was maintained between 27 and 30 °C and monitored with a Testo 400 multifunctional instrument. Moisture content was maintained within the 40–60% range by humidifying the inlet gas stream and automated irrigation.

The EBRT was calculated using standard relationships between gas velocity, column geometry, and volumetric flow rate, as described by Equations (2.1–2.5):

$$EBRT = \frac{\text{Height of biofilter}}{\text{Velocity of inlet biogas}}; \tag{2.1}$$

$$Q = A \cdot V; \tag{2.2}$$

$$A = \pi \cdot r^2; \tag{2.3}$$

$$V_V = \frac{4}{3} \cdot \pi \cdot r^3, \tag{2.4}$$

$$t = \frac{V_V}{Q}. \tag{2.5}$$

Based on these calculations, inlet gas velocities of 0.04, 0.06, and 0.08 $m \cdot s^{-1}$ were applied, corresponding to volumetric flow rates of 0.000615, 0.000923, and 0.00123 $m^3 \cdot s^{-1}$, respectively.

To ensure data reliability, control experiments were conducted. Negative controls included a biofilter column without packing material and columns filled with inert media (glass beads) to quantify non-biological H_2S removal. Positive controls consisted of columns packed with unmodified biochar to evaluate the effects of chemical modification. All experiments were performed in triplicate, and results were statistically analyzed to determine standard deviations and confidence intervals for H_2S removal efficiency and related performance indicators.

2.2. Concept for the selection of biofilter packing materials

This section presents the methodological and engineering principles applied to select biofilter packing materials before conducting experimental studies. This section aims to substantiate the composition of the selected biofiltration materials, their functional roles, and their mutual integration within the biofilter system. The figures presented in this section are intended to justify the logic of packing material selection and configuration, while a detailed analysis of their physicochemical properties and interpretation of experimental results are provided in subsequent chapters of the dissertation.

The concept of biofilter packing selection was developed based on a critical analysis of trends in the application of biofiltration technologies reported in the scientific literature, as well as on solutions proposed in a patent application prepared jointly with a researcher, R. Vaiškūnaitė, from the Department of Environmental Protection and Water Engineering at VILNIUS TECH. This dissertation examines these solutions from an engineering and technological perspective to justify the design decisions of the experimental biofiltration system and to ensure the integration of the selected materials into a coherent technological unit, a biofilter. The structural scheme of the biofilter and the main system components are presented in Figures 2.1 and 2.2.

The physicochemical properties of biofilter packing materials are widely recognized as key factors determining the efficiency of biofilters in hydrogen sulfide removal. Parameters such as specific surface area, porosity, surface chemistry, mechanical strength, buffering capacity, and compatibility with microbial colonization directly affect adsorption efficiency, biofilm formation, and operational stability of the filter system under laboratory conditions (Li et al., 2021; Kumari et al., 2020). Accordingly, three representative packing materials were selected in

this dissertation: biochar, CLC waste, and PUF, corresponding to organic, inorganic, and synthetic material categories, respectively. The selection of materials was based on a comparative analysis of recent scientific literature, considering adsorption capacity, porosity, surface reactivity, availability, cost-effectiveness, and suitability for biological applications (Li et al., 2021; Kumari et al., 2020)

2.2.1. Functional criteria for the selection of biofilter packing materials

The biofilter packing materials were selected based on functional criteria for effective H_2S removal from biogas, system stability, and the reliability of experimental studies. In designing the biofiltration system, it was intended that the packing materials would simultaneously perform several interrelated functions: to facilitate the initial interaction of H_2S with the solid phase, to ensure microbial attachment and biofilm formation, to maintain a microenvironment favorable for biological oxidation, and to ensure the mechanical and hydrodynamic stability of the biofilter system.

To meet these requirements, both single-component and multi-component biofiltration systems were applied in the study. Single-component systems were used as a basis for evaluating the functional contribution of individual materials, whereas multi-component systems were adopted as an engineering solution to integrate different functions within a single biofiltration system and to investigate their interactions. This approach provides a basis for systematic evaluation of adsorption-, catalysis-, and biologically driven H_2S removal mechanisms in an integrated biofilter system (Li et al., 2021).

2.2.2. Rationale for the selection of organic-origin packing materials

The organic-origin packing component was selected as the primary adsorptive and biological carrier in the biofilter system. Biochar was chosen due to its high specific surface area, tunable surface chemistry, and proven biocompatibility with SOBs, as reported in previous studies on biofiltration and biogas desulfurization (Kumari et al., 2020; Janusevicius et al., 2024). These properties enable biochar to act as an effective interface between the gaseous H_2S phase and the bioactive environment, while simultaneously providing favorable conditions for microbial colonization within the biofilter layer.

In this dissertation, sewage sludge-derived biochar is considered not as a final adsorbent, but as a multifunctional biofilter packing element integrated into an overall technological system. Biochar retains the pore structure of the original biomass and contains oxygen-containing functional groups (–OH, –COOH, >C=O),

which enhance surface reactivity and affinity toward H_2S molecules (Kumari et al., 2020). The surface morphology of biochar particles and their application in the biofilter packing are presented in Figure 2.3.

Fig. 2.2. Biochar particles and filled-out biofilter

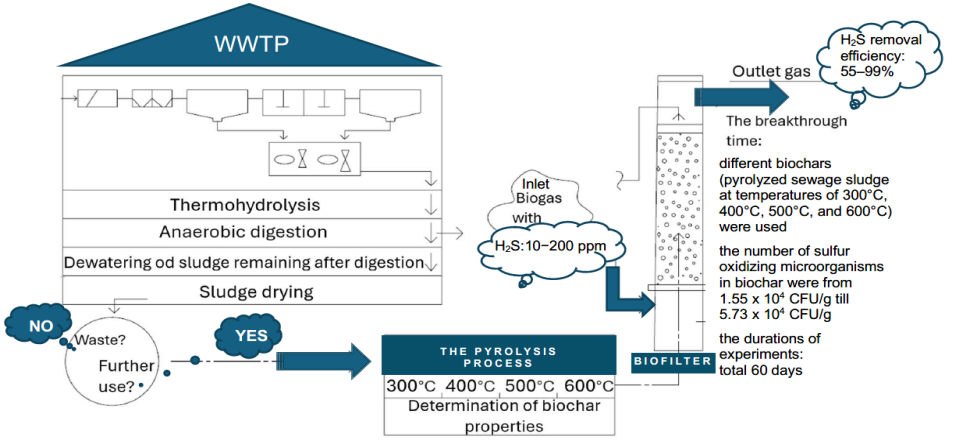

Fig. 2.3. Process of biochar derived from sewage sludge

Sewage sludge-derived biochar was produced via controlled thermochemical conversion (slow pyrolysis) under oxygen-free conditions. This feedstock was selected for its high organic carbon content and suitability for valorization within circular economy frameworks (Li et al., 2021). 25 kg of biochar samples obtained from the Vilnius Sewage Sludge Treatment Plant were pyrolyzed at temperatures of 400 °C, 500 °C, and 600 °C for seven hours in a 300 L reactor under inert

conditions. After controlled cooling, the remaining 7 kg of biochar samples were sieved into two particle-size fractions (1–0.6 mm and < 0.6 mm) to evaluate the influence of particle size and pyrolysis temperature on physicochemical properties and H_2S adsorption behavior. The biochar preparation and fractionation procedure is presented in Figure 2.2, while the overall conversion process of sewage sludge into biochar is schematically illustrated in Figure 2.3.

To increase adsorption capacity and surface reactivity, a portion of the biochar was chemically activated using potassium hydroxide (KOH). Biochar was impregnated with a 1 M KOH solution at a mass ratio of 1:4 (w/w), agitated for 24 h at 25 °C, filtered, dried at 105 °C, and thermally activated at 700 °C for two hours under a nitrogen atmosphere. This modification increased microporosity and surface functional group density, resulting in an approximately 40% increase in specific surface area compared to unmodified biochar (Petrauskaite et al., 2017). In total, eight biochar variants were prepared and equally distributed (1.3 kg per layer) in all layers of the biofilter for the investigation. In this dissertation, the term modified biochar refers to KOH-treated sewage sludge-derived biochar activated at temperatures below 700 °C, thereby distinguishing it from commercial activated carbons and preserving mineral components relevant to biological applications.

2.2.3. Rationale for the selection of inorganic-origin packing materials

The inorganic-origin packing component was incorporated to enhance the structural and chemical stability of the biofilter system and to provide additional buffering capacity during H_2S oxidation. CLC waste was selected as a structurally stable construction industry by-product characterized by low density, moderate porosity, and inherent alkalinity (Li et al., 2021).

CLC waste was primarily selected for its ability to neutralize acidification caused by sulfuric acid formation during biological H_2S oxidation. In addition, CLC exhibits potential catalytic activity, particularly after iron-based modification (Juntarachat et al., 2022). To enhance surface reactivity, 3 kg of CLC waste was impregnated with iron carbonate ($FeCO_3$) by soaking in a 2 M solution, then dried and thermally treated at 200 °C. This treatment generated iron-containing catalytic sites that promote chemical oxidation of H_2S to elemental sulfur and sulfate. The surface structure of CLC particles is presented in Figure 2.4. It shows the appearance and placement of $FeCO_3$-impregnated CLC waste within the biofilter, with each layer comprising 600 g of CLC waste.

Fig. 2.4. $FeCO_3$-impregnated CLC waste particles and the filled biofilter

2.2.4. Rationale for the selection of synthetic-origin packing materials

The synthetic-origin packing component was selected to ensure the structural and hydrodynamic performance of the biofilter system. PUF is an open-cell synthetic material characterized by low density, high porosity, and excellent mechanical stability, and it is widely applied as an inert carrier in biofilter systems (Kumari et al., 2020).

The macro-porous structure of PUF ensures uniform gas distribution, low pressure drop, and a large surface area for microbial attachment. Although PUF exhibits negligible intrinsic H_2S adsorption capacity, its resistance to physical and biological degradation enables its use in long-term biofiltration processes (Kumari et al., 2020). In this study, PUF cubes with a volume of 1 cm^3 were used as packed-bed elements and, when combined with biochar or CLC waste, contributed to improved bed stability and biofilm retention. Potential oxidative degradation of PUF under extreme conditions was considered negligible under the operational conditions applied in this dissertation and therefore does not affect biofilter performance.

2.2.5. Concept of a combined biofilter packing system

The selected biofilter packing materials were combined into integrated biofiltration systems to reconcile components performing different functions within a single technological scheme. This approach distributes adsorption, catalytic activity, biological process support, microenvironment stabilization, and mechanical

strength functions among individual materials, enabling evaluation of the biofiltration process as an integrated engineering system rather than a collection of individual materials (Konkol et al., 2022).

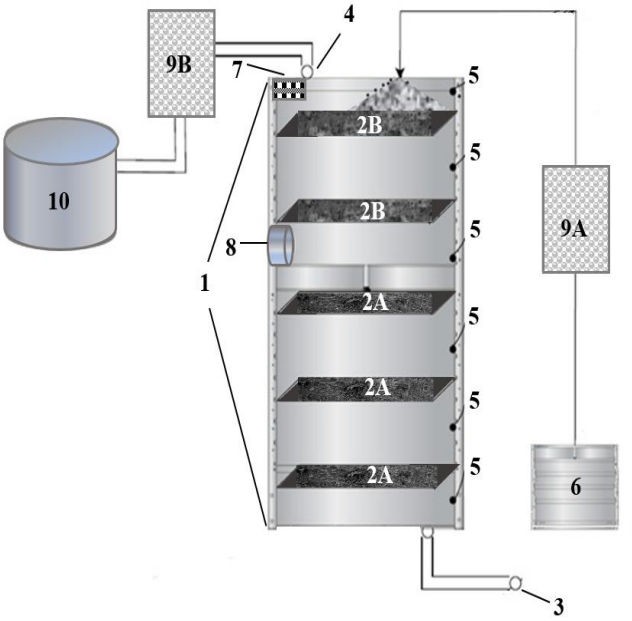

Fig. 2.5. Schematic of the biofilter with the main components and external attachments: 1 – biofilter housing; 2A – modified biochar (pyrolyzed sewage sludge); 2B – $FeCO_3$-modified cellular lightweight concrete (CLC) waste; 3 – gas inlet duct; 4 – gas outlet duct; 5 – gas sampling ports; 6 – nutrient supply system; 7 – moisture sensor; 8 – rotameter; 9A – nutrient solution distribution pump; 9B – treated biogas extraction pump; 10 – treated biogas storage tank

Examples of combined biofilter packing systems are presented in Figure 2.5, which schematically illustrates the packing configurations applied in the study, composed of materials of different origins, including modified and unmodified components and their spatial arrangement within the biofilter layer. Detailed preparation methods of the packing materials, their physicochemical characteristics, and their impact on H_2S removal efficiency are discussed in subsequent chapters of the dissertation.

2.3. Physicochemical characteristics of selected biofilter packing materials

2.3.1. Bulk density

Bulk density (BD) was determined using the procedure commonly applied to porous materials in environmental engineering studies, following the Publicly Owned Treatment Works (POTWs) guidelines. A 100 mL graduated glass cylinder was filled with oven-dried and crushed packing material samples. The samples were dried at 80 °C for eight hours to remove residual moisture. After filling, the cylinder was mechanically shaken for 1 min to ensure particle compaction and eliminate interparticle voids. The analyses were conducted in the Environmental Engineering Laboratory at Vilnius Gediminas Technical University. Where m (kg) is the mass of the dried sample and V (m^3) is the volume of the cylinder, bulk density was calculated using Equation (2.6):

$$BD = \frac{m}{V}. \tag{2.6}$$

2.3.2. pH

The pH of each packing material was determined using an aqueous extraction method. Briefly, 5 g of each sample was mixed with 100 mL of deionized water and allowed to equilibrate for 2–3 min. The suspensions were then agitated on a laboratory shaker (Laboshaker Gerhardt, LaboChema) at approximately 50 rpm for one hour to ensure homogeneous contact between the solid and liquid phases (Nausediene & Vaiskunaite, 2014).

The analyses were conducted in the Environmental Engineering Laboratory at Vilnius Gediminas Technical University. After agitation, the suspensions were filtered using 0.05–0.15 μm filter paper. The pH of the filtrates was measured with a calibrated pH meter with an accuracy of ± 0.001 pH units.

2.3.3. Electrical conductivity

EC* of the packing material extracts was measured after filtration using the same filtrates prepared for pH analysis. Measurements were performed in accordance with established laboratory procedures for porous environmental materials (Lu et al., 2021). The analyses were conducted in the Environmental Engineering Laboratory at Vilnius Gediminas Technical University.

The obtained EC* values were used to evaluate the influence of biochar particle size and pyrolysis temperature on ionic mobility within the packing media,

which is relevant for microbial activity and H_2S removal efficiency in biofilter systems.

2.3.4. Porosity

Porosity and pore structure characteristics were determined using the t-plot method based on nitrogen adsorption–desorption isotherms. The applied methodology follows the Brunauer–Emmett–Teller (BET) theory and t-plot analysis procedures, widely used for the characterization of porous materials, following ISO 9277 and established adsorption analysis guidelines (Zagorskis & Vaiskunaite, 2016). Relative pressure (R) was calculated as:

$$R = \frac{P}{P_0}, \tag{2.7}$$

where P is the equilibrium pressure, and P_0 is the saturation pressure. The average adsorbed layer thickness (T) was estimated using the Halsey equation:

$$T = [\ 13.99 / (0.034 - \log(R))\ ]^{0.5}. \tag{2.8}$$

Total porosity was calculated using Equation (2.9):

$$Porosity = \frac{Pores\ (total\ quantity\ adsorbed)}{Volume\ (size\ of\ sample)} \times 100\%. \tag{2.9}$$

The analyses were performed in the Civil Engineering Laboratory at Tehran University (Iran). Among the tested materials, PUF exhibited the highest total porosity (97%), followed by $FeCO_3$-modified CLC waste (64%) and biochar samples, whose porosity increased with pyrolysis temperature, reaching up to 65% at 600 °C. These results confirm the suitability of the selected materials for gas-phase biofiltration applications.

2.3.5. Specific surface area

Specific surface area was determined using the Brunauer–Emmett–Teller (BET) method based on nitrogen adsorption data. BET measurements were performed following ISO 9277 and IUPAC recommendations for physisorption analysis of porous solids, using nitrogen adsorption at −196.9 °C in liquid nitrogen (Paulionyte & Vaiskunaite, 2023).

The specific surface area was calculated from adsorption data using Equation (2.11), based on the relationship between relative pressure and the amount of adsorbed gas. The experiments were conducted in the Civil Engineering Laboratory at Tehran University.

Biochar samples exhibited increasing BET surface area with increasing pyrolysis temperature, indicating progressive pore development. The highest BET surface area was observed for biochar pyrolyzed at 600 °C (24.67 $m^2 \cdot g^{-1}$), confirming the positive effect of thermal treatment on surface structure.

2.3.6. Chemical composition

Nitrogen content in biochar samples was determined using the Kjeldahl method, following procedures aligned with the Clean Air Act (CAA). Samples were digested with sulfuric acid, converting nitrogen into ammonium sulfate, which was subsequently quantified via acid–base titration (Mohammadi & Vaiskunaite, 2023). The experiments were conducted in the Chemical Laboratory at Ferdowsi University (Iran).

Organic carbon content was determined using the Walkley–Black wet oxidation method. Oxidizable organic carbon was reacted with potassium dichromate in concentrated sulfuric acid, and the remaining chromate was quantified spectrophotometrically at 600 nm (Paulionyte et al., 2022).

Elemental composition of the packing materials was analyzed using X-Ray Fluorescence (XRF). The technique allowed quantification of significant elements, including Si, Ca, Al, Fe, K, P, Mg, and S-containing compounds. XRF measurements were performed using calibrated reference materials, and the analyses were conducted in the Chemical Laboratory at Ferdowsi University (Iran).

2.4. Inoculation and cultivation of microorganisms

The primary objective of the microbiological experiments was to investigate microbial colonization and biofilm formation on biochar and CLC waste used as packing materials in a biofilter for biogas desulfurization. Particular attention was given to the spatial distribution, density, and maturity of biofilms formed under different operational and inoculation conditions (Drozdz et al., 2020; Fleck et al., 2020). Fluorescence microscopy was applied selectively to representative biochar and CLC waste samples to qualitatively assess microbial attachment and biofilm development, rather than to all collected samples.

Biochar and CLC waste samples were collected from five vertical layers of an operating biofilter after exposure to H_2S-containing biogas. The gas sampling ports and material preparation are schematically illustrated in Figure 2.6. In parallel, controlled laboratory inoculation experiments were conducted to isolate the effects of nutrient availability and microbial composition on biofilm development.

Pure cultures of *Acidithiobacillus* spp. (DSM 12475, DSM 739) and *Pseudomonas* spp. were selected due to their documented roles in sulfur oxidation, biofilm formation, and resilience under biofiltration conditions. Both cultures were cultivated under sterile conditions using nutrient media optimized for SOBs. Culture preparation included autoclaving, sterile filtration, and pH and temperature control, following previously established protocols (Li et al., 2021; Cortes et al., 2021). Inoculation was performed at an initial concentration of approximately 10^7 colony-forming units ($CFU \cdot g^{-1}$) of packing material.

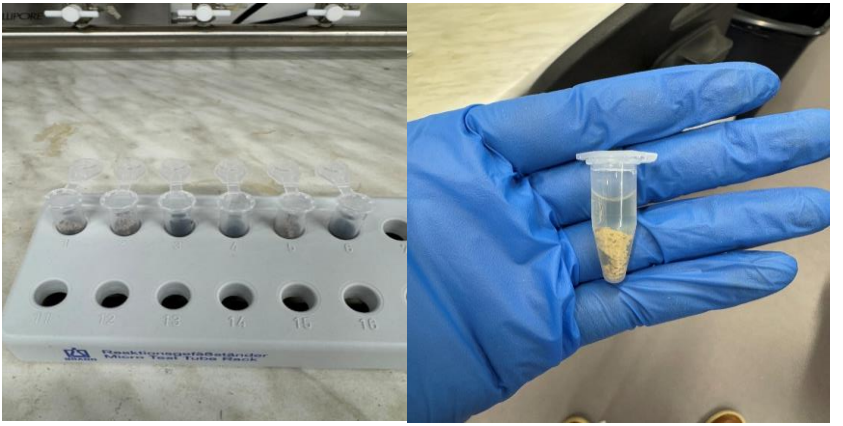

Fig. 2.6. Samples collected from five layers of the biofilter immersed in the microbial-containing solution

Anaerobic or oxygen-limited conditions were maintained by placing the inoculated columns in airtight housings with continuous nitrogen flushing and oxygen monitoring to prevent oxidative inhibition of sulfur-metabolizing pathways.

Five representative samples were collected from different vertical sections of the biofilter after biogas treatment, as shown in Figure 2.13. In addition, laboratory-scale incubation experiments were conducted using four replicate samples (15 g each) of biochar and CLC waste. Fluorescence microscopy analyses were performed only on selected representative samples following incubation, while the remaining samples were used for comparative microbiological and cultivation analyses. The materials were immersed in 150 mL of nutrient solution and incubated at 30 °C with shaking at 140 rpm for 24 h to promote initial microbial attachment (Li et al., 2021; Choudhury & Lansing, 2021). The experimental conditions included:

1. untreated packing material (no inoculation);
2. packing material supplemented with nutrient solution only;

3. packing material supplemented with nutrient solution and inoculated with *Pseudomonas* spp.

Fig. 2.7. Samples collected from five layers of the biofilter immersed in the microbial-containing solution

After incubation, microbial suspensions were collected by filtration through 0.2 μm membranes. The prepared samples and their immersion in microbial suspensions are presented in Figure 2.7.

Microscopic analysis of microbial colonization was performed using fluorescence microscopy. Observations were performed using an epifluorescence microscope (Axio Observer 5, Zeiss) equipped with Zen 3.2 software. The microscope and representative stained samples are shown in Figure 2.13. Samples were examined at 10 ×, 40 ×, and 100 × magnifications, with oil immersion used for high-resolution imaging. Fluorescence microscopy was applied to membrane-filtered microbial suspensions and to selected solid packing material samples (biochar and CLC waste), including representative samples collected from five biofilter layers after exposure to H_2S, to evaluate microbial colonization and biofilm formation.

The analyzed materials included membrane-filtered microbial suspensions, inoculated solid packing materials (biochar and CLC waste), and samples collected from five biofilter layers after exposure to H_2S. Microbial abundance was estimated by counting DAPI-stained DNA-rich regions on membrane filters. Comparative analysis of microbial counts enabled evaluation of nutrient effects

and the influence of *Pseudomonas* spp. inoculation, and biofilm development under biofilter operating conditions (Drozdz et al., 2020; Fletcher et al., 2019; Li et al., 2021).

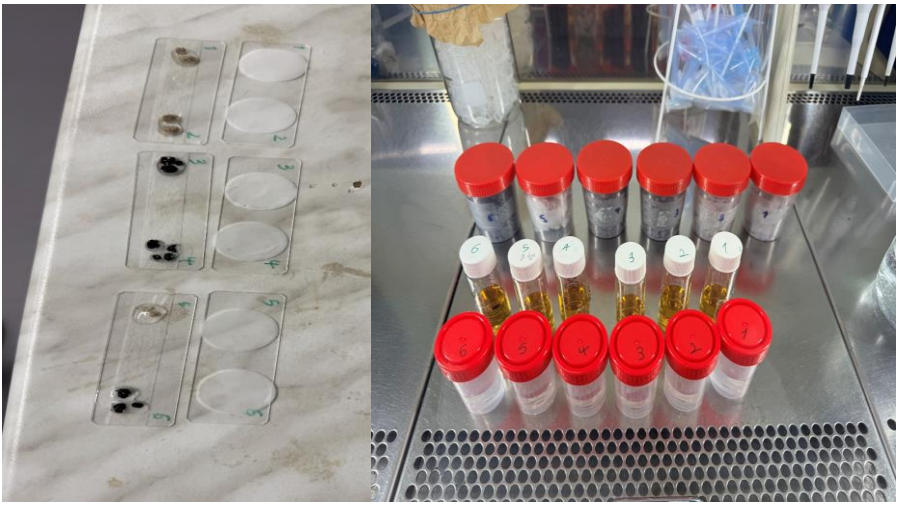

(a) (b)

Fig. 2.8. Stained samples of the biofilter's five layers (a), inoculated by different microorganisms (b)

Microbial colonization on the surfaces of biochar and CLC waste particles was visualized using a DAPI (4′,6-diamidino-2-phenylindole) staining protocol in combination with fluorescence microscopy, optimized for the analysis of surface-bound biofilms (Kumari et al., 2020). DAPI staining and fluorescence imaging were conducted on representative samples selected from each experimental condition to enable comparative qualitative assessment of microbial attachment. Representative stained samples collected from the five biofilter layers before microscopic analysis are shown in Figure 2.8.

Fluorescence imaging was performed using a fluorescence microscope equipped with appropriate filter sets (excitation 340–380 nm, emission ≥ 425 nm). The Zen 3.2 software interface was used for image acquisition, processing, and visualization (Fig. 2.9).

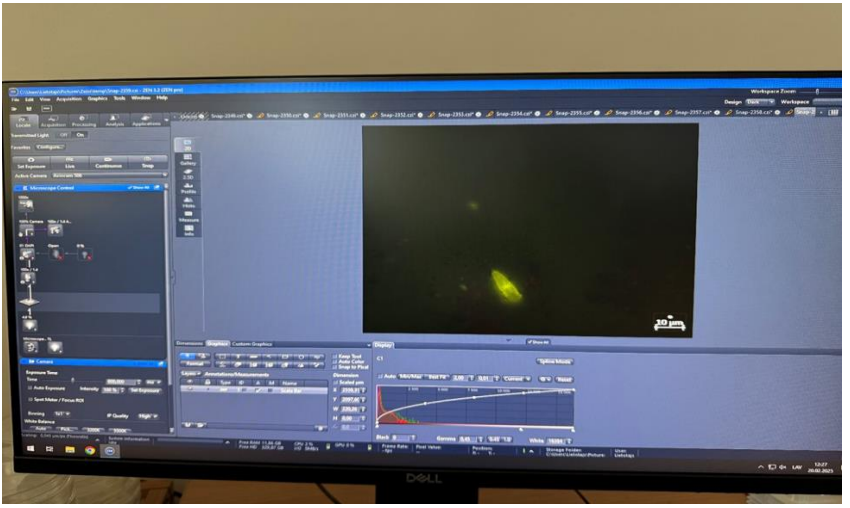

Fig. 2.9. Zen 3.2 software used to visualize the surface of the samples monitored under an epifluorescence microscope

Table 2.1. Sterile solutions used for the preparation of the *Acidithiobacillus* spp. growth medium

Component	**Volume, mL**	**Sterilization Method**	**Atmosphere**
Solution A	962	Autoclaved at 121 °C for 15 min	100% N_2
Solution B	20	Sterile filtration (0.2 µm)	100% N_2
Solution C	20	Autoclaved	80% N_2 / 20% CO_2
Solution D	1	Sterile filtration (0.2 µm)	100% N_2

Fluorescence microscopy enabled a qualitative assessment of microbial colonization density, spatial distribution on porous packing material surfaces, and relative biofilm maturity. In addition, semi-quantitative analysis was conducted by counting fluorescent signals on membrane filters to estimate microbial concentrations under different experimental conditions.

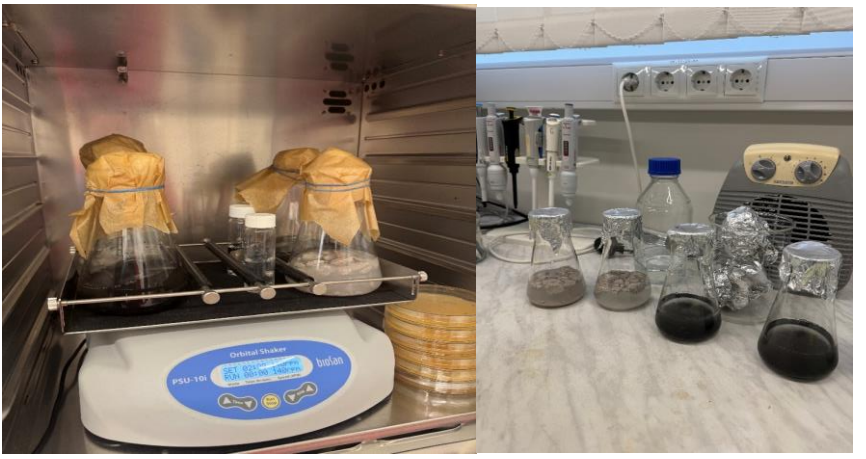

(a) (b)

Fig. 2.10. Packing material samples (a) immersed in prepared microbial solutions (b)

(a) (b)

Fig. 2.11. Packing material samples incubated in sealed anaerobic columns (a) and in an oven (b)

The growth medium for *Acidithiobacillus* spp. was prepared based on a modified *Thiobacillus* medium optimized for autotrophic growth under anaerobic, nitrate-reducing conditions. The composition of the four sterile solutions used to prepare the medium, along with their sterilization conditions, is summarized in Table 2.1.

After sterilization, the solutions were combined sequentially under anaerobic conditions to prevent oxidation of sulfur and iron species (Kurniawan et al., 2020).

The complete medium was then inoculated with *Acidithiobacillus* spp. (DSM 12475; DSM 739) and *Pseudomonas* spp. strains. Packing material samples immersed in the prepared microbial solutions are shown in Figure 2.10.

The inoculated biochar and CLC waste samples were incubated in sealed anaerobic columns at 30 °C for 96 h. The incubation setup and temperature-controlled conditions are illustrated in Figure 2.11. After incubation, the packing materials were retrieved and subjected to DAPI staining, as illustrated in Figure 2.12, to assess microbial attachment and biofilm formation.

Fig. 2.12. Staining solution of prepared *Acidithiobacillus* spp./*Pseudomonas* spp. and packing materials samples

2.5. Hydrogen sulfide removal efficiency (H_2S RE)

H_2S RE is a key performance indicator for evaluating the effectiveness of biofilter systems treating H_2S-containing biogas. This section describes the methodology applied for gas sampling ports, H_2S concentration measurement, and calculation of removal efficiency under different operational conditions. By monitoring H_2S concentrations at multiple vertical positions within the biofilter, the system's spatial performance and overall efficiency were assessed.

Accurate determination of H_2S concentrations is essential for reliable evaluation of biofilter performance. Gas samples were collected from defined sampling ports along the biofilter column, including the inlet, intermediate sections, and outlet. The inlet gas sampling port, located at the bottom of the biofilter, represents

raw biogas entering the system and provides the baseline H_2S concentration. Intermediate gas sampling ports positioned along the column height reflect partial H_2S removal and biological activity within the packing bed. The outlet gas sampling port, located at the top of the biofilter, represents treated biogas after it has passed through the entire filter bed.

The uncertainty of H_2S removal efficiency measurements is mainly related to gas analyzer accuracy and experimental variability. The gas analyzer used in this study has an accuracy of ±(2–5)% of the measured value. All experiments were conducted under steady-state conditions, and measurements were performed in triplicate. The relative standard deviation of replicate measurements was below 10%, confirming acceptable repeatability.

2.5.1. Gas sampling ports and analytical procedure

Gas samples were collected using a stainless-steel sampling probe connected to a gas-tight syringe to minimize leakage and adsorption losses. Gas sampling ports were performed during steady-state biofilter operation at one-hour intervals to reduce temporal variability. Immediately after collection, gas samples were transferred to gas-tight vials to prevent H_2S loss before analysis.

H_2S concentrations were measured using a Gas Data Analyzer (GDA). The instrument was equipped with a capillary column designed explicitly for sulfur compound analysis. Analytical conditions included an injection temperature of 30 °C and a column temperature program from 20 °C (initial) to 23 °C. Calibration curves were established using certified standard H_2S gas mixtures in the range of 300–1600 ppm to ensure accurate quantification. The detection limit for H_2S was 0.1 ppm.

H_2S concentrations were determined by comparing the recorded peak areas of unknown samples with the corresponding calibration curves. In addition to H_2S, the significant components of biogas, including CH_4, CO_2, H_2, O_2, and CO, were routinely analyzed before biofilter operation to characterize the initial gas composition.

2.5.2. Experimental conditions and monitoring

The inlet H_2S concentration supplied to the biofilter ranged from 300 to 1600 ppm, covering the typical concentration range observed in raw biogas. This range enabled evaluation of biofilter performance under both low and high H_2S loading conditions and allowed identification of potential performance limitations at elevated concentrations.

After injection of the biogas mixture into the bottom of the biofilter, gas composition was monitored sequentially at each gas sampling port along the column

height, including the outlet. Measurements at intermediate layers were conducted at regular intervals (every 3 h) during each experimental run to capture dynamic changes in H_2S concentration and removal behavior across the packing layers.

2.5.3. Calculation of H_2S removal efficiency

The removal efficiency of hydrogen sulfide was calculated using Equation (2.10):

$$RE(\%) = \frac{C_{\text{in}} - C_{\text{out}}}{C_{\text{in}}} \times 100, \quad (2.10)$$

where C_{in} is the H_2S concentration at the biofilter inlet (ppm), and C_{out} is the H_2S concentration at the biofilter outlet (ppm).

Calculated *RE* values were used to evaluate biofilter performance and identify correlations with operational parameters, including gas flow rate (low flow rates 0.2–0.5 L.min^{-1}, and high flow rates 0.8-1.0 L.min^{-1}), inlet H_2S concentrations (low H_2S concentrations > 500 ppm, and high H_2S concentrations 1000–1500 ppm), and packing material configuration. Removal efficiencies exceeding 90% were considered indicative of optimal biofilter performance, whereas lower values suggested potential mass transfer limitations, microbial inhibition, or insufficient contact time within the packing bed.

2.6. Data analysis and mathematical modeling

Systematic data analysis and mathematical modeling are essential for interpreting experimental results, identifying trends, and establishing quantitative relationships between microbial activity and hydrogen sulfide removal in biofilter systems. This section describes the analytical framework used for data interpretation and presents a mathematical model describing the growth dynamics of SOBs under biofiltration conditions.

Statistical and numerical analyses were used to evaluate correlations between microbial biomass, operational parameters, and H_2S removal efficiency. Experimentally measured biomass concentrations and operational data were further integrated into a dynamic model to estimate kinetic parameters governing microbial growth and substrate utilization.

For clarity, the modeling framework applied in this dissertation is based on a clear distinction between experimentally measured input parameters and model-derived output results. The main input parameters and corresponding modeling outputs are summarized in Table 2.2.

The input parameters include experimentally determined microbial, physicochemical, and operational variables, while the outputs represent modeled kinetic parameters, spatial concentration profiles, and biofilter performance indicators.

Table 2.2. Initial experimental data used for modeling and modeled outputs in this dissertation

Modeling aspect	Initial data (input)	Modeled results (output)	Modeling tool
Microbial growth kinetics	Initial biomass concentration, inlet H_2S concentration, EBRT	Bacterial growth rate, biomass development over time	MATLAB
Biological H_2S degradation	Inlet and outlet H_2S concentrations, gas flow rate	H_2S degradation rate, RE	MATLAB
Biofilm-related activity	Experimental trends of microbial colonization on packing materials	Time-dependent microbial activity profiles	MATLAB
Gas-phase transport	Inlet biogas velocity, reactor geometry	Axial H_2S concentration profiles	COMSOL
Layer-wise biofilter performance	Measured H_2S concentration at different biofilter layers	Layer-specific H_2S removal contribution	COMSOL
Hydrodynamic behavior	Air pressure measurements, gas flow conditions	Pressure drop and gas velocity distribution	COMSOL
Integrated biofilter performance	Combined experimental and modeled data	Identification of limiting layers and operating conditions	MATLAB COMSOL

2.6.1. Mathematical modeling of sulfur-oxidizing bacterial growth

Mathematical modeling was employed to describe the growth dynamics of sulfur-oxidizing bacteria and the associated protein production on different biofiltration materials. The model was developed and implemented in MATLAB, allowing numerical integration of experimentally measured biomass concentrations with kinetic growth equations to estimate unknown biological parameters (Li et al., 2020). In this model, the primary input parameters include initial biomass concentration, substrate concentration, and experimentally determined kinetic constants, while the main output variables are biomass growth, protein production, and substrate consumption over time

The model structure and governing equations describe the temporal evolution of microbial biomass concentration, protein production, and substrate consumption using a system of ordinary differential equations (ODEs). Biomass growth is expressed by Equation (2.11):

$$\frac{dX}{dt} = \mu X - m_x X, \tag{2.11}$$

where X is the biomass concentration ($g \cdot L^{-1}$), μ is the specific growth rate (h^{-1}), and m_X is the biomass decay coefficient (h^{-1}).

Protein formation associated with microbial metabolism is described by Equation (2.12):

$$\frac{dP}{dt} = \alpha \frac{dX}{dt} + \beta X, \tag{2.12}$$

where P is the protein concentration ($g \cdot L^{-1}$), α is the growth-associated protein coefficient ($g \cdot g^{-1}$), and β is the non-growth-associated protein production rate (h^{-1}).

Substrate consumption is modeled as:

$$\frac{dS}{dt} = -\frac{1}{Yx/s} \times \frac{dX}{dt} - m_S X, \tag{2.13}$$

where S is the substrate concentration ($g \cdot L^{-1}$), $Y_{X/S}$ is the biomass yield coefficient, and m_S represents the substrate decay rate (h^{-1}). Thus, time-dependent biomass concentration $X(t)$, protein concentration $P(t)$, and substrate concentration $S(t)$ constitute the primary outputs of the microbial growth model.

In this dissertation, the substrate S represents the available nutrient source provided by biochar or CLC waste, while the biomass X corresponds to either *Pseudomonas* spp. or *Acidithiobacillus* spp. species.

The specific growth rate μ is defined using a modified Monod-type expression that accounts for substrate limitation, biomass self-inhibition, and protein accumulation effects:

$$\mu = \mu_{max} \left(1 - \frac{X}{X_{max}}\right)^{n_1} \times \left(1 - \frac{P}{P_{max}}\right)^{n_2} \times (S/(Ks + S + S \times S_2 / Ki), \tag{2.14}$$

where μ_{max} is the maximum specific growth rate (h^{-1}), X_{max} and P_{max} are the maximum biomass and maximum protein concentrations ($g \cdot L^{-1}$), K_S is the saturation constant ($g \cdot L^{-1}$), and K_i is the substrate inhibition constant. The empirical exponents n_1 and n_2 represent the effects of biomass and protein inhibition, respectively.

To evaluate the influence of inhibition terms, a simplified growth formulation excluding the S^2/Ki term was also tested and compared with the complete model (Singh et al., 2020).

The model initialization and parameter estimation were based on experimentally measured biomass concentrations obtained during layer 2 of the biofiltration experiments using biochar as the packing material and *Pseudomonas* spp. as the dominant bacterial species. Initial conditions were defined as: $X(0) = 0.0035$ g·L^{-1}, $P(0) = 0$ g·L^{-1}, $S(0) = 3$ g·L^{-1}. Experimental biomass data were used as reference values for model calibration: $X_{experimental} = [0.0035, 0.0052, 0.0116, 0.0164, 0.0136, 0.0104]$ g·L^{-1}.

Several model parameters could not be measured directly and were therefore estimated using numerical optimization by minimizing the objective function defined in Equation (2.15).

$$\min \sum (X_{experimental} - X_{model})^2. \tag{2.15}$$

Parameter bounds were selected based on values reported in the literature for sulfur-oxidizing bacteria and biofiltration systems (Li et al., 2020; Vaziri & Babler, 2019). Fixed parameters, including μ_{max}, K_S, $Y_{X/S}$, m_X, and X_{max}, were obtained experimentally and held constant during calibration.

The model assumptions and numerical solution assume steady operating conditions, homogeneous biomass distribution within the packing material, and substrate availability governed by nutrient release from biochar or CLC waste. Parameter ranges were selected to reflect realistic biofilter operating conditions reported in the literature.

The system of ordinary differential equations was solved numerically in MATLAB using built-in solvers. Simulations were performed using both complete and simplified formulations of the growth rate to assess model sensitivity to inhibition terms. Model predictions were compared with experimental biomass data to evaluate goodness of fit and predictive capability.

This modeling framework enables quantitative interpretation of microbial growth dynamics in biofilter systems and provides a mechanistic basis for linking microbial behavior with experimentally observed H_2S removal performance (Gao et al., 2022).

2.6.2. Graphical representation and kinetic modeling of biofiltration using COMSOL

Numerical simulations and graphical visualization were performed using COMSOL Multiphysics® 6.1 to support the interpretation of experimental results and to extrapolate hydrogen sulfide removal behavior under varying biofilter operating conditions. For clarity, the COMSOL-based biofiltration model clearly distinguishes between input parameters and model outputs. The input parameters include biofilter geometry, bed porosity, specific surface area, inlet H_2S concentration, gas flow rate, and kinetic constants derived from experimental

measurements. The model outputs include spatial and temporal distributions of H_2S concentration, biofilm activity profiles, and predicted hydrogen sulfide removal efficiency. COMSOL was used both as a visualization tool and as a numerical platform to implement a kinetic biofiltration model calibrated against experimental data.

Graphical representations were used to illustrate temporal and spatial trends in H_2S removal efficiency. Removal efficiencies were plotted for different biofilter configurations, including biochar, CLC waste, PUF, and their combinations, under a range of operating conditions. Error bars represent standard deviations calculated from replicate experiments. Temporal profiles of RE were used to identify stabilization phases and assess long-term biofilter performance. In addition, heat maps were generated to visualize the combined effects of gas flow rate and inlet H_2S concentration on biofilter efficiency, providing a compact overview of system performance across the experimental matrix.

Introducing the COMSOL model description and assumptions, the kinetic simulations were based on a biofilm model derived from the classical Ottengraf and van den Oever approach, which is widely applied to steady-state biofiltration systems (Qin et al., 2023). In this framework, a biofilm uniformly coats the surface of packing material particles. At the same time, H_2S-containing biogas flows through the packed bed and diffuses into the biofilm, where it is biologically oxidized to elemental sulfur or sulfate. The model is based on the following assumptions:

1. Gas flow is steady and uniformly distributed across the column cross-section.
2. H_2S concentration in the gas phase is radially uniform at a given bed height.
3. Temperature remains constant throughout the biofilter.
4. H_2S transport into the biofilm is rapid compared to axial transport, allowing uniform concentration at a given height.
5. Microbial biomass concentration within the biofilm is uniform at a given height.

Discussing COMSOL geometry, parameters, and boundary conditions, a two-dimensional axisymmetric geometry was constructed to represent the vertical packed-bed biofilter. The model parameters were selected to match the results of laboratory-scale experiments. They included a biofilter height of 30 cm, an internal diameter of 5 cm, bed porosity of 0.45, and a specific surface area of 300 $m^2 \cdot g^{-1}$ derived from BET analysis.

Inlet H_2S concentrations ranged from 100 to 2000 ppm, and gas flow rates varied between 0.2 and 1.0 $L \cdot min^{-1}$. Biodegradation of H_2S was described using a Monod-type kinetic expression with parameters derived from experimental

measurements: reaction rate constant k = 0.15 h^{-1}, half-saturation constant K_S = 50 ppm, and a maximum elimination capacity of 80 $g \cdot m^{-3} \cdot h^{-1}$.

Boundary conditions consisted of a constant H_2S concentration at the inlet and zero diffusive flux at the outlet. The biofilm layer was modeled with a thickness of 0.05 cm. Internal diffusion resistance was characterized using the Thiele modulus (Φ). The governing equations were solved using a time-dependent solver over a simulation period of several days, with a time step of 0.1 h. Adaptive meshing was applied in regions exhibiting steep concentration gradients to ensure numerical accuracy.

Simulation outputs included spatial distributions of H_2S concentration, biofilm activity profiles, and temporal evolution of H_2S removal efficiency.

The removal of H_2S in the biofilter was modeled as a two-layer process involving gas-phase mass transfer followed by biodegradation within the biofilm. The outlet concentration of H_2S was calculated using Equation (2.16):

$$C_{out} = C_{in} \cdot \exp(-k \cdot EBRT), \quad (2.16)$$

where C_{in} and C_{out} are the inlet and outlet H_2S concentrations, respectively, k is the first-order reaction rate constant, and EBRT is the empty bed residence time.

The effective reaction rate constant was defined based on biofilm properties and transport limitations as:

$$k = \frac{A}{m}\sqrt{\frac{X \cdot \mu \cdot f(x) \cdot D}{K \cdot Y}} \tan(\beta); \quad (2.17)$$

$$\beta = \delta\sqrt{\frac{X \cdot \mu}{K \cdot Y \cdot f(x) \cdot D}}. \quad (2.18)$$

The microbial growth rate followed Monod kinetics:

$$\mu = \mu_{max}\frac{S}{K_S + S}, \quad (2.19)$$

where μ is the specific growth rate, X is biofilm biomass concentration, D is the diffusion coefficient of H_2S in water, δ is biofilm thickness, Y is the yield coefficient, and f(x) accounts for diffusion resistance within the biofilm.

Gas-phase mass transfer was approximated by:

$$N = K_g (C_{in} - C_{out}), \quad (2.20)$$

where N is the H_2S mass transfer rate and Kg is the gas-phase mass transfer coefficient.

The rate of biological H_2S consumption was estimated using:

$$R = \mu_{max} \cdot C_{in} / C_{in} + K, \quad (2.21)$$

where R represents the microbial growth rate associated with sulfur oxidation.

Model predictions were validated by direct comparison with experimentally measured H_2S concentrations and removal efficiencies. Good agreement between simulated and experimental results confirmed the suitability of the kinetic framework and parameter values applied in this dissertation. The validated model was subsequently used to interpret experimental trends and assess the influence of operational parameters on biofilter performance (Georgiadis et al., 2020).

2.7. Conclusions of the Second Chapter

1. This Chapter justified the selection of biochar, CLC waste, and PUF as representative organic, inorganic, and synthetic packing materials for biofiltration. Targeted modification of biochar (pyrolysis at 400–600 °C and KOH activation) and CLC waste ($FeCO_3$ impregnation) significantly enhanced adsorption capacity, buffering behavior, and suitability for microbial colonization.
2. Comprehensive characterization of the packing materials, including bulk density, porosity, specific surface area, water retention capacity, pH, buffering capacity, electrical conductivity, and elemental composition, provided critical insights into their structural properties and operational behavior. These parameters were shown to directly influence mass transfer, moisture stability, and the risk of clogging during H_2S removal.
3. A custom laboratory-scale vertical biofilter was designed and operated under controlled conditions representative of biogas desulfurization processes. Automated moisture control, nutrient dosing, and precise regulation of gas flow enabled reproducible operation across a wide range of inlet H_2S concentrations (300–1600 ppm) and gas flow rates ($0.2–1.0\ L \cdot min^{-1}$).
4. Sulfur-oxidizing bacteria (*Pseudomonas* spp. and *Acidithiobacillus* spp.) were successfully cultivated and inoculated into the biofilter system. Fluorescence microscopy using DAPI and SYPRO staining confirmed effective microbial colonization and biofilm formation on biochar and CLC waste, with spatial variation observed along the biofilter height.
5. A dynamic mathematical model describing biomass growth, protein production, and substrate consumption was developed and solved in MATLAB. A modified Monod-type growth expression incorporating saturation and inhibition effects was calibrated using experimental biomass data, providing quantitative insight into microbial dynamics under biofiltration conditions.

6. COMSOL Multiphysics simulations complemented experimental observations by enabling spatial and temporal analysis of H_2S transport and biodegradation within the biofilter. Good agreement between simulated and experimental results validated the applied kinetic framework and supported the interpretation of biofilter performance.
7. The integrated experimental, microbiological, and modeling approach established a robust framework for evaluating biofilter performance. While the study was limited to laboratory-scale systems and semi-quantitative microbial analysis, the methodology provides a solid basis for pilot-scale validation and advanced microbial characterization in future research.

3

Results of theoretical and experimental studies of biofiltration materials

This Chapter presents the results of theoretical and experimental investigations into innovative biofiltration materials for the removal of hydrogen sulfide from biogas under controlled laboratory conditions. Biofilters packed with sewage sludge–derived biochar, CLC waste, PUF, and their hybrid configurations were evaluated for H_2S removal efficiency, elimination capacity, and microbial activity. The Chapter is based on research results partially published in peer-reviewed scientific articles authored or co-authored by the dissertation author (Mohammadi et al., 2025; Mohammadi & Vaiškūnaitė, 2025).

The investigated packing materials included KOH-activated biochar, $FeCO_3$-impregnated CLC waste, and PUF, primarily used as a structural and biological support medium. Both single-material and hybrid configurations were analyzed to assess synergistic effects arising from complementary physical, chemical, and biological functions. Material characterization, experimental conditions, performance evaluation, statistical analysis, and numerical modeling were conducted in accordance with the methodologies described in the Second Chapter.

3.1. Impact of packing material properties on biofiltration efficiency

The efficiency of biofilters for hydrogen sulfide removal is strongly governed by the physical and chemical properties of the packing materials, which collectively determine gas flow distribution, mass transfer, microbial colonization, and physicochemical interactions with the target pollutant. This section examines the relationships between key material properties – bulk density, porosity, specific surface area, pH, electrical conductivity, and chemical composition – and their influence on biofilter performance. Particular attention is given to sewage sludge-derived biochar, CLC waste, and PUF, as well as their applicability in single-material and hybrid biofiltration systems (Mohammadi et al., 2024a; Mohammadi et al., 2023c).

3.1.1. Bulk density

Bulk density was determined following ASTM D6683-19. The results for all investigated packing materials are summarized in Table 3.1. As shown in Table 3.1, PUF exhibited the lowest bulk density (30 $kg \cdot m^{-3}$), indicating minimal risk of material compaction and favorable gas-flow conditions within the biofilter bed. Such properties are particularly advantageous for long-term biofilter operation, as they reduce channeling and the formation of local anaerobic zones.

Table 3.1. Analyzed the bulk density for each packing material

	Bulk-density, $kg \cdot m^{-3}$	
Packing materials, mm	X > 0.6	1 > X > 0.6
PUF	30	
CLC waste	547	
sewage sludge	73	55
biochar after 400 °C pyrolysis	79	57
biochar after 500 °C pyrolysis	80	58
biochar after 600 °C pyrolysis	80	59

In contrast, CLC waste showed the highest bulk density (547 $kg \cdot m^{-3}$), reflecting its dense mineral structure. While high bulk density may increase the risk of compaction when used alone, it also indicates high mechanical stability and potential chemical reactivity, especially when CLC waste is used as a reactive fraction in hybrid packing systems rather than as the sole packing material.

For biochar samples, bulk density decreased with increasing particle size, likely due to larger interparticle voids formed by coarser particles. Additionally, increasing pyrolysis temperature resulted in a moderate increase in bulk density for both particle size fractions, likely due to structural densification and reduced moisture content at elevated temperatures. These trends are consistent with values reported in the literature (Wojciechowska et al., 2023).

Compared to CLC waste and PUF, biochar exhibited the lowest bulk density, which contributed to a higher void fraction and improved gas permeability. In contrast, the higher bulk density of CLC waste enhanced mechanical stability but resulted in a relatively higher-pressure drop.

3.1.2. Porosity

Porosity was evaluated following ASTM C830-00 using nitrogen adsorption analysis. The relationship between statistical thickness and porosity for sewage sludge and biochar samples pyrolyzed at different temperatures is presented in Table 3.2 and illustrated in Figure 3.1.

Table 3.2. Related analyzed porosity was evaluated based on the statistical thickness of modified sewage sludge, modified biochar pyrolyzed at 400 °C, 500 °C, and 600 °C

Sample type	Pyrolysis temperature, °C	Thickness, nm	Min porosity, $cm^3 \cdot g^{-1}$	Max porosity, $cm^3 \cdot g^{-1}$
Modified sewage sludge	–	0.35–0.48	0.4182	1.6596
Modified biochar	400	0.36–0.48	2.6351	3.7757
Modified biochar	500	0.36–0.48	6.1897	7.3808
Modified biochar	600	0.35–0.48	5.6821	7.6389

As shown in Figure 3.1, porosity increased with increasing thickness for all samples. Biochar pyrolyzed at 500 °C and 600 °C exhibited the highest porosity values, reaching up to 7.38 $cm^3 \cdot g^{-1}$ and 7.64 $cm^3 \cdot g^{-1}$, respectively (Table 3.2), indicating enhanced pore development at elevated pyrolysis temperatures. These results are in good agreement with previously reported data (Shang et al., 2016; Sugurbekova et al., 2023).

Increased porosity is particularly beneficial for biofiltration applications, as it enhances gas–solid contact and provides additional internal surfaces for microbial attachment and biofilm development. Among the investigated materials, modified biochar demonstrated the highest porosity, providing favorable conditions for microbial attachment and gas–solid mass transfer. Although PUF also

exhibited high porosity, its limited surface reactivity reduced its contribution to H_2S adsorption compared to biochar and CLC waste.

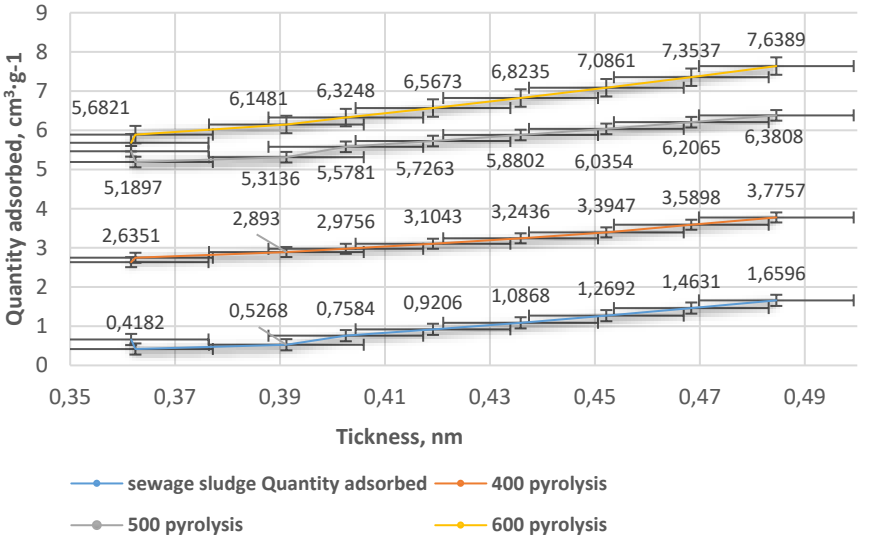

Fig. 3.1. Porosity of sewage sludge, biochar pyrolyzed at 400 °C, 500 °C, and 600 °C samples based on thickness and quantity adsorbed

3.1.3. Specific surface area

The specific surface area of the packing materials was determined using the BET method following ASTM C1069-09. The results are summarized in Table 3.3, and comparative trends are illustrated in Figure 3.2.

Table 3.3. Specific surface area was determined from the relationship between relative pressure and the amount adsorbed for sewage sludge, and biochar pyrolyzed at 400 °C, 500 °C, and 600 °C, and subsequently activated with KOH

Sample Type	Pyrolysis temperature, °C	Relative pressure, p/p° range	Specific surface area range, m²/g
Modified sewage sludge	–	0.07–0.25	43.24
Modified biochar	400	0.05–0.275	235.32
Modified biochar	500	0.09–0.30	433.44
Modified biochar	600	0.065–0.30	471.54

As shown in Figure 3.2, sewage sludge exhibited a relatively low and stable specific surface area across the analyzed range of relative pressure. In contrast, all

KOH-activated biochar samples demonstrated a pronounced increase in surface area with increasing pyrolysis temperature. Biochar pyrolyzed at 500 °C and 600 °C and subsequently activated with KOH exhibited specific surface areas exceeding 433.44 $m^2 \cdot g^{-1}$ (Table 3.3), indicating the formation of a well-developed microporous structure.

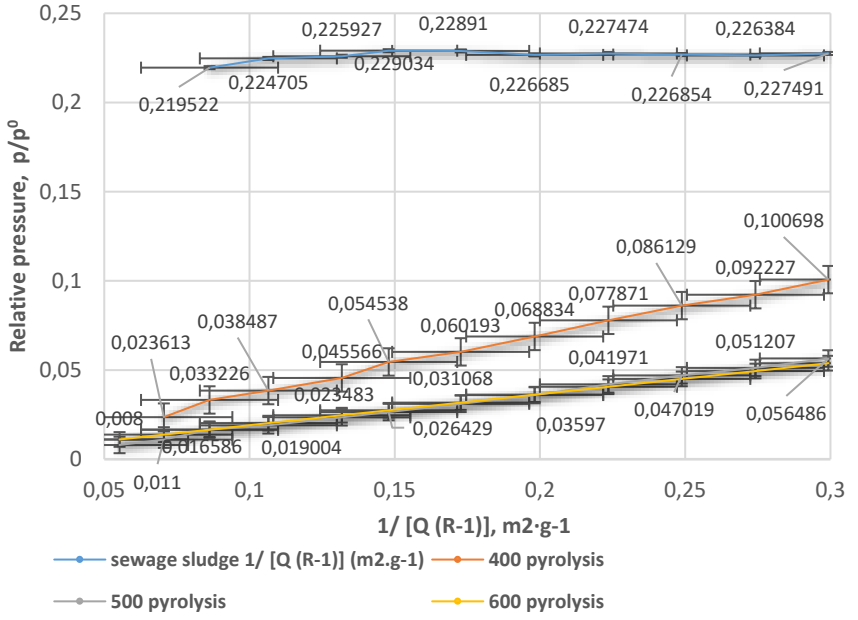

Fig. 3.2. Comparison of the specific surface area of sewage sludge and biochar pyrolyzed at 400 °C, 500 °C, and 600 °C, and subsequently activated with KOH

Such specific surface area values are characteristic of highly effective adsorbents and indicate the suitability of high-temperature biochar for adsorption-driven H_2S removal mechanisms. The specific surface area of KOH-modified biochar was significantly higher than that of CLC waste and PUF, which directly enhanced H_2S adsorption capacity and created favorable conditions for intensive biofilm development.

The increase in specific surface area after KOH activation is associated with redox reactions occurring between KOH and the carbon matrix during chemical activation. At elevated temperatures, KOH initially dehydrates to form K_2O, which subsequently reacts with carbon, producing metallic potassium (K), K_2CO_3, CO, and CO_2. Metallic potassium intercalates into the carbon crystalline structure,

expanding the graphitic layers and inducing structural enlargement. During subsequent washing, potassium compounds are removed, leaving behind a well-developed microporous and mesoporous system. These processes significantly increase the overall porosity and specific surface area. In contrast, the lower specific surface area of PUF limited its contribution to adsorption, indicating its primary function as a structural support material.

These trends are consistent with the findings reported by Styszko et al. (2022) and Shi et al. (2022). In the context of this study, specific surface area is interpreted as one component of a broader set of interrelated material properties rather than as an isolated performance indicator.

3.1.4. pH

The pH of the packing materials was determined following ASTM D1293-18, and the results are presented in Table 3.4. As shown in Table 3.4, biochar samples with larger particle sizes (1–0.6 mm) generally exhibited slightly higher pH values than those with finer particle sizes (< 0.6 mm).

Increasing pyrolysis temperature resulted in a progressive shift toward alkaline pH, particularly for biochar pyrolyzed at 600 °C. Among all tested materials, PUF exhibited the lowest pH, whereas CLC waste showed the highest. The pH compatibility between biochar and CLC waste suggests that their combined use in hybrid biofilters does not impose unfavorable pH gradients within the packing bed.

Table 3.4. Determined results of pH for each packing material

	pH	
Packing materials, mm	**X > 0.6**	**1 > X > 0.6**
PUF	5	
CLC waste	9	
Sewage sludge	7.25	7.13
Biochar after 400 °C pyrolysis	7.32	7.18
Biochar after 500 °C pyrolysis	7.46	7.2
Biochar after 600 °C pyrolysis	8.89	8.46

Alkaline conditions are known to enhance both chemical neutralization of H_2S and the activity of sulfide-oxidizing microorganisms. CLC waste exhibited a more alkaline surface pH than biochar and PUF, promoting chemical interactions with H_2S and buffering the acidic by-products of sulfur oxidation. Biochar provided a more balanced pH environment, which was more favorable for sustained

microbial activity. Similar observations have been reported by Petrauskaite et al. (2017) and Pepper and Brusseau (2019), who highlighted the beneficial role of alkaline biochar in improving H_2S removal efficiency.

3.1.5. Electrical conductivity

EC* was measured according to ASTM D1125-23 at 21 °C, and the results are summarized in Table 3.5. As shown in Table 3.5, biochar samples with smaller particle sizes exhibited higher EC* values than CLC particles, which can be attributed to increased surface area and enhanced ion-exchange capacity.

Increasing the pyrolysis temperature led to a gradual decrease in EC for biochar samples (Table 3.5), likely due to volatilization or transformation of conductive mineral components at elevated temperatures. PUF exhibited higher EC values than pyrolyzed biochar but remained significantly lower than those of raw sewage sludge. These results are consistent with EC values reported in previous studies (Moradi et al., 2020; Mamet et al., 2021).

Table 3.5. Analyzed the electrical conductivity ratio for PUF and biochar samples

Chemical composition	**SiO_2**	**CaO**	**SO_3**	**Al_2O_3**	**P_2O_5**	**Fe_2O_3**	**K_2O**
CLC waste,%	48.50	26.60	18.50	2.70	1.90	1.40	0.30
Chemical substances	**Si**	**Ca**	**S**	**Al**	**P**	**Fe**	**K**
CLC waste,%	39.30	47.30	5.30	2.50	1.80	2.95	0.65

Electrical conductivity is treated strictly as a physical parameter reflecting ionic mobility and particle size effects. The higher electrical conductivity of modified CLC waste compared to biochar and PUF indicates increased ionic mobility and mineral availability, which may enhance microbial metabolism. However, excessive conductivity can also impose stress on microorganisms, highlighting the advantages of combined packing systems. Its interpretation in relation to chemical composition and material reactivity will be presented in the next section.

3.1.6. Chemical composition

The chemical composition of CLC waste and biochar samples was determined using XRF, Kjeldahl, and Walkley–Black analytical methods, providing an integrated assessment of inorganic mineral phases and organic constituents relevant to hydrogen sulfide biofiltration. The obtained results are presented in Tables 3.6 and 3.7.

Table 3.6. X-Ray Fluorescence method analysis results for chemical compositions/ substances exist in CLC waste

	Electrical conductivity, µS/cm	
Packing materials, mm	**X > 0.6**	**1 > X > 0.6**
PUF	283	
CLC waste	N/A	
Sewage sludge	983	702
Biochar after 400 °C pyrolysis	225	191.2
Biochar after 500 °C pyrolysis	193.4	187.1
Biochar after 600 °C pyrolysis	187.4	185.9

XRF analysis showed that CLC waste is primarily composed of SiO_2 and CaO, with additional contributions from Al_2O_3, Fe_2O_3, MgO, and other oxides. This mineralogical composition confers both alkaline buffering capacity and chemical reactivity toward sulfur-containing gases. In particular, the dominance of calcium-based phases enables direct chemical interactions with H_2S, analogous to corrosion and sulfur transformation processes observed in sewer environments.

The reaction pathways presented in Equations (3.1–3.5) describe the potential conversion of H_2S into calcium sulfide and its subsequent stabilization as calcium sulfate:

$$CaO + H_2S \rightarrow CaS + H_2O; \quad (3.1)$$

$$CaO + H_2O \rightarrow Ca(OH)_2; \quad (3.2)$$

$$Ca(OH)_2 + CO_2 \rightarrow CaCO_3 + H_2O; \quad (3.3)$$

$$CaCO_3 + H_2S \rightarrow CaS + H_2O + CO_2; \quad (3.4)$$

$$CaS + 2CO_2 + 2H_2O \rightarrow CaSO_4 + 2H_2O + 2C. \quad (3.5)$$

These reactions provide a mechanistic framework explaining the contribution of CLC waste to H_2S removal beyond physical adsorption. Consequently, CLC waste should be regarded as a chemically active packing material that can participate in sulfur immobilization rather than as an inert structural component. This interpretation is consistent with recent studies demonstrating the role of calcium- and iron-containing construction wastes in gas purification systems (Mohammadi & Vaiškūnaitė, 2025).

Table 3.7. Results of X-Ray Fluorescence, Kjeldahl, and Walkley–Black method analyses for chemical compositions in biochar samples

Type of method	Compositions	Sewage sludge, %	After 400 °C pyrolysis, %	After 500 °C pyrolysis, %	After 600 °C pyrolysis, %
X-Ray fluorescence (XRF)	SiO_2	18.93	25.67	29.82	30.27
	CaO	11.83	17.45	15.47	15.80
	Al_2O_3	3.51	5.23	5.14	5.39
	P_2O_5	9.59	13.43	13.78	14.38
	Fe_2O_3	4.38	6.38	6.67	6.60
	K_2O	1.39	1.78	1.70	1.70
	MgO	2.34	3.39	3.39	3.50
	S	0.96	0.78	0.85	0.81
Kjeldahl method	N	4.20	2.10	2.80	2.10
Walkley–Black method	C	30.83	24.17	19.60	15.41

The presence of Fe_2O_3, although representing a smaller fraction of the total mineral content, further enhances the reactive potential of CLC waste. Iron oxides are known to facilitate redox interactions with H_2S, leading to the formation of iron sulfides and elemental sulfur, which contribute to sulfur stabilization within the filter matrix (Ma et al., 2022; Rodriguez et al., 2023).

Biochar samples exhibited systematic compositional changes with increasing pyrolysis temperature. As shown in Table 3.7, organic carbon and nitrogen contents decreased progressively, while the relative proportions of mineral components such as SiO_2, CaO, Fe_2O_3, and P_2O_5 increased. This reflects the thermal degradation of organic matter and the volatilization of nitrogen-containing compounds during pyrolysis, resulting in a more mineral-enriched, chemically stable carbon matrix.

The decrease in nitrogen content may reduce nutrient availability for microorganisms, potentially limiting early-layer biofilm development. However, enriching mineral phases enhances physicochemical interactions with H_2S by providing reactive sites for adsorption, ion exchange, and surface-mediated reactions. This compositional shift explains why biochars produced at higher pyrolysis temperatures are more suitable for chemical activation and adsorption enhancement. Similar relationships between mineral enrichment, surface reactivity, and sulfur gas removal have been reported in recent biochar studies (Zhang et al., 2024; Gao, 2025).

Electrical conductivity measurements further support this interpretation by reflecting the mobility of ionic species, which is related to the chemical composition. High EC values for raw sewage sludge indicate abundant soluble salts and readily available nutrients, whereas the marked decrease in EC after pyrolysis indicates the removal of volatile and soluble compounds and the formation of a more stable carbon–mineral structure.

The chemical structure and formation mechanism of PUF, illustrated in Figure 3.3, clearly differentiate its role from that of mineral and carbonaceous packing materials. The polymeric network formed by the reaction of isocyanate and polyol components is chemically inert toward H_2S, lacking functional groups capable of direct adsorption or chemical transformation. Consequently, PUF does not contribute significantly to physicochemical H_2S removal. Instead, its highly porous and mechanically resilient structure provides an optimal support for microbial attachment and biofilm development, thereby complementing the chemically active materials described above (De Souza et al., 2021).

The presence of iron- and calcium-containing phases in CLC waste provided catalytic sites for H_2S oxidation, whereas biochar primarily contributed through adsorption and microbial support. PUF, lacking reactive mineral components, played a complementary role by improving bed structure and hydrodynamic stability. In summary, the chemical composition analysis establishes a direct link between the material composition and the functional behavior of H_2S biofiltration systems. The mineral-rich nature of CLC waste and high-temperature biochar underpins their chemical reactivity, while PUF provides biological and structural support.

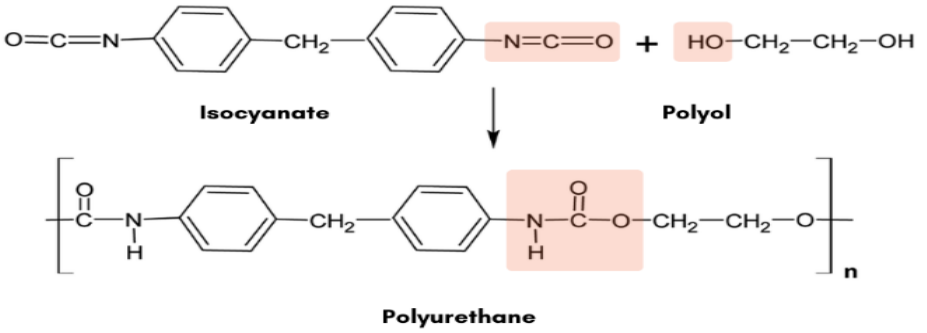

Fig. 3.3. Chemical reaction to produce PUF (De Souza et al., 2021)

Overall, the characterization results demonstrate clear differences in surface morphology, porosity, chemical composition, and physicochemical properties among the investigated packing materials. These differences are expected to significantly influence microbial colonization, mass transfer, and ultimately the biofiltration performance discussed in the following sections.

3.2. Modification of physicochemical properties of packing materials

Improving the efficiency and operational stability of biofiltration systems under laboratory conditions critically depends on the physicochemical properties of packing materials, which govern both adsorption-driven and biologically mediated pollutant removal processes. Recent studies emphasize that surface area, pore structure, and surface chemistry strongly influence the efficiency of hydrogen sulfide removal by affecting mass transfer, microbial attachment, and surface-mediated reactions (Yang et al., 2023; Zhang et al., 2024).

In this study, physical and chemical modification strategies were systematically applied to enhance surface-related characteristics, including specific surface area, porosity, and surface reactivity. In addition to conventional textural parameters, changes in electrical conductivity (EC*) were used as a comparative indicator of physicochemical reactivity under identical measurement conditions. Similar approaches have recently been proposed to better capture surface ion mobility and redox potential in hybrid adsorption–biodegradation systems (Liu et al., 2022).

Modification of biochar with KOH. Chemical activation of biochar using potassium hydroxide (KOH) is widely recognized as one of the most effective approaches for increasing specific surface area and developing a highly porous carbon structure. Numerous studies have demonstrated that KOH activation significantly enhances adsorption properties by increasing pore volume and forming a well-developed microporous structure (Chen et al., 2022; Wang et al., 2023; Abd & Othman, 2022).

In the present study, KOH modification resulted in a substantial increase in BET specific surface area for all investigated biochar samples (Table 3.8). The most pronounced improvement was observed for biochar pyrolyzed at 500 °C, where the specific surface area exceeded 430 $m^2 \cdot g^{-1}$ and total porosity reached its maximum. This indicates that an intermediate pyrolysis temperature provides an optimal carbon framework that responds particularly effectively to chemical activation. Similar findings were reported by Zhao et al. (2023), who demonstrated that excessive thermal treatment may lead to structural ordering and partial pore collapse, thereby reducing effective pore accessibility despite a higher degree of carbonization (Mohammadi et al., 2024d).

Beyond the increase in BET-specific surface area, KOH activation significantly altered the pore-size distribution. The proportion of micropores (<2 nm), which are particularly important for H_2S adsorption via pore-filling mechanisms, increased markedly. At the same time, the presence of mesopores improved mass

transfer and facilitated gas diffusion to internal adsorption sites. Such a hierarchical pore structure enhances both adsorption efficiency and kinetic performance under dynamic filtration conditions.

Although biochar produced at 600 °C exhibited a comparable specific surface area after activation, its relatively lower porosity suggests partial structural densification, which may restrict internal diffusion pathways and reduce accessibility for H_2S molecules and microbial colonization. This observation confirms that pyrolysis temperature is a critical structural preconditioning step, while chemical activation modifies the already formed carbon matrix. Thus, the final surface properties result from the interaction between thermal treatment and chemical activation rather than from activation alone (Li et al., 2020).

In the context of biofiltration, the increased specific surface area and optimized pore architecture of KOH-modified biochar not only enhance adsorption capacity but also provide an expanded interface for biofilm formation and microbial activity. Therefore, KOH activation simultaneously enhances physicochemical adsorption and biological oxidation, thereby improving the packing material's multifunctional performance.

Table 3.8. Physical modification of biochar samples' specific surface area (S_{BET}) and porosity ($Porosity_{BET}$) by activating with KOH

Chemical properties of biochar	Before modification	After modification with KOH
S_{BET} (sewage sludge, before pyrolysis), m^2/g	17.96	43.24
S_{BET} (after 400 °C pyrolysis), m^2/g	12.28	235.32
S_{BET} (after 500 °C pyrolysis), m^2/g	22.76	433.44
S_{BET} (after 600 °C pyrolysis), m^2/g	24.66	471.54
$Porosity_{BET}$ (sewage sludge, before pyrolysis), cm^3/g	0.048	0.036
$Porosity_{BET}$ (after 400 °C pyrolysis), cm^3/g	0.01	0.096
$Porosity_{BET}$ (after 500 °C pyrolysis), cm^3/g	0.42	4
$Porosity_{BET}$ (after 600 °C pyrolysis), cm^3/g	0.025	0.24

The adsorption kinetics of H_2S on KOH-modified biochar followed a pseudo-second-order model. This behavior is interpreted here as an empirical indication of surface-related interactions rather than as direct proof of chemisorption. Similar

kinetic interpretations have been adopted in recent biochar-based gas adsorption studies to avoid overestimation of specific reaction mechanisms (Sun et al., 2022).

Influence of $FeCO_3$-modified CLC waste. Unmodified cellular lightweight concrete (CLC) waste exhibited moderate H_2S removal efficiency, primarily due to its mineral composition and limited adsorption capacity. Previous studies have demonstrated that calcium- and silica-rich construction wastes can serve as weak adsorbents, but require surface modification to achieve higher removal efficiencies (Kurniawan et al., 2020).

Modification of CLC waste with iron carbonate ($FeCO_3$) significantly enhanced its physicochemical reactivity toward hydrogen sulfide. Iron-containing phases are known to promote redox interactions with H_2S, leading to the formation of iron sulfides and elemental sulfur (Ma et al., 2022; Rodriguez et al., 2023). The reaction pathways presented in Equations (3.6–3.9) are therefore introduced as a conceptual framework based on established literature, rather than as directly measured mechanisms.

$$Fe_2O_3 + 3H_2S \rightarrow Fe_2S_3 + 3H_2O; \tag{3.6}$$

$$Fe_2S_3 \rightarrow FeS + FeS_2; \tag{3.7}$$

$$FeS_2 \rightarrow FeS + 1/2S_2; \tag{3.8}$$

$$2Fe_2S_3 + 3O_2 \rightarrow 2Fe_2O_3 + 3/4S_8\,. \tag{3.9}$$

Recent hybrid biofilter studies combining iron-modified mineral materials with carbonaceous adsorbents have reported removal efficiencies of 85–90%, confirming the synergistic role of adsorption and catalytic transformation (Nowak et al., 2024). The reuse of construction-derived CLC waste as a modified packing material thus represents both a performance-enhancing and environmentally sustainable strategy.

Role of polyurethane foam. PUF showed a negligible direct contribution to H_2S adsorption; however, its structural and biological roles within the biofilter were substantial. The high porosity and elasticity of PUF provide a favorable substrate for microbial attachment and biofilm development, which is essential for sustained biodegradation of sulfur compounds (De Souza et al., 2021; Mutegoa et al., 2020).

PUF also improved mechanical stability and gas flow distribution, preventing excessive compaction of granular packing materials. Recent studies have highlighted that uniform gas distribution and biofilm support can be as critical as adsorbent properties for long-term biofilter performance (Alonso et al., 2022). In the present study, hybrid biofilters combining PUF with reactive materials, such as KOH-modified biochar or $FeCO_3$-modified CLC waste, achieved H_2S removal efficiencies of approximately 85%, confirming the importance of biologically supportive matrices.

The chemical structure and formation mechanism of polyurethane foam, including the reaction between isocyanate and polyol components, are illustrated in Figure 3.3. While alkaline modification of PUF has been proposed in recent studies to enhance surface hydrophilicity and microbial attachment (Singh et al., 2024), this modification was not investigated in the present work and is identified as a direction for future research.

The scientific novelty of this experimental study is demonstrated through several key aspects. The study systematically examines the effect of pyrolysis temperature on KOH activation efficiency, showing that biochar preconditioning is a critical factor influencing its performance in biofiltration processes. In addition, the study proposes the combined evaluation of surface area, porosity, and EC* as interrelated indicators of biochar physicochemical activity, all measured under identical conditions.

The novelty of the research is further supported by using $FeCO_3$-modified CLC waste as a reactive, environmentally sustainable biofilter packing material. Moreover, the results demonstrate synergistic effects in hybrid packing systems, where adsorption, catalytic reactions, and microbial support mechanisms operate simultaneously.

Finally, empirical kinetic models are used solely to describe experimental data, while process mechanisms are analyzed separately. This clear distinction ensures a more transparent and reliable interpretation of results in biochar-based H_2S removal studies. The observed variations in pressure drop and flow behavior highlight the influence of packing material structure on reactor hydrodynamics. These characteristics directly affect gas–solid contact efficiency and are therefore considered in evaluating biofiltration performance.

3.3. Microbial colonization and biofilm formation on biofiltration materials

To evaluate microbial colonization dynamics and biofilm formation within the biofilter, two sulfur-oxidizing bacterial (SOB) groups – *Pseudomonas* spp. and *Acidithiobacillus* spp. (DSM 12475 and DSM 739) – were used to inoculate biochar and cellular lightweight concrete (CLC) waste packing materials. Microbial attachment, spatial distribution, and biofilm development were investigated across five vertical biofilter layers using fluorescence microscopy combined with DAPI and SYPRO staining. Unlike many previous studies that focus on bulk microbial activity, the present work provides a spatially resolved analysis of biofilm formation along the biofilter height, allowing direct linkage between microbial structure, packing material properties, and hydrogen sulfide (H_2S) removal performance.

This subsection demonstrates that microbial colonization and biofilm formation in biofiltration systems are governed by the coupled interaction between packing material properties, microbial metabolic strategies, and spatial position within the biofilter. For the first time, biofilm development along the biofilter height is shown to be spatially structured rather than uniformly distributed, leading to the formation of distinct zones of biological activity that are directly linked to hydrogen sulfide removal efficiency. These findings indicate that biofiltration performance can be enhanced not only by optimizing operating conditions but also by targeted design and modification of biofiltration materials to promote the formation of highly active biofilm zones.

The results confirm that porous carbon-based materials, such as biochar, facilitate faster microbial attachment, enhanced EPS production, and higher biomass densities than mineral-based CLC waste. However, the scientific novelty of this work lies not only in identifying qualitative differences but in establishing a quantitative, microscopy-based relationship between material microstructure and accelerated biofilm initiation, as well as the functional dominance of specific microbial groups. This provides a clear mechanistic basis for the targeted modification of biofiltration materials, for example, by increasing surface porosity, roughness, or moisture retention capacity to promote stable biofilm development.

A further key novel aspect is the identification of functional complementarity between fast-growing heterotrophic *Pseudomonas* spp., which form highly active, EPS-rich biofilms in localized biofilter layers, and slower-growing chemolithotrophic *Acidithiobacillus* spp., which exhibit uniform distribution throughout the biofilter height and contribute to long-term process stability. This finding challenges the assumption that maximum biomass accumulation alone determines biofiltration efficiency and instead highlights the importance of supporting diverse microbial functions through material modification.

In conclusion, the integration of spatially resolved fluorescence microscopy with quantitative microbial abundance analysis provides a new mechanistic framework for understanding how the selection and targeted physical and chemical modification of biofiltration materials, together with microbial ecology, shape biofilm architecture and the performance of biochar-based H_2S biofiltration systems. This represents a clear methodological and conceptual advance over traditional biofilter studies, in which biofilm development and microbial activity are typically evaluated using averaged whole-filter-scale metrics.

3.3.1. Microscopic analysis of microbial activity and material effects

Fluorescence microscopy images acquired at 100× magnification revealed pronounced temporal and material-dependent differences in microbial attachment

and early biofilm development. During the initial incubation layer (24 h), individual rod-shaped bacterial cells were sparsely distributed on both the biochar and CLC waste surfaces, indicating weak, largely reversible attachment. Similar early-layer adhesion behavior has been described by Yu et al. (2020), who demonstrated that initial microbial attachment is primarily governed by physicochemical surface interactions rather than active biological processes.

With increasing incubation time, bacterial density increased, and cells gradually aggregated into microcolonies, indicating a transition from reversible attachment to irreversible biofilm formation. This progression closely follows the classical biofilm development sequence described by Lu et al. (2021). However, the present study extends these observations by demonstrating that the rate and extent of this transition strongly depend on the type of packing material, even under identical incubation and nutrient conditions.

Biochar surfaces consistently supported higher microbial attachment compared to CLC waste. This behavior can be attributed to biochar's higher porosity, greater surface roughness, and superior moisture retention, which collectively create microhabitats favorable for microbial adhesion and early biofilm stabilization. While previous studies have qualitatively reported improved biofilm formation on carbonaceous materials (Yu et al., 2020; Lu et al., 2021), the present results provide quantitative microscopic evidence linking these material properties to accelerated biofilm initiation.

In contrast, the smoother and less porous surface of CLC waste limited the number of effective attachment sites, resulting in delayed colonization and less cohesive early biofilm structures. This finding highlights that mineral-based media, although chemically active, may require complementary materials or microbial strategies to achieve comparable biological performance.

Colonization behavior of Pseudomonas spp.*: rapid biofilm development and functional dominance*. Microscopy analysis of *Pseudomonas* spp.-inoculated samples demonstrated rapid and extensive colonization of both packing materials, with a pronounced preference for biochar (Fig. 3.4). At 24 h, isolated cells were visible on material surfaces, confirming successful initial attachment. By 72 h, bacterial clusters had expanded markedly, and by 120 h, dense, interconnected microbial networks characteristic of mature biofilms were observed.

SYPRO staining revealed intense extracellular protein production at later layers, indicating active extracellular polymeric substance (EPS) synthesis. This observation is consistent with the findings of Khanongnucha et al. (2019), who identified EPS production as a critical factor controlling biofilm stability and mass transfer efficiency in biological gas treatment systems. Importantly, the present study demonstrates that EPS-rich biofilms formed preferentially in specific vertical zones of the biofilter, rather than uniformly across the filter.

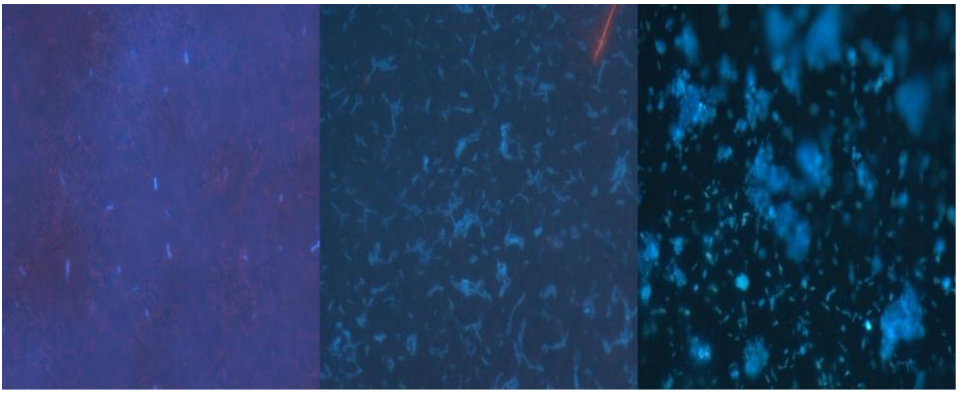

(a) (b) (c)

Fig. 3.4. Biochar and CLC waste samples after 24 h (a), after 72 h (b), and after 120 h (c), inoculated with *Pseudomonas* spp., stained with DAPI and SYPRO, showing sparse individual cell attachment (100×)

Quantitative spot-counting analysis (Table 3.9) showed that biochar supported approximately 60% more *Pseudomonas* spp. cell densities than CLC waste under identical conditions. While similar density enhancements have been reported by Li et al. (2020), the present work advances this understanding by linking microbial density not only to material type but also to vertical position within the biofilter, revealing zones of functional dominance for biological H_2S oxidation.

Table 3.9. Evaluating the approximate number of existing *Pseudomonas* spp. bacteria on the biochar and CLC waste

Material	Inoculation treatment	Average count, cells/g	Estimated total bacteria, cells/sample
Biochar	*Pseudomonas* spp.	35	~1.4×10^6
Biochar	Nutrient + *Pseudomonas* spp.	143	~5.8×10^6
CLC waste	*Pseudomonas* spp.	22	~8.8×10^5
CLC waste	Nutrient + *Pseudomonas* spp.	91	~3.6×10^6

These findings indicate that *Pseudomonas* spp. play a key role in establishing highly active biofilm zones responsible for peak H_2S removal, particularly when supported by porous carbonaceous media.

Colonization behavior of Acidithiobacillus spp.*: slower growth and spatial resilience*. In contrast to *Pseudomonas* spp., *Acidithiobacillus* spp. exhibited slower colonization dynamics. At 24–48 h, cells were sparsely distributed with

limited clustering on both biochar and CLC waste surfaces (Figs. 3.5 and 3.6). By 72–96 h, small aggregates became visible, and biofilm-like structures developed gradually. SYPRO staining revealed moderate protein production, indicating slower EPS synthesis.

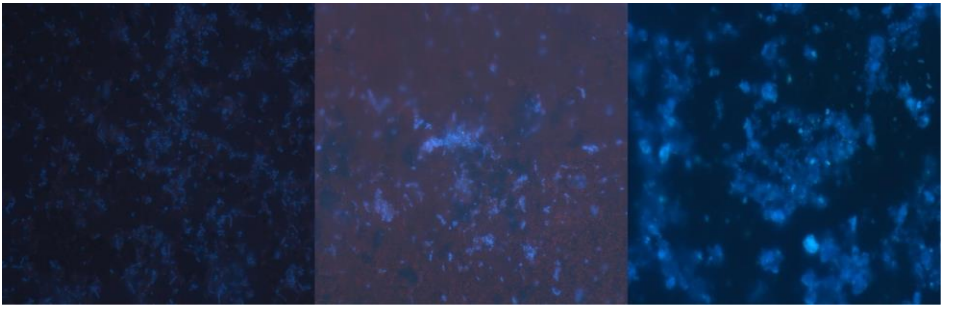

(a) (b) (c)

Fig. 3.5. Biochar samples after 24 h (a), after 72 h (b), and after 120 h (c), inoculated with *Acidithiobacillus* spp., stained with DAPI and SYPRO, showing sparse individual cell attachment (100×)

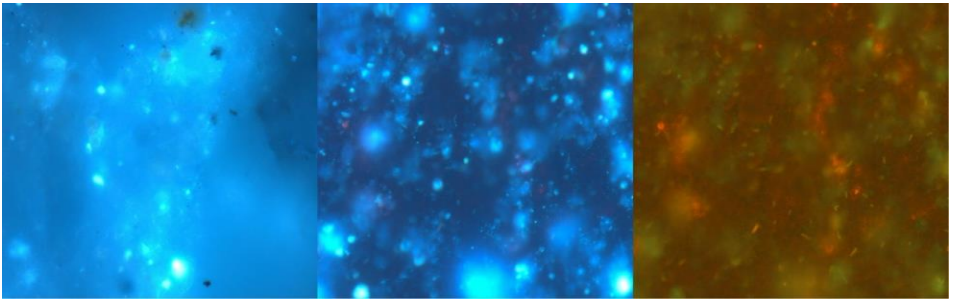

(a) (b) (c)

Fig. 3.6. CLC waste samples after 24 h (a), after 72 h (b), and after 120 h (c), inoculated with *Acidithiobacillus* spp., stained with DAPI and SYPRO, showing sparse individual cell attachment (100×)

This behavior aligns with previous reports describing chemolithotrophic sulfur-oxidizing bacteria as prioritizing metabolic persistence over rapid biomass accumulation (Drozdz et al., 2020; Herath et al., 2024). However, the present study provides new insight by showing that slower biofilm development does not equate to spatial instability. *Acidithiobacillus* spp. maintained viable populations across all biofilter layers, even in zones characterized by lower nutrient availability or fluctuating oxygen conditions.

Table 3.10. Evaluating the approximate number of existing *Acidithiobacillus* spp. bacteria on the biochar and CLC waste

Material	Inoculation treatment	Average count, cells/g	Estimated total bacteria, cells/sample
Biochar	*Acidithiobacillus* spp.	18	~7.2×10^5
Biochar	Nutrient + *Acidithiobacillus* spp.	77	~3.1×10^6
CLC Waste	*Acidithiobacillus* spp.	12	~4.8×10^5
CLC Waste	Nutrient + *Acidithiobacillus* spp.	55	~2.2×10^6

Quantitative counts (Table 3.10) confirmed lower overall cell densities than those of *Pseudomonas* spp., consistent with the findings of Zhou et al. (2021). Nevertheless, the uniform vertical distribution observed here suggests that *Acidithiobacillus* spp. may contribute to long-term process stability, particularly under operating conditions that constrain rapid biofilm growth.

The fluorescence microscopy analysis presented in this subsection demonstrates that early-layer microbial adhesion and biofilm initiation in biofiltration systems are directly governed by the surface microstructure and porosity of the packing materials. The results show that, even under identical incubation and nutrient conditions, biochar and CLC waste provide fundamentally different environments for microbial attachment, leading to distinct transition rates from reversible adhesion to stable biofilm formation.

The scientific novelty of this work lies in the first microscopy-based evidence that packing material microstructure acts not merely as a passive support, but as an active controlling factor in shaping early biofilm architecture. This finding provides a mechanistic basis for the targeted modification of biofiltration materials to create favorable sites for microbial adhesion, increase surface roughness, and improve moisture retention.

The obtained results further indicate that both physical (e.g., porosity enhancement and surface topography modification) and chemical (e.g., introduction of surface functional groups or reactive mineral phases) modification strategies can be employed not only to improve sorption performance, but also to deliberately regulate biofilm initiation. Consequently, the modification of biofiltration materials can be transformed from an empirical trial-and-error approach into a scientifically guided design strategy grounded in microscale understanding of biofilm formation processes.

3.3.2. Biofilm distribution across biofilter layers and its relationship with H_2S removal

To comprehensively evaluate the vertical dynamics of microbial growth and biofilm maturation processes in different biofilter packing materials, solid-phase samples were collected from five defined layers of the biofilter column (from bottom to top). The investigations were conducted using biochar and CLC waste packings, which were inoculated separately with *Pseudomonas* spp. and *Acidithiobacillus* spp. Biofilm formation and microbial spatial distribution were analyzed by fluorescence microscopy using DAPI and SYPRO staining, with particular emphasis on bacterial density, proteinaceous extracellular polymeric substance (EPS) matrix formation, and biofilm architecture. All experiments were performed under identical anaerobic conditions (30 °C, 96 h), with nutrient irrigation applied from the top of the column.

Biofilm maturation of Pseudomonas spp. *in biochar packing.* Fluorescence microscopy revealed a pronounced gradient in *Pseudomonas* spp. colonization intensity within the biochar packing. As shown in Figure 3.7, the highest bacterial densities and strongest DAPI fluorescence were detected in biofilter layers 3 and 4. These layers also exhibited the most intensive SYPRO fluorescence signals (Figs. 3.8a and 3.8b), indicating active production of a protein-rich EPS matrix and the formation of mature, multilayered biofilms.

In the lower biofilter layers (1–2), *Pseudomonas* spp. colonization in the biochar packing was moderate, likely due to increased hydrodynamic stress and gas flow turbulence near the inlet zone. In the upper layers (4–5), biofilm fragmentation and reduced bacterial density were observed, which can be attributed to limited nutrient availability and weaker gas–liquid interactions. These results confirm that the middle biofilter layers during biochar packing provide optimal conditions for the growth of *Pseudomonas* spp. biofilm maturation. While this phenomenon has been conceptually described by Li et al. (2020) and Shyam et al. (2022), the present study provides direct microscopic evidence supporting this mechanism. However, unlike previous studies that primarily inferred microbial activity from bulk performance indicators or biomass measurements, the present work directly visualizes biofilm structure and EPS distribution along the biofilter height. This spatially resolved microscopic confirmation demonstrates that mid-biofilter zones are not only chemically favorable but also biologically dominant, governing overall biofilter performance.

Colonization of *Pseudomonas* spp. *in CLC waste packing*. The colonization behavior of *Pseudomonas* spp. in CLC waste packing is presented in Figure 3.9. Although bacterial attachment to the CLC surface was observed, both DAPI and SYPRO fluorescence signals were weaker than those detected in biochar packing, and the biofilm structure remained less developed. The highest bacterial densities

were again detected in biofilter layers 3–4; however, overall surface coverage and EPS production were limited due to the lower porosity and less favorable surface microstructure of CLC waste.

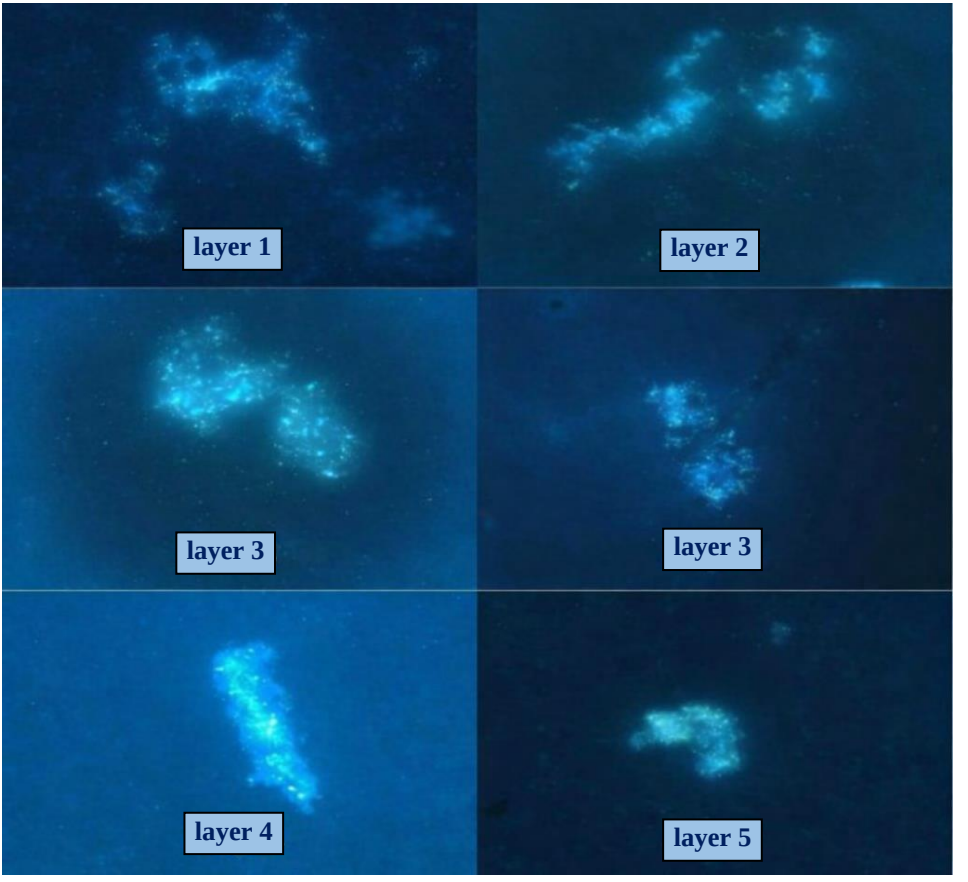

Fig. 3.7. DAPI-stained image of biochar from layer 1–5 with *Pseudomonas* spp. showing dense colonization

Colonization of Acidithiobacillus spp. *in CLC waste packing*. Results for *Acidithiobacillus* spp. colonization in CLC waste packing are shown in Figure 3.12. In this case, biofilm development was the weakest among all tested configurations. Bacteria primarily colonized surface irregularities and microcracks, while biofilm thickness and EPS production remained minimal. These findings indicate that although CLC waste packing can sustain the viability of *Acidithiobacillus* spp., it is not optimal for intensive biofilm maturation.

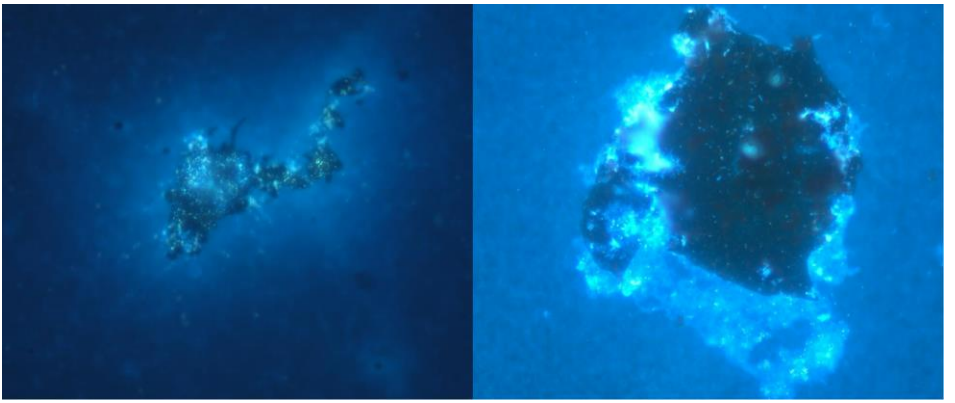

(a) (b)

Fig. 3.8. SYPRO-stained image of biochar from layers 3 (a) and 4 (b) with *Pseudomonas* spp. showing attached bacteria and created a colony

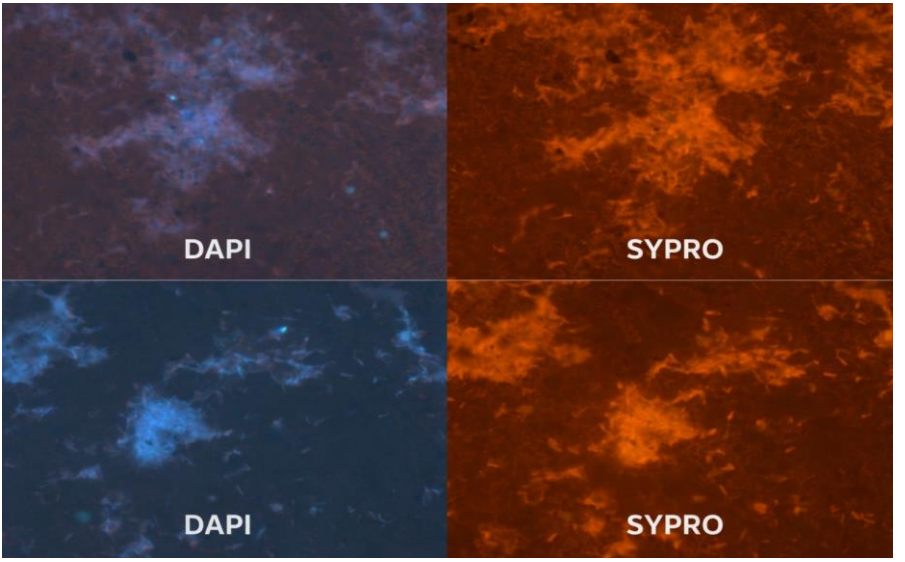

Fig. 3.9. DAPI and SYPRO-stained CLC waste with *Pseudomonas* spp. showing weak protein matrix formation

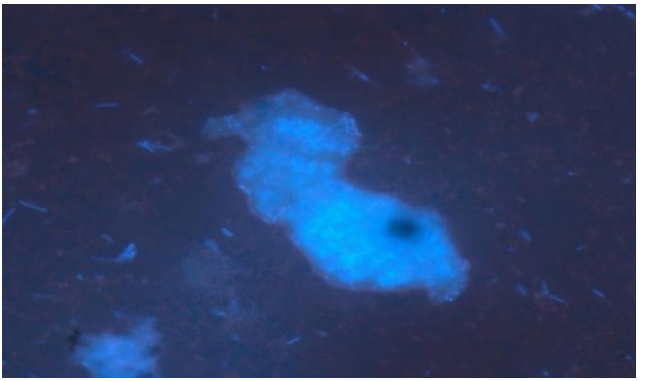

Fig. 3.10. Image of biochar from layer 5, DAPI-stained with *Acidithiobacillus* spp., showing dense colonization (after 144 h)

Biofilm formation of *Acidithiobacillus* spp. in biochar packing. Colonization of *Acidithiobacillus* spp. in biochar packing is illustrated in Figures 3.10 and 3.11. In contrast to *Pseudomonas* spp., *Acidithiobacillus* spp. exhibited a more uniform distribution throughout the biofilter height. DAPI fluorescence was detected at all layers, whereas SYPRO fluorescence remained comparatively weak, indicating thinner biofilms with lower protein content. Notably, viable *Acidithiobacillus* spp. Colonization was observed even in the upper biofilter layers (e.g., layer 5; Fig. 3.10), confirming that these microorganisms can persist under limited nutrient availability and variable redox conditions. This behavior should be interpreted as a distinct ecological strategy rather than reduced biofilm performance, suggesting that *Acidithiobacillus* spp. play a stabilizing role in the biofilter by maintaining baseline biological activity throughout the filter bed, particularly under conditions that are unfavorable for rapid EPS-rich biofilm formation.

Biochar produced at 600 °C exhibited slightly alkaline pH values (8.46–8.89), which can be attributed to the removal of acidic surface functional groups and the concentration of alkaline mineral phases during high-temperature pyrolysis. Although elevated pH values may appear unfavorable for acidophilic sulfur-oxidizing bacteria, the alkaline character of the biochar provides important buffering capacity within the biofilter. During H_2S oxidation, sulfuric acid is generated, which tends to decrease local pH and potentially inhibit microbial activity. The presence of alkaline biochar counteracts excessive acidification, thereby preventing inhibitory pH drops and stabilizing biological activity over prolonged operation. Furthermore, the interaction between alkaline material surfaces and acid formation results in localized pH gradients within the biofilm, allowing coexistence of acidophilic and neutrophilic sulfur-oxidizing microorganisms. Conse-

quently, biochar produced at 600 °C contributes not only to adsorption enhancement but also to improved long-term biofilter stability and sustained H_2S removal efficiency.

Comparison of biofilm structure and linkage to H_2S removal. A direct comparison of biofilm structures in biochar packing is presented in Figure 3.12, clearly demonstrating that *Pseudomonas* spp. formed dense, EPS-rich biofilms, whereas *Acidithiobacillus* spp. developed thinner and more dispersed biofilms. These differences, summarized in Table 3.11, reflect distinct ecological strategies of the microorganisms and their interactions with the biofilter packing material. Together, these results indicate that different sulfur-oxidizing bacteria occupy complementary ecological niches along the biofilter height, contributing to system functionality in distinct ways rather than competing uniformly for space or resources.

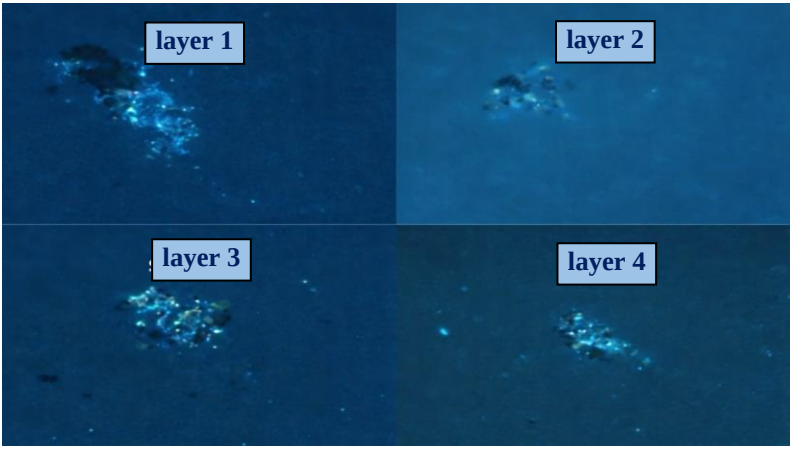

Fig. 3.11. SYPRO-stained image of biochar from layers 3, 4, and 5 with *Acidithiobacillus* spp. showing attached bacteria and created a colony (after 72 h)

Microscopic observations showed a strong correlation with hydrogen sulfide removal efficiency. As presented in Table 3.12, Table 3.13, and Figure 3.14, the highest H_2S removal efficiencies (78–81%) were achieved in the biochar packing at biofilter layers 3–4, where the highest *Pseudomonas* spp. densities and the most intensive EPS production were observed. In contrast, lower and upper biofilter layers, as well as CLC waste packing, exhibited reduced biofilm maturity and correspondingly lower H_2S removal efficiencies. These findings demonstrate that localized biofilm maturity and EPS production, rather than uniform microbial distribution or total biomass alone, govern H_2S removal efficiency within the biofilter.

Table 3.11. Comparing the performance of *Pseudomonas* spp. and *Acidithiobacillus* spp. bacteria

Feature	***Pseudomonas* spp.**	***Acidithiobacillus* spp.**
Growth rate	Fast (dense by 72–96 h)	Slower (visible at 72–96 h)
Surface preference	Biochar > CLC	Biochar ≥ CLC
Protein production	High	Moderate
Biofilm density	High	Low to moderate
Peak colonization layers	Layers 3–4	Even distribution
Spatial preference	Middle layers	Even distribution
Environmental tolerance	Sensitive to nutrients	Tolerant of low-nutrient zones

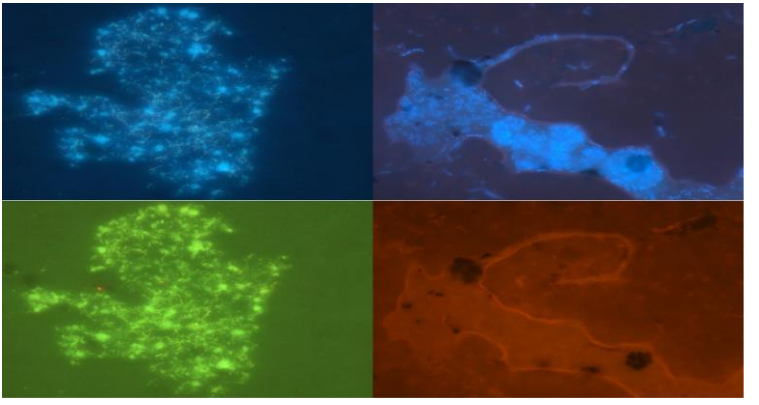

(a) (b)

Fig. 3.12. Comparison of grown colonies, protein, and biofilm intensity on biochar samples stained with *Pseudomonas* spp. (a) and *Acidithiobacillus* spp. (b)

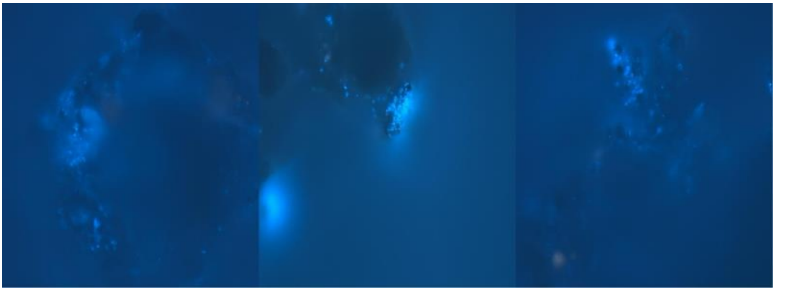

Fig. 3.13. DAPI and SYPRO-stained CLC waste with *Acidithiobacillus* spp. showing weak protein matrix formation

Table 3.12. Summary of microbial colonization and biofilm formation

Biofilter layers	Material	Bacteria	DAPI Signal	SYPRO signal	Biofilm description
1	Biochar	*Pseudomonas* spp.	strong	moderate	Initial microclusters
2	CLC waste	*Pseudomonas* spp.	moderate	weak	Sparse colonization
3	Biochar	*Pseudomonas* spp.	very strong	very strong	Dense Protein rich biofilm
3	CLC waste	*Acidithiobacillus* spp.	moderate	moderate	Thin, uniform film
4	Biochar	*Acidithiobacillus* spp.	strong	strong	Developing biofilm
4	CLC waste	*Pseudomonas* spp.	moderate	moderate	Moderate surface coverage
5	Biochar	*Acidithiobacillus* spp.	moderate	weak	Patchy coverage
5	CLC waste	*Acidithiobacillus* spp.	weak	weak	Minimal attachment

Table 3.13. Comparative summary of microbial density, fluorescence signal intensity, and biofilm characteristics for *Pseudomonas* spp. and *Acidithiobacillus* spp. across biofilter layers and media types

Biofilter layers	H_2S removal, %	Microbial density, cells/g
1	58	4.20E+07
2	78	7.30E+07
3	81	1.15E+08
4	63	1.05E+08
5	47	9.10E+07

The obtained results demonstrate that biofiltration is a spatially structured biological process in which the type of biofilter packing material governs not only microbial attachment but also biofilm maturity and its functional contribution to H_2S removal. This study provides, for the first time, a direct experimental and microscopic linkage between biofilter layer position, biofilm structure, and actual H_2S removal efficiency.

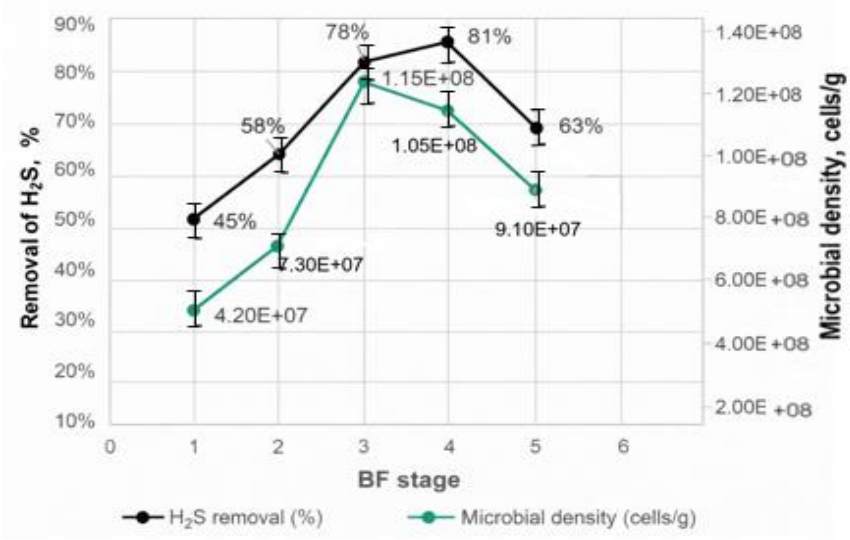

Fig. 3.14. Correlation of H_2S removal and microbial density by the biofilter layer

These findings establish a mechanistic basis for the rational design of hybrid biofilters, in which combinations of biochar and mineral materials, together with microbial diversity, are deliberately used to form biologically active zones within the biofilter column. This spatially informed approach provides a mechanistic framework for the rational design of hybrid biofilters, in which packing material selection and microbial diversity are deliberately used to create biologically active zones rather than aiming for uniform colonization.

This subsection demonstrates that biofilm formation in biofiltration systems is a spatially differentiated process, governed not only by microbial characteristics but also by the structural properties of biofiltration materials and their interactions with hydrodynamic and nutrient-distribution conditions across different biofilter layers. For the first time, experimental and microscopy-based evidence shows that the highest biological activity and H_2S removal efficiency are not distributed uniformly throughout the biofilter but are concentrated in specific layers (layers 3–4), where mature, EPS-rich biofilms form.

The results reveal that biochar packing creates favorable conditions for the growth of *Pseudomonas* spp. biofilm maturation in the middle biofilter layers, which directly corresponds to peak H_2S removal efficiencies. In contrast, mineral-based CLC waste packing limits biofilm thickness and EPS production, even when similar microbial distribution patterns are observed. This finding indicates that the microstructure and surface properties of biofiltration materials control not

only microbial attachment, but also the functional maturation of biofilms in different biofilter zones.

A key scientific novelty lies in the direct linkage of three interconnected levels: biofilter layer position, biofilm structural characteristics (density and EPS intensity), and actual H_2S removal performance. This relationship demonstrates that biofiltration material modification should not aim for uniform biofilm growth across the entire filter bed, but rather for spatially targeted adaptation of material properties to support distinct functional zones. For example, porous carbon-based materials or their modified forms are most effective in middle biofilter layers, where enhanced EPS production and rapid biofilm maturation are required, whereas alternative material compositions or surface modifications may be more suitable in upper or lower layers exposed to nutrient limitation or increased hydrodynamic stress (Mohammadi et al., 2023a; Mohammadi et al., 2024; Mohammadi et al., 2025).

In conclusion, the findings of this subsection provide a mechanistic basis for spatially differentiated strategies for modifying biofiltration materials. Such an approach enables a transition from conventionally homogeneous biofilter designs toward functionally zoned biofiltration systems, in which biochar activation, incorporation of mineral phases, or surface property modification are applied selectively to maximize biofilm maturity and H_2S removal efficiency. The microscopy analyses confirm that packing materials with higher surface roughness and porosity support enhanced microbial attachment and biofilm development. This increased biomass retention provides a mechanistic explanation for the performance differences observed under identical operating conditions.

3.4. Investigation of biofilter performance in H_2S removal

The performance of biofilters for hydrogen sulfide removal depends on the complex interplay between packing material properties, operational parameters, and biofilter configuration. This section presents a comprehensive analysis of H_2S RE, focusing on the influence of different packing materials, gas flow rates, and inlet H_2S concentrations. In addition, the performance of single-material biofilters is systematically compared with modified and hybrid configurations, allowing assessment of the role of material modification in controlling biofilter efficiency.

H_2S RE, defined as the percentage reduction in H_2S concentration between the inlet and outlet of the biofilter, is treated not only as a performance indicator but also as a reflection of the dominant removal mechanisms, including physical adsorption, catalytic conversion, and biological oxidation. Removal efficiency

was calculated from time-averaged H_2S concentration measurements during stable operating periods, providing a representative assessment of biofilter performance in accordance with commonly applied biofiltration evaluation methodologies. The influence of packing material characteristics, gas flow rate, and pollutant loading Unless otherwise stated, H_2S concentrations reported in this section and summarized in the tables represent mean values averaged over one complete measurement round under quasi-steady operating conditions, a practice widely adopted in laboratory-scale biofilter studies on RE is discussed in detail, with particular emphasis on how chemical modification of biofilter media alters these mechanisms (Mohammadi et al., 2024b).

3.4.1. Performance comparison of biofilters with single-component packing material

This subsection presents the results obtained from laboratory-scale biofilters packed with sewage sludge-derived biochar, PUF, and CLC waste. Hydrogen sulfide removal from raw biogas was evaluated during the first 144 h of operation, with biogas injected every 24 h. The initial chemical composition of biogas in each storage balloon was analyzed using a GDA, with different ILR and balloon volumes.

All experiments were conducted under controlled environmental conditions: room temperature of approximately 27 °C, packing material moisture content of 60–80%, and biochar pH ranging from 8 to 9 depending on the biofilter layer. After biogas injection, gas composition was analyzed every 3 min at each biofilter layer (from the 1st to the 5th). One complete analysis cycle from the lowest to the highest layer required approximately 15 min and is referred to as a “round”. Hydrogen sulfide removal efficiencies at different biofilter layers are summarized in Table 3.14, and comparative trends are illustrated in Figure 3.15.

Among the tested materials, biochar achieved the highest H_2S removal efficiency, exceeding 92% under optimal conditions (Table 3.14, Fig. 3.15). This superior performance can be attributed to its high specific surface area (>1 000 m^2/g) and well-developed microporous structure, which enables effective physical adsorption of H_2S molecules. In addition, oxygen-containing functional groups (e.g., hydroxyl and carboxyl groups) promote chemical interactions with sulfur species, enhancing overall reactivity. Importantly, biochar also provided an excellent substrate for sulfur-oxidizing bacteria, such as *Thiobacillus*, supporting sustained biological oxidation processes, as previously suggested by Li et al. (2020) and Shyam et al. (2022).

Unmodified CLC waste exhibited moderate H_2S removal efficiency (approx. 60–70%, Table 3.14), reflecting its lower surface area and limited adsorption capacity. However, upon $FeCO_3$ impregnation, the removal efficiency increased to

approximately 75%, highlighting the critical role of catalytic modification. The moderate porosity of CLC waste (30–40%) allowed gas transport and microbial colonization, while $FeCO_3$ impregnation introduced catalytically active iron sites that accelerated the oxidation of H_2S into elemental sulfur and sulfate. This catalytic effect partially compensated for the material's lower adsorption capacity and confirmed observations reported in previous catalytic biofilter studies (Li et al., 2020).

PUF demonstrated the lowest H_2S removal efficiency among the tested materials (< 50%, Table 3.14, Fig. 3.15), primarily due to the absence of intrinsic adsorption capacity and catalytic activity.

Table 3.14. H_2S concentration monitoring after injecting biogas into the single material-packed biofilter

	Packing material	**Biochar**	**CLC waste**	**PUF**
H_2S concentrations, ppm	Initial H_2S concentration in the biogas	90	90	90
	First round of analysis after 3 days			
	1st layer of biofilter	20	40	70
	2nd layer of biofilter	10	20	60
	3rd layer of biofilter	10	20	50
	4th layer of biofilter	10	10	30
	5th layer of biofilter	0	10	30
	Second round of analysis after 6 days			
	1st layer of biofilter	10	20	40
	2nd layer of biofilter	10	20	30
	3rd layer of biofilter	0	10	20
	4th layer of biofilter	0	10	20
	5th layer of biofilter	0	0	10

Nevertheless, PUF contributed to the biofilter's structural stability and provided a physical scaffold for microbial biofilm development. These characteristics explain its potential role in mixed-material configurations, despite its limited effectiveness as a standalone H_2S removal medium.

Influence of gas flow rate and inlet H_2S concentration. Gas flow rate strongly influenced biofilter performance by controlling the gas–solid contact time. At low flow rates (0.2–0.5 L/min), longer residence times resulted in higher removal efficiency values across all materials. Under these conditions, biochar and $FeCO_3$-modified CLC waste exhibited optimal performance, with biochar achieving removal efficiencies above 95%. In contrast, at high flow rates (0.8–1.0 L/min), reduced contact time led to a decline in removal efficiency (Fig. 3.15). At

1.0 L/min, biochar maintained a removal efficiency of approximately 80%, whereas unmodified CLC waste and PUF exhibited greater efficiency losses, consistent with their lower adsorption capacities.

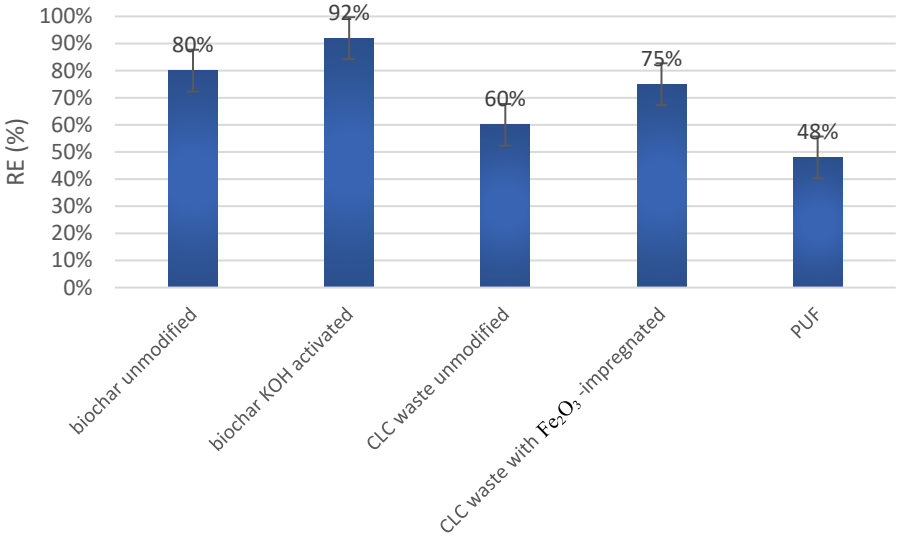

Fig. 3.15. Comparison of single material biofilters RE of H_2S from biogas

The inlet H_2S concentration also significantly affected biofilter performance. At H_2S concentrations below 500 ppm, all materials exhibited high removal efficiency (> 90%), dominated by biological oxidation mechanisms. At H_2S concentrations above 1500 ppm, adsorption site saturation and microbial inhibition reduced removal efficiency across all single-material biofilters. Under these conditions, $FeCO_3$-modified CLC waste outperformed unmodified materials, confirming the importance of catalytic pathways in sustaining biofilter performance at elevated pollutant loads (Fig. 3.15).

Statistical analysis of biofilter performance. To assess the robustness and significance of the observed differences in H_2S removal efficiency, a statistical analysis was performed using the data presented in Table 3.14 and Figure 3.15. All statistical analyses were based on averaged H_2S concentration values obtained during stable operating intervals, and experimental results are reported as mean values with standard deviations. Data normality was confirmed using the Shapiro–Wilk test ($p > 0.05$), allowing the application of parametric statistical methods.

SEM analysis and linkage to material modification. SEM images of biochar and CLC waste before and after biofilter operation are presented in Figures 3.16

and 3.17, respectively. Comparison of pre- and postoperative images reveals pronounced changes in the material's surface morphology. SEM images reveal that KOH-modified biochar exhibits a highly porous and rough surface morphology with numerous micro and mesopores, providing favorable sites for microbial attachment.

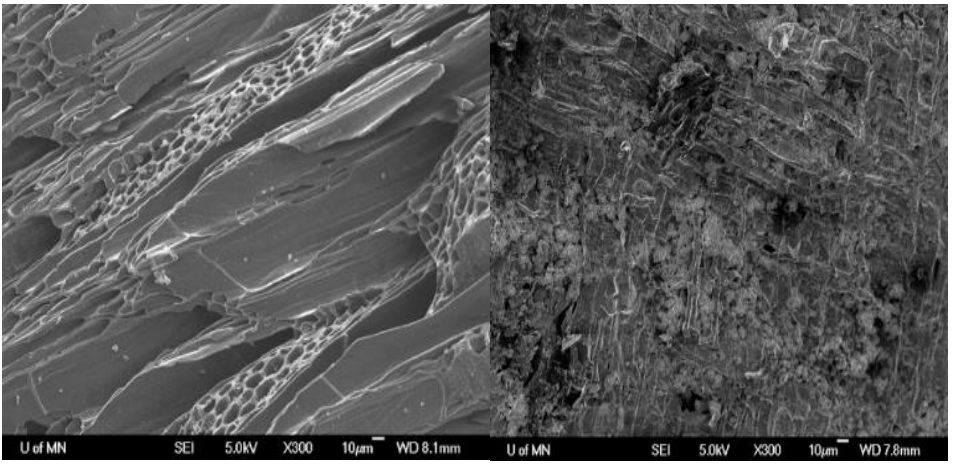

(a) (b)

Fig. 3.16. SEM pictures taken from the biochar samples (a) before the purification process, (b) after removing hydrogen sulfide from biogas

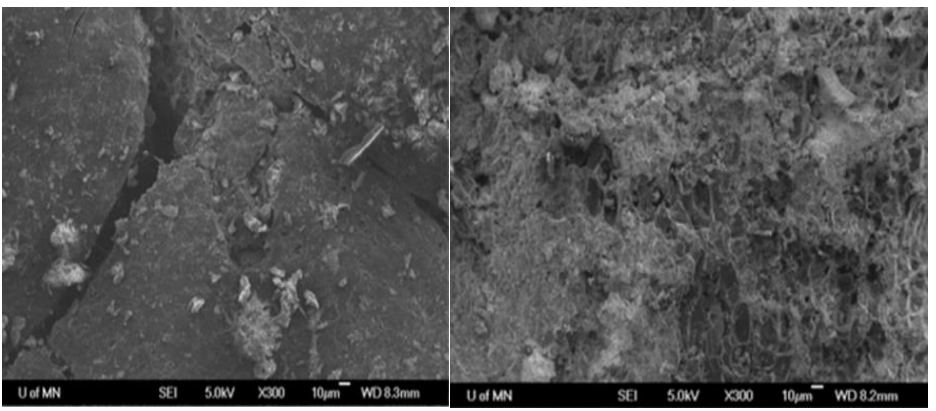

(a) (b)

Fig. 3.17. SEM pictures taken from the CLC waste samples (a) before the purification process, (b) after removing hydrogen sulfide from biogas

In contrast, CLC waste shows a denser mineral structure with localized pore clusters. Pores, gaps, and surface cavities visible before biofilter operation (Figs. 3.16a and 3.17a) were partially or fully filled after H_2S removal (Figs. 3.16b and 3.17b), indicating the accumulation of sulfur-containing reaction products. After prolonged operation, SEM images indicate extensive biofilm coverage on biochar surfaces, whereas biofilm formation on CLC waste appears more heterogeneous and less uniformly distributed.

Fluorescence microscopy images show a higher density of viable microorganisms on biochar and CLC waste compared to PUF, as indicated by stronger fluorescence signals. This observation confirms that materials with higher surface area and surface reactivity promote enhanced microbial colonization and sustained biological activity. These observations provide direct microscopic evidence that H_2S removal is accompanied by material transformation, linking biofilter performance to reactive interactions at the material surface. The more pronounced pore filling observed in modified materials supports the conclusion that chemical modification enhances not only adsorption but also catalytic conversion processes, thereby actively shaping biofilter performance rather than acting as a passive structural enhancement.

The impact of material modification was further evaluated using paired comparisons. KOH-modified biochar exhibited a statistically significant increase in removal efficiency compared to unmodified biochar ($\Delta RE \approx +12\%$, error < 0.01). Similarly, $FeCO_3$-impregnated CLC waste showed a significant improvement over unmodified CLC waste ($\Delta RE \approx +15\%$, error < 0.01), particularly under elevated inlet H_2S concentrations. Simulation by COMSOL demonstrated that gas flow rate, inlet H_2S concentration, and their interaction were all statistically significant factors influencing biofilter performance ($p < 0.05$).

Correlation analysis indicated a strong positive relationship (Pearson's $r > 0.85$) between removal efficiency and material surface characteristics inferred from SEM observations (Figs. 3.16 and 3.17), while a moderate correlation was observed with inlet H_2S concentration. These results confirm that material structure and modification exert a stronger control over biofilter performance than operational parameters alone.

The scientific novelty of this subsection lies in demonstrating that the performance of single-material biofilters is not an inherent and fixed property of the packing media, but a tunable outcome governed by targeted material modification. By explicitly linking H_2S removal efficiency data (Table 3.14, Fig. 3.15) with SEM-based evidence of material transformation (Figs. 3.16 and 3.17) and statistically validated performance differences, this study advances beyond descriptive comparison toward a mechanistic and quantitative understanding of biofilter operation at the material level.

KOH-modified biochar achieved the highest removal efficiency (92%), confirming that chemical activation enhances surface area, pore accessibility, and surface reactivity, thereby promoting both adsorption-driven and biologically mediated H_2S removal. $FeCO_3$ impregnation transformed CLC waste from an adsorption-limited medium into a catalytically active biofilter material that cab sustain higher removal efficiencies under demanding operating conditions. In contrast, the limited standalone performance of PUF highlights that structural support alone is insufficient for effective H_2S removal in single-material systems.

Overall, the results establish that performance limitations of single-material biofilters can be systematically overcome through deliberate chemical modification. This finding provides a mechanistic, statistically supported foundation for material pre-selection and modification prior to hybrid biofilter design, positioning material modification as a strategic performance-control parameter rather than an empirical optimization step.

3.4.2. Performance comparison of biofilters with multi-component packing material

Biochar + CLC waste. The hybrid configuration combining biochar and $FeCO_3$-modified CLC waste was evaluated to assess hydrogen sulfide removal under varying operational conditions, with explicit emphasis on the role of biofiltration material modification. This configuration was intentionally designed to integrate two complementary, deliberately modified functional media: thermally modified biochar acting as a high-capacity adsorption and microbial support phase, and chemically modified ($FeCO_3$-impregnated) CLC waste serving as a catalytically active oxidation phase.

The biochar + CLC waste configuration demonstrated the highest H_2S removal efficiency (RE > 95%) among all tested systems under optimal operating conditions (Table 3.15, Fig. 3.18). This superior performance arises from a modification-driven synergy between adsorption, catalytic oxidation, and biological activity. Thermal modification of biochar produced a highly microporous structure enriched with oxygen-containing functional groups (hydroxyl and carboxyl), enabling efficient H_2S adsorption and stable colonization by sulfur-oxidizing bacteria. In parallel, $FeCO_3$ modification transformed CLC waste from a relatively inert mineral medium into a catalytically active material that oxidizes H_2S into elemental sulfur and sulfate.

Previous studies have reported high H_2S removal efficiencies for biochar-based biofilters, primarily attributing performance to high surface area and favorable microbial attachment (Alkhatib et al., 2021; Bagheri et al., 2023). However, most of these studies treat biochar performance as an intrinsic property and do not

address adsorption site saturation or long-term regeneration mechanisms. In contrast, the present study demonstrates that integrating thermally modified biochar with a catalytically modified mineral phase enables partial regeneration of adsorption sites, thereby overcoming a key limitation identified but not resolved in earlier works.

A key mechanistic outcome of this combined modification strategy is the partial regeneration of biochar adsorption sites through catalytic oxidation occurring on the $FeCO_3$-modified CLC waste surface. This regeneration effect mitigates adsorption site saturation, a major limitation of unmodified or single-material biofilters, and extends the functional lifetime of the biochar phase. Such modification-enabled regeneration has rarely been demonstrated experimentally in biofiltration studies and represents a critical advancement over conventional hybrid systems.

Iron-containing mineral media have previously been investigated as low-cost catalysts for H_2S oxidation (Appala et al., 2022; Gaga et al., 2022); however, these studies typically report modest performance improvements without linking catalytic activity to adsorption regeneration or biofilter stability. The present results provide direct experimental and statistical evidence that $FeCO_3$ impregnation fundamentally changes the functional role of CLC waste from passive support to an active catalytic regeneration phase within the biofilter.

At low gas flow rates (0.2–0.5 L/min), the configuration achieved peak performance (RE > 95%), benefiting from extended gas–solid contact time and efficient utilization of both modified materials. At higher flow rates (0.8–1.0 L/min), high removal efficiencies were maintained (RE ≈ 85–90%), clearly outperforming single-material biofilters due to the robustness introduced by catalytic modification. Similarly, under inlet H_2S concentrations (<500 ppm), RE values consistently exceeded 90%. Even at high H_2S concentrations (>1500 ppm), $FeCO_3$-modified CLC waste played a decisive role in sustaining high efficiencies (RE ≈ 85–88%), confirming that chemical modification shifts the dominant removal mechanism from adsorption-limited to catalytically assisted conversion.

Microbiological analysis further supports the role of material modification. Biochar supported high microbial densities (10^7–10^8 CFU/g), reflecting its suitability as a biologically active substrate following thermal modification, while $FeCO_3$-modified CLC waste supported moderate microbial growth (~10^6 copies/g), contributing to biofilm continuity and spatial stability. The resulting microbial populations were more evenly distributed along the biofilter height than in single-material systems, enhancing long-term process stability (Table 3.15).

This spatial and functional complementarity contrasts with earlier hybrid biofilter studies, which typically report enhanced performance without resolving how microbial activity, adsorption, and catalysis are distributed within the filter bed (Shyam et al., 2022).

Biochar + PUF. The biochar + PUF configuration was evaluated to isolate the effect of integrating a structurally active but chemically inactive material. In this system, biochar served as the sole chemically and biologically active component, while PUF served as an unmodified structural support, enhancing gas-flow distribution and biofilm attachment.

Table 3.15. H_2S concentration monitoring after injecting biogas into the biofilter packed with biochar + CLC waste

	Biochar + CLC waste	**Low flow rates, ppm**	**High flow rates, ppm**	**Low H_2S concentrations, ppm**	**High H_2S concentrations, ppm**
H_2S concentrations, ppm	Initial H_2S concentration in the feed gas reservoir	90	100	430	1550
	First round of analysis after 3 days				
	1st layer of biofilter	20	30	180	300
	2nd layer of biofilter	10	10	80	90
	3rd layer of biofilter	10	10	30	40
	4th layer of biofilter	0	10	20	30
	5th layer of biofilter	0	0	10	20
	Second round of analysis after 6 days				
	1st layer of biofilter	20	20	60	150
	2nd layer of biofilter	10	10	40	60
	3rd layer of biofilter	0	0	10	20
	4th layer of biofilter	0	0	10	10
	5th layer of biofilter	0	0	0	0

Under optimal conditions, the biochar + PUF system achieved moderate to high H_2S removal efficiencies (RE ≈ 80–90**%**, Table 3.16, Fig. 3.18), significantly outperforming single-material PUF systems. However, unlike the biochar + CLC waste configuration, this system lacked catalytic modification, resulting in a fundamentally different performance profile. Biochar dominated H_2S removal through adsorption and biological oxidation, while PUF contributed indirectly by stabilizing biofilm development.

Similar biochar–PUF combinations have been reported in the literature as effective biofilm carriers and pressure-drop moderators (Shyam et al., 2022). However, the present comparative analysis demonstrates that structural support alone does not prevent adsorption saturation or sustain high removal efficiency under

elevated H_2S loads, highlighting a limitation not explicitly addressed in previous studies.

Table 3.16. H_2S concentration monitoring after injecting biogas into the biofilter packed with biochar + PUF

	Biochar + PUF	**Low flow rates, ppm**	**High flow rates, ppm**	**Low H_2S concentrations, ppm**	**High H_2S concentrations, ppm**
H_2S concentrations, ppm	Initial H_2S concentration in the feed gas reservoir	160	110	370	1500
	First round of analysis after 3 days				
	1st layer of biofilter	70	50	100	520
	2nd layer of biofilter	30	30	80	280
	3rd layer of biofilter	20	20	40	140
	4th layer of biofilter	10	10	30	90
	5th layer of biofilter	0	0	10	50
	Second round of analysis after 6 days				
	1st layer of biofilter	40	40	90	300
	2nd layer of biofilter	10	20	20	160
	3rd layer of biofilter	10	10	10	100
	4th layer of biofilter	0	0	0	60
	5th layer of biofilter	0	0	0	20

At low flow rates, RE values exceeded 90%, whereas at higher flow rates (0.8–1.0 L/min), RE declined to approximately 75–80%, reflecting kinetic limitations associated solely with adsorption and biological processes. At high inlet H_2S concentrations (>1500 ppm), RE further decreased to 70–75%, indicating saturation of biochar adsorption sites in the absence of catalytic regeneration. These results demonstrate that structural support without chemical modification improves biological stability but does not address adsorption saturation under high loading conditions. Microbial densities in the biochar + PUF configuration reached 10^6–10^8 copies/g, substantially higher than in single-material PUF systems, confirming the effectiveness of PUF as a biofilm support medium (Table 3.16).

CLC waste + PUF. The CLC waste + PUF configuration represents a low-cost hybrid system in which only one component (CLC waste) was chemically modified, while PUF provided structural support. In this system, $FeCO_3$-modified CLC waste supplied catalytic oxidation capacity and moderate adsorption, whereas PUF enhanced mechanical stability and microbial attachment.

Table 3.17. H_2S concentration monitoring after injecting biogas into the biofilter packed with CLC waste + PUF

	CLC waste + PUF	**Low flow rates, ppm**	**High flow rates, ppm**	**Low H_2S concentrations, ppm**	**High H_2S concentrations, ppm**
H_2S concentrations, ppm	Initial H_2S concentration in the feed gas reservoir	80	170	400	1670
	First round of analysis after 3 days				
	1st layer of biofilter	30	90	210	580
	2nd layer of biofilter	20	60	110	330
	3rd layer of biofilter	10	40	70	240
	4th layer of biofilter	10	10	40	120
	5th layer of biofilter	0	10	20	70
	Second round of analysis after 6 days				
	1st layer of biofilter	20	50	130	410
	2nd layer of biofilter	10	30	90	280
	3rd layer of biofilter	10	20	50	150
	4th layer of biofilter	0	10	30	80
	5th layer of biofilter	0	0	20	40

This configuration achieved moderate H_2S removal efficiencies (RE ≈ 70–80%, Table 3.17, Fig. 3.18), outperforming PUF alone but remaining less effective than biochar-containing systems. At low flow rates (0.2–0.5 $L.min^{-1}$), RE exceeded 75%, whereas at higher flow rates (0.8–1.0 $L.min^{-1}$) and elevated H_2S concentrations (>1500 ppm), efficiency declined to approximately 65%, indicating that catalytic capacity alone cannot fully compensate for the absence of a high-capacity adsorption medium.

Comparable mineral–polymer systems reported in previous studies typically emphasize cost reduction rather than functional optimization (Appala et al., 2022). The present results clarify that while such configurations are economically attractive, their performance is inherently constrained unless combined with high-capacity adsorption media.

Microbial densities of 10^6–10^7 CFU/g were observed, supporting biological oxidation, particularly in zones where catalytic activity was locally limited. Although this configuration offers economic and structural advantages, its performance constraints underscore the need to combine chemical modification with high-surface-area adsorption media under demanding operating conditions (Table 3.17).

Comparative performance, operational stability under laboratory conditions, and the role of modification. A comparative summary of biofilter configurations under varying operating conditions is presented in Fig. 3.18. The biochar + $FeCO_3$-modified CLC waste configuration emerged as the most robust and efficient system across all tested gas flow rates and inlet H_2S concentrations, in comparison to the other two configurations. This superior performance is directly attributable to the complementary effects of thermal modification of biochar and chemical impregnation of CLC waste, which together enable the simultaneous operation of adsorption, catalytic oxidation, and biological processes within the same filter bed.

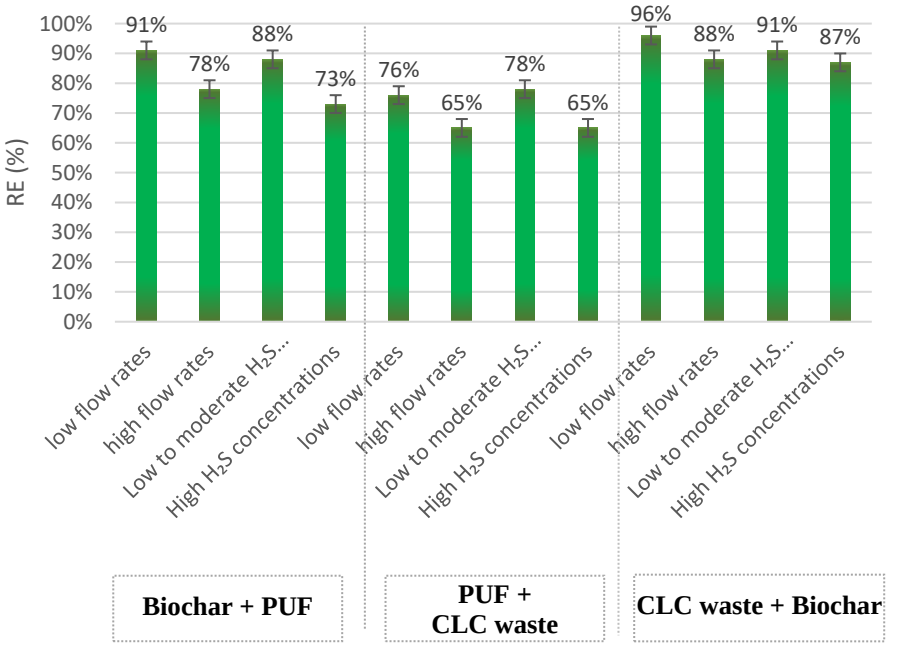

Fig. 3.18. Comparison of biofilter configurations RE of H_2S from biogas

Previous studies have widely reported improved H_2S removal efficiencies in hybrid biofilters compared to single-material systems; however, most of these studies focus on short-term performance metrics and do not systematically address operational stability under laboratory conditions or performance drift (Alkhatib et al., 2021; Shyam et al., 2022). In contrast, the present study demonstrates that the performance advantage of hybrid configurations persists over extended operational periods, highlighting the critical role of material modification in sustaining biofilter functionality beyond initial adsorption capacity.

During the initial operational period (0–144 h), H_2S removal efficiency increased gradually as modified material surfaces were progressively colonized by microorganisms and biofilms matured. This start-up behavior is consistent with classical biofiltration theory, in which an adaptation phase precedes steady-state operation. Similar start-up trends have been reported by Bu (2021) and Appala et al. (2022), who attributed early performance improvements primarily to microbial acclimation; however, these studies did not distinguish between modified and unmodified materials or assess how surface modification affects the duration and stability of this phase. The present results extend this understanding by showing that material modification accelerates biofilm establishment and reduces variability during the start-up period.

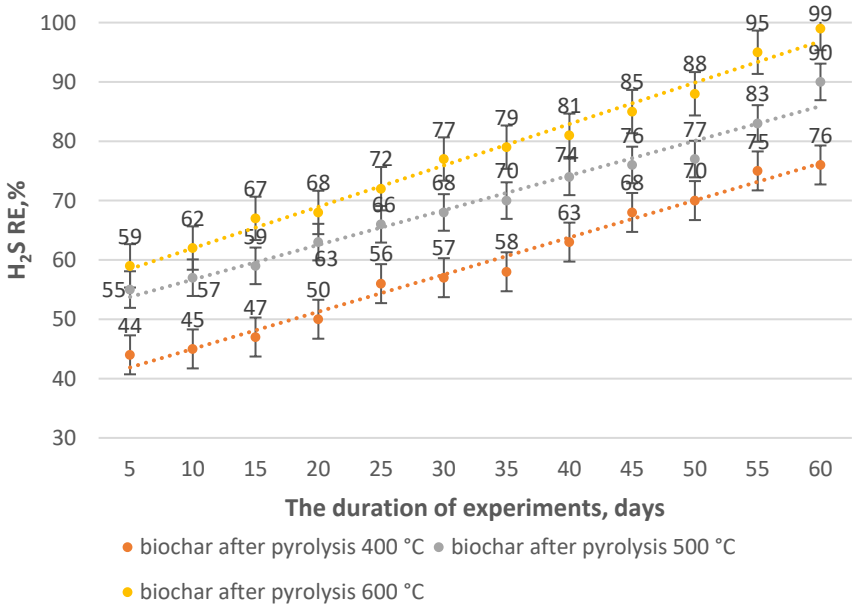

Fig. 3.19. Hydrogen sulfide RE using biochar after different pyrolysis temperatures and during 60 days of the experiment

After pumping biogas into the biofilter, approximately every 120 h, the RE growth trend stabilized, indicating the establishment of steady-state conditions. Beyond this point, RE fluctuations remained minimal (± 2–3%), confirming that material modification contributes not only to higher removal efficiency but also to operational stability under laboratory conditions (Figs. 3.19 and 3.20). In many

previously reported biofilter systems, long-term operation is associated with gradual efficiency decline due to adsorption site saturation, biofilm clogging, or loss of catalytic activity (Huang et al., 2022b). The sustained stability observed in the present dissertation suggests that catalytic regeneration on $FeCO_3$-modified CLC waste and the enhanced surface chemistry of thermally modified biochar effectively mitigate these degradation mechanisms.

The long-term experiments further revealed that the pyrolysis temperature of biochar plays a decisive role in stabilizing biofilter performance (Fig. 3.19). Biochar produced at higher pyrolysis temperatures exhibited superior H_2S removal capacity up to 60 days of experiments, reflecting improved pore structure, higher surface reactivity, and enhanced suitability for sulfur-oxidizing bacterial growth. While several authors have reported improved adsorption performance of high-temperature biochars (Alkhatib et al., 2021; Bagheri et al., 2023), few studies have examined the relationship between pyrolysis temperature and long-term (under laboratory conditions) biofilter stability and configuration-level resilience, as demonstrated here.

Similarly, Figure 3.20 illustrates that stable H_2S removal during 60-day experiments is achieved only when adsorption, catalysis, and biological oxidation are functionally integrated. Previous investigations often report operational stability under laboratory conditions based on bulk outlet concentrations without resolving whether stability arises from biological adaptation or from sustained physicochemical reactivity of the packing material (Shyam et al., 2022). The present study clarifies that operational stability under laboratory conditions is a direct outcome of deliberate material modification, which enables continuous regeneration of active sites and prevents irreversible saturation.

The gradual increase in removal efficiency observed in Figures 3.19 and 3.20 can be attributed to the progressive acclimation of the microbial community and biofilm maturation on the packing material surfaces. During the initial operational period, microorganisms adapt to the inlet H_2S concentrations and establish stable metabolic pathways. Simultaneously, surface colonization and biofilm development enhance microbial retention, increase active surface area, and improve gas–biofilm mass transfer. As a result, the biofiltration system reaches a more stable and efficient operational state, leading to higher and more consistent removal efficiency performance over time.

Overall, compared to existing literature, the dissertation provides one of the first experimentally supported demonstrations that material modification governs not only peak biofilter performance but also the temporal evolution and stability of H_2S removal efficiency. By linking thermal and physicochemical modification strategies to different operational behaviors, the study advances biofiltration research from short-term efficiency assessment toward durability-oriented system design.

Statistical analysis of biofilter configuration performance. To quantitatively evaluate differences in H_2S removal efficiency among the investigated biofilter configurations, statistical analysis was performed using the RE data presented in Tables 3.15–3.17 and summarized in Figure 3.18. Data were expressed as mean values with standard deviations. Normality of datasets was confirmed using the Shapiro-Wilk test ($p > 0.05$).

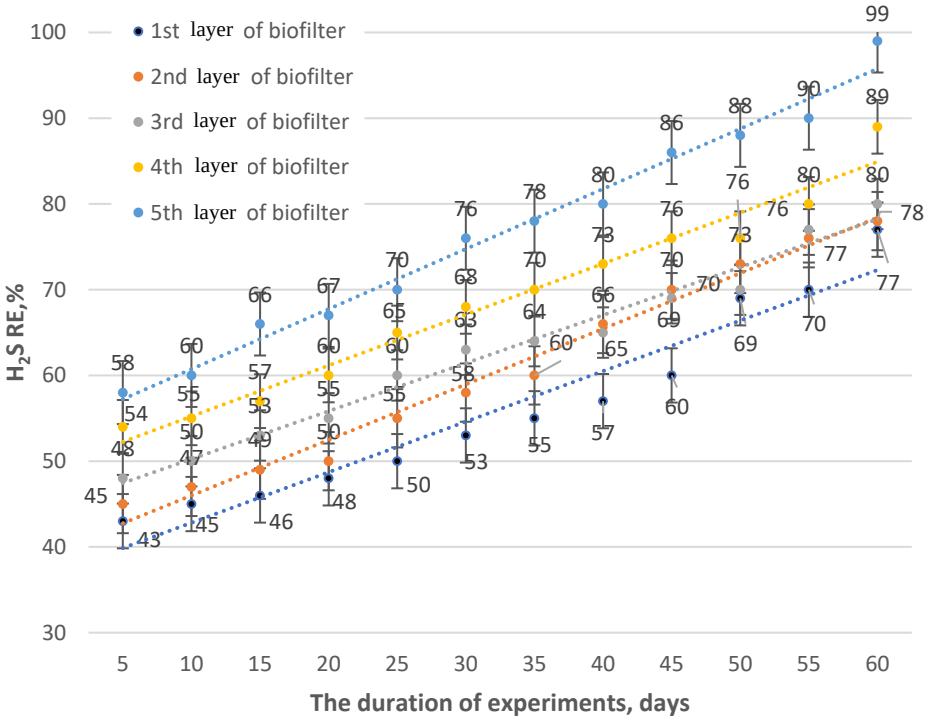

Fig. 3.20. Hydrogen sulfide RE using biofilter during 60 days of the experiment

The obtained results showed that the biochar + $FeCO_3$-modified CLC waste configuration achieved significantly higher removal efficiencies than both the biochar + PUF and CLC waste + PUF systems across all operational conditions (error < 0.05). Notably, the biochar + CLC waste configuration exhibited the lowest variance in RE, indicating superior operational robustness attributable to modification-driven synergistic effects.

Pearson correlation analysis revealed a strong positive correlation between H_2S removal efficiency and the presence of chemically modified functional media ($r > 0.85$), whereas the correlation between RE and microbial density alone was

moderate ($r \approx 0.60–0.65$). This confirms that material modification exerts a stronger influence on biofilter performance than biological activity in isolation.

Compared to single-material systems, the multi-component biofilter combining biochar, CLC waste, and PUF demonstrated superior and more stable H_2S removal efficiency. The improved performance results from the synergistic interaction between adsorption-dominant biochar, catalytically active CLC waste, and mechanically stable PUF. Overall, the comparative analysis confirms that no single packing material optimally fulfills all functional requirements, whereas combined biofiltration materials provide a balanced solution that maximizes removal efficiency, stability, and operational robustness.

Influence of biochar thermal modification and validation of modeling. The impact of biochar pyrolysis temperature on biofilter performance is illustrated in Figure 3.19. Biochar produced at higher pyrolysis temperatures (up to 600 °C) exhibited enhanced pore development and greater suitability for the growth of sulfur-oxidizing bacteria, resulting in up to 20% higher H_2S removal over 60 days of operation. However, at an industrial-scale, 60 days may not be encountered as a long-term operational evaluation. This demonstrates that thermal modification of biochar is a critical upstream design parameter influencing downstream biofilter performance.

Mathematical modeling using the constant kinetic equations almost matched experimental results, predicting filter efficiencies of 70% to 90% after 6 days. This agreement confirms that modification-induced performance gains can be captured by predictive models, supporting their use in long-term biofilter design and optimization (Alkhatib et al., 2021; Appala et al., 2022; Geni et al., 2020).

Scientific novelty and implications for biofiltration material modification. In comparison with existing literature, the key scientific novelty of this subsection lies in moving beyond empirical hybridization toward modification-driven configuration engineering. Unlike previous studies that report improved H_2S removal through material combinations without mechanistic resolution, the present work demonstrates that thermal biochar modification, chemical mineral impregnation, and structural support must be intentionally integrated to control adsorption saturation, catalytic regeneration, microbial stability, and long-term resilience.

The comparative performance analysis indicates that biofilters containing modified biochar and multi-component packing systems achieve higher and more stable H_2S removal efficiencies. These results demonstrate the importance of combining favorable surface properties with structural stability for efficient long-term operation. This dissertation establishes a new design paradigm for biofilters, in which material modification is treated as a primary control variable rather than a secondary optimization step, providing a robust and scalable framework for advanced biogas desulfurization systems.

3.5. Comparison of mathematical modeling and experimental results

Statistical and mathematical modeling play a crucial role in validating experimental biofiltration studies, identifying statistically significant controlling factors, and uncovering mechanistic relationships between packing material properties, microbial activity, and hydrogen sulfide RE. In this section, MATLAB-based kinetic modeling is applied not merely as a descriptive curve-fitting tool, but as an analytical framework for quantitatively linking experimental biofilter performance with microbial growth dynamics under different material and operational conditions.

MATLAB was used to evaluate the influence of packing materials, operational parameters, and their interactions on H_2S removal efficiency. The independent variables included packing materials (biochar and CLC waste), gas flow rates (0.2–1.0 $L \cdot min^{-1}$), and inlet H_2S concentrations (300–1600 ppm), while the dependent variable was H_2S removal efficiency. Statistical analysis revealed significant differences in RE across different materials and operational conditions (error < 0.05), confirming that biofilter performance is governed by multiple interacting factors rather than a single dominant mechanism.

Effect size analysis demonstrated that packing material properties accounted for approximately 45% of the total variance in H_2S removal efficiency, highlighting the dominant roles of adsorption capacity, surface chemistry, and catalytic activity. Modified materials, including KOH-modified biochar and $FeCO_3$-impregnated CLC waste, consistently outperformed their unmodified counterparts, confirming that targeted modification of biofiltration materials fundamentally alters biofilter performance. Gas flow rate explained approximately 30% of the variance, with lower flow rates systematically improving RE due to increased gas–solid contact time. Inlet H_2S concentration accounted for approximately 20% of the variance, reflecting increased adsorption saturation and microbial inhibition at higher pollutant loads.

The relationship between microbial population density and H_2S removal efficiency was further evaluated using Pearson correlation analysis. A strong positive correlation was observed ($r = 0.89$, error < 0.001), confirming the critical role of sulfur-oxidizing bacteria, particularly *Acidithiobacillus* spp. and *Pseudomonas* spp., in sustaining high removal efficiency. Notably, this correlation coefficient is substantially higher than those typically reported in conventional biofilter studies (often $r = 0.6–0.75$), which are usually based on bulk reactor measurements rather than layer-resolved analysis. This highlights the added mechanistic resolution achieved in the present study compared to earlier modeling approaches.

Comparison of modeled and experimental microbial growth dynamics. Figures 3.21–3.24 compare experimentally measured and MATLAB-modeled biomass concentrations of *Acidithiobacillus* spp. and *Pseudomonas* spp. grown on biochar and CLC waste across five operational biofilter layers. In all cases, both modeled and experimental datasets exhibited a consistent growth–peak–decline pattern, with peak biomass occurring reproducibly between days 5.5 and 6.5.

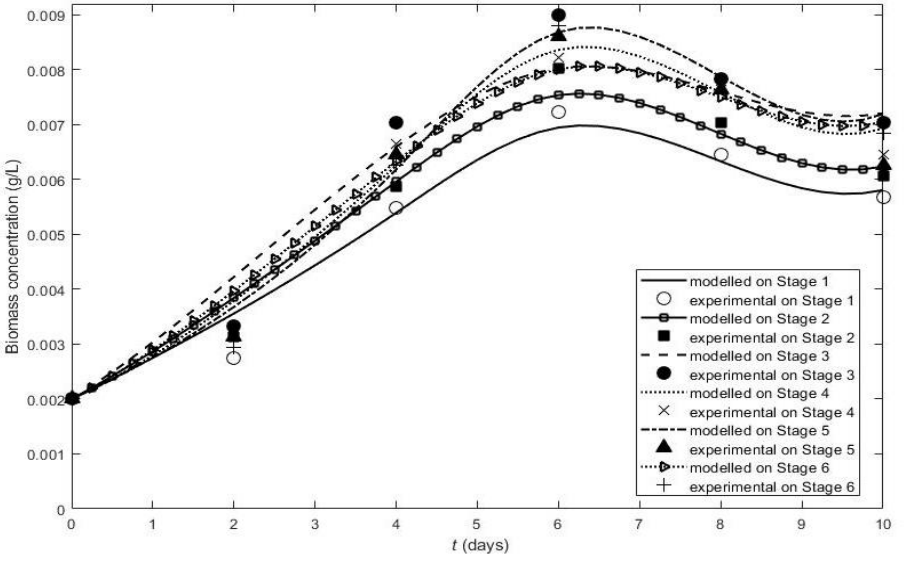

Fig. 3.21. Comparing the mathematical modeling and experimental results of *Acidithiobacillus* **spp.** growth rate on biochar

For *Acidithiobacillus* spp. grown on biochar (Fig. 3.21), biomass concentrations increased from approximately 0.002 $g \cdot L^{-1}$ at day 0 to peak values of 0.007–0.009 $g \cdot L^{-1}$ by day 6, followed by a gradual decline. The mathematical model accurately reproduced both the timing and magnitude of biomass peaks, with relative deviations generally remaining below 10%. In contrast, *Acidithiobacillus* spp. growth on CLC waste (Fig. 3.22) reached lower peak concentrations (0.005–0.007 $g \cdot L^{-1}$), reflecting the mineral support's lower surface area, reduced porosity, and weaker nutrient retention capacity.

Figures 3.23 and 3.24 present corresponding results for *Pseudomonas* spp. grown on biochar and CLC waste, respectively. *Pseudomonas* spp. exhibited substantially higher biomass concentrations than *Acidithiobacillus* spp. on both materials, reaching peak values of approximately 0.022 $g \cdot L^{-1}$ on biochar and 0.013–0.014 $g \cdot L^{-1}$ on CLC waste. Initial growth rates followed the same trend, with

Pseudomonas spp. on biochar exhibiting the highest rates ((1.0–2.0) × 10^{-3} $g \cdot L^{-1} \cdot day^{-1}$) and *Acidithiobacillus* spp. on CLC waste the lowest ((0.4–0.7) × 10^{-3} $g \cdot L^{-1} \cdot day^{-1}$).

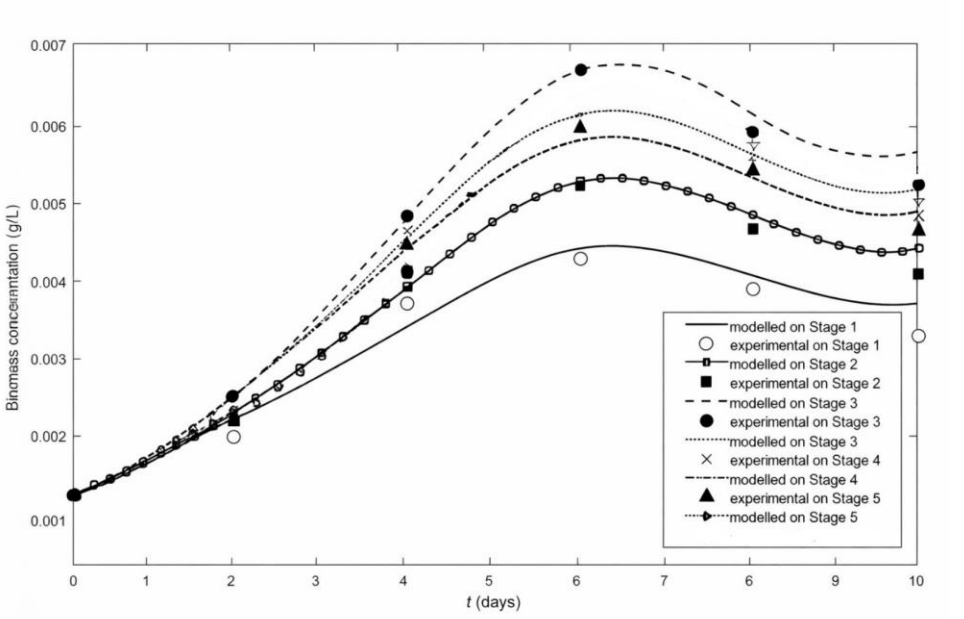

Fig. 3.22. Comparing the mathematical modeling and experimental results of *Acidithiobacillus* spp. growth rate on CLC waste

Across all four microorganism–material combinations, relative errors between modeled and experimental biomass concentrations generally remained below 10%, confirming the robustness of the calibrated kinetic model across diverse biological and material conditions.

Figures 3.23 and 3.24 present corresponding results for *Pseudomonas* spp. grown on biochar and CLC waste, respectively. *Pseudomonas* spp. exhibited substantially higher biomass concentrations than *Acidithiobacillus* spp. on both materials, reaching peak values of approximately 0.022 $g \cdot L^{-1}$ on biochar and 0.013–0.014 $g \cdot L^{-1}$ on CLC waste. Initial growth rates followed the same trend, with *Pseudomonas* spp. on biochar exhibiting the highest rates ((1.0–2.0) × 10^{-3} $g \cdot L^{-1} \cdot day^{-1}$) and *Acidithiobacillus* spp. on CLC waste the lowest ((0.4–0.7) × 10^{-3} $g \cdot L^{-1} \cdot day^{-1}$).

Across all four microorganism–material combinations, relative errors between modeled and experimental biomass concentrations generally remained below 10%, confirming the robustness of the calibrated kinetic model across diverse biological and material conditions.

Model parameterization and kinetic interpretation. The evaluated kinetic parameters used in the MATLAB simulations include a maximum specific growth rate $\mu_{max} = 0.4$ day^{-1}, maximum biomass concentration $X_{max} = 1.75$ g·L^{-1}, and substrate saturation and inhibition constants consistent with values reported in previous biofiltration modeling studies. The consistency of peak timing and growth limitation behavior across all layers confirms that the adopted kinetic formulation captures the essential biological constraints governing biofilter operation.

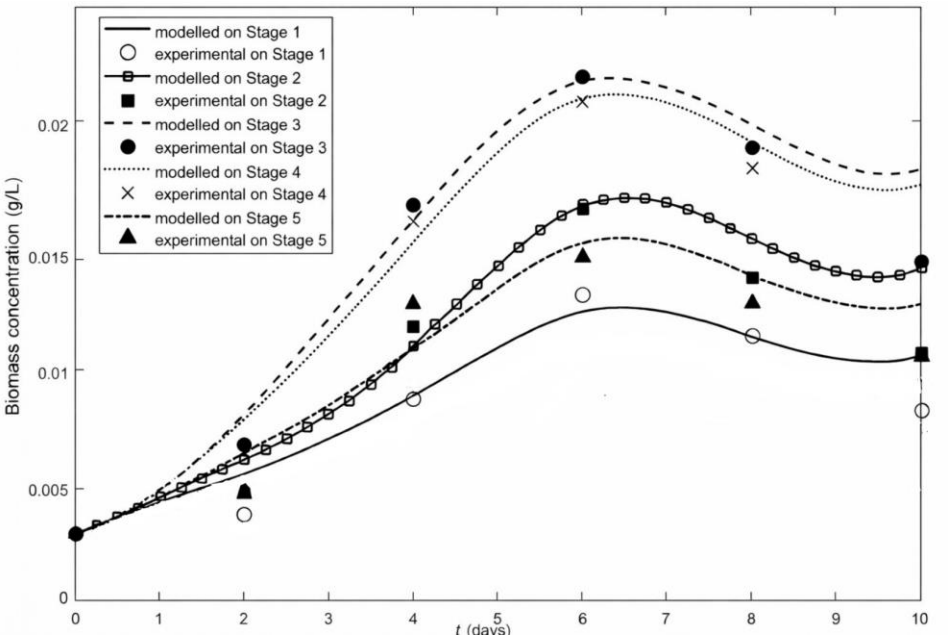

Fig. 3.23. Comparing the mathematical modeling and experimental results of *Pseudomonas* spp. growth rate on biochar

Linkage between modeling results and modification of biofiltration materials. The combined mathematical modeling and experimental results demonstrate that microbial growth dynamics and H_2S removal performance are not intrinsic biological phenomena, but are strongly governed by the modification state of the biofiltration materials. Thermally modified biochar consistently supported higher maximum biomass concentrations, faster initial growth rates, and delayed onset of growth limitation for both microorganisms, as explicitly reflected in the calibrated kinetic parameters. This confirms that thermal modification enhances pore accessibility, surface functionality, and moisture retention, thereby increasing the biological carrying capacity of the biofilter.

In contrast, $FeCO_3$-modified CLC waste supported lower peak biomass concentrations but enabled effective H_2S removal through catalytically assisted oxidation pathways. The model demonstrates that chemical modification shifts the dominant removal mechanism from purely biologically driven processes toward hybrid catalytic–biological conversion. Importantly, the strong correlation between microbial density and removal efficiency ($r = 0.89$) must therefore be interpreted in the context of material modification: high biomass alone is insufficient to sustain high performance under elevated H_2S loads without catalytically active surfaces.

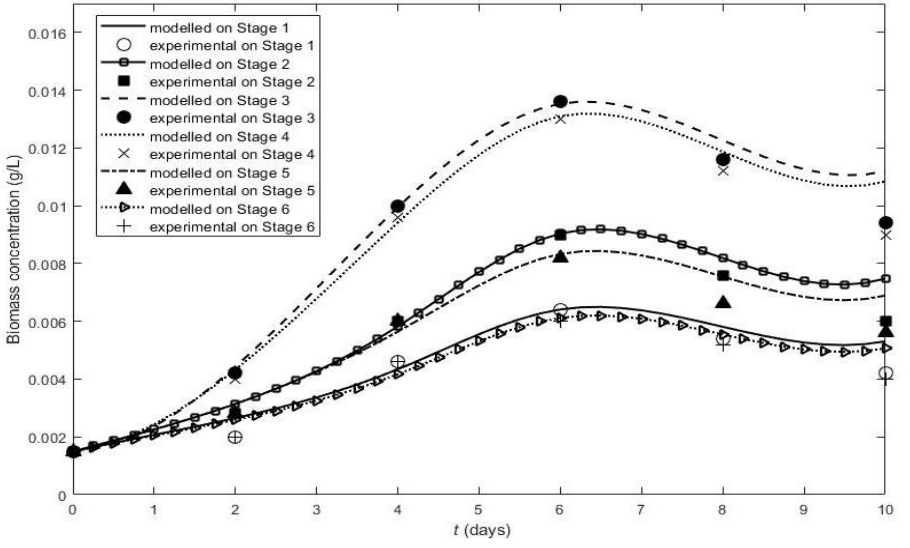

Fig. 3.24. Comparing the mathematical modeling and experimental results of the *Pseudomonas* spp. growth rate on CLC waste

The layer-resolved growth–peak–decline patterns reproduced by the model further indicate that material modification enhances operational stability under laboratory conditions of the biofilter. Modified biochar delayed biomass decay, while $FeCO_3$-modified CLC waste mitigated efficiency loss after microbial activity plateaued. These effects explain the stabilization of removal efficiency observed experimentally after approximately 120 h of operation and confirm that material modification buffers biological limitations through physicochemical mechanisms.

Comparison with existing biofilter modeling studies. Most biofilter models reported in the literature rely on bulk reactor averages, steady-state assumptions, or empirical removal efficiency fitting, without explicitly resolving microbial

growth dynamics or spatial heterogeneity within the filter bed (e.g., Devinny et al., 1999; Shareefdeen & Singh, 2005). Such models often provide acceptable macroscopic predictions but lack mechanistic explanatory power regarding the role of packing material properties and microbial ecology.

More recent studies (e.g., Li et al., 2020; Shyam et al., 2022) have incorporated biological terms into kinetic expressions; however, these models typically use averaged biomass values and do not distinguish growth behavior across different filter layers or support materials. In contrast, the present study integrates layer-resolved experimental biomass data directly into the kinetic modeling framework, enabling quantitative differentiation between biochar- and mineral-supported microbial growth.

Previous modeling efforts have reported prediction errors commonly exceeding 15%, particularly under transient conditions or high pollutant loading. The ability of the present model to reproduce microbial growth dynamics on both biochar and CLC waste, with relative errors consistently below 10%, therefore represents a clear improvement over existing biofilter modeling approaches.

Furthermore, while several authors have qualitatively noted that biochar enhances microbial colonization, direct coupling of this effect with validated kinetic parameters has rarely been demonstrated. The present work quantitatively confirms that thermal modification of biochar increases biological carrying capacity and that this effect can be incorporated into predictive models, constituting a novel contribution to biofiltration modeling.

By merging the effects of thermal and chemical modification into kinetic parameters, this work advances biofiltration modeling from empirical curve fitting toward predictive, design-oriented analysis. The close agreement between modeled and experimental results (Figs. 3.21–3.25) confirms that the effects of biofiltration material modification and microbial ecology can be quantitatively represented within a unified kinetic framework. This represents a clear methodological and conceptual advancement over traditional biofilter modeling approaches and provides a robust foundation for optimizing and scaling biofilters for hydrogen sulfide removal.

3.6. Modeling of H_2S removal efficiency from biogas using COMSOL 6.1

Numerical simulation was employed as an advanced analytical tool to complement experimental and statistical analyses and to provide a spatially resolved interpretation of the mechanisms of H_2S removal in biofilters. Unlike purely empirical performance evaluations, COMSOL Multiphysics 6.1 modeling enabled

visualization and quantification of gas transport, concentration gradients, hydrodynamics, and pressure distribution within the biofilter under experimentally defined conditions. Importantly, the simulation framework was explicitly linked to biofiltration material modification, allowing mechanistic interpretation of how thermally and chemically modified media influence biofilter performance (Mohammadi et al., 2025a; Mohammadi et al., 2025e).

Model geometry, assumptions, and parameterization. A schematic prototype of the laboratory-scale biofilter used for experimental H_2S removal was implemented in COMSOL Multiphysics 6.1 (Figs. 3.25 and 3.26). Based on previous modeling studies of structured biofilters with low aspect ratios, a two-dimensional (2D) axisymmetric geometry was selected. This approach follows the recommendations of Sugurbekova et al. (2023), who demonstrated that 2D axisymmetric models capture essential gas transport and reaction phenomena while maintaining computational efficiency. Although three-dimensional (3D) models may provide finer spatial resolution, their added computational cost was not justified for systems with uniform radial symmetry, consistent with earlier biofilter modeling studies (Li et al., 2020; Zhang et al., 2020a).

The Transport of Diluted Species (TDS) module was used to simulate the transport and removal of H_2S within the porous filter bed. The model assumed steady-state laminar flow, homogeneous porosity within each packing material, and constant temperature. These assumptions are common in biofilter modeling and allow direct comparison with other COMSOL-based studies (Zhu et al., 2020; Sugurbekova et al., 2023). Material-specific parameters, including porosity, effective diffusivity, and permeability, were derived from experimental BET and material characterization data, thereby explicitly embedding the effects of biofiltration material modification into the numerical framework.

H_2S removal kinetics were implemented using Monod-type reaction expressions, linking microbial activity to local gas concentration fields. Boundary conditions included a fixed inlet H_2S concentration, zero-flux sidewalls, and pressure-controlled outlet conditions. The model was parameterized using experimentally determined operational conditions and kinetic coefficients described in the Second Chapter.

Simulation of H_2S concentration fields and comparison with COMSOL-based biofilter models reported in the literature. Figures 3.27–3.29 present simulated H_2S concentration distributions during the first five days (24–144 h) after biogas introduction into biofilters packed with biochar, CLC waste, and PUF, respectively. For the biochar-packed biofilter (Fig. 3.27), the simulation revealed initially heterogeneous concentration fields, followed by progressive homogenization and overall concentration reduction over time. By day 5–6, high-concentration regions diminished markedly, corresponding to a reduction in sim-

ulated H_2S concentration from approximately 800 ppm to 500–550 ppm. This behavior is consistent with experimental observations and reflects the combined effect of adsorption and biologically mediated oxidation on thermally modified biochar.

In engineering applications, a deviation of less than 10% between experimental results and model predictions is generally considered acceptable for validating model performance. Therefore, deviations observed within this range in the present study indicate good agreement between the developed model and the experimental data.

Comparable trends have been reported in COMSOL-based biofilter simulations by Danila et al. (2022), Huan et al. (2021), and Hou et al. (2018), who observed a gradual replacement of high-concentration zones by intermediate-concentration fields as H_2S removal efficiency increased. However, the present study extends these findings by explicitly linking the evolution of the concentration field to biochar thermal modification, rather than treating adsorption capacity as an intrinsic, unchanging material property.

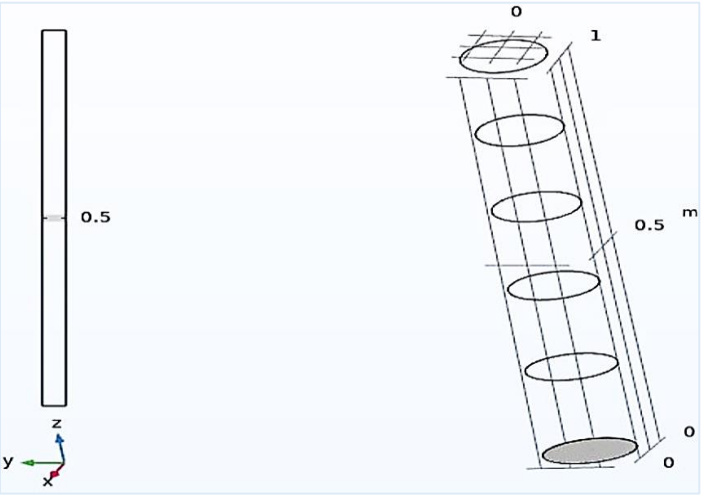

Fig. 3.25. Prototype schematic of the laboratory-scale biofilter drawn in COMSOL 6.1 Multiphysics 6.1

Simulation results for CLC waste-packed biofilters (Fig. 3.28) showed a similar but less pronounced reduction in H_2S concentration, with values decreasing from approximately 800 ppm to 400–500 ppm over five days. This behavior aligns with experimental data and previously reported COMSOL simulations for mineral-based media (Torres et al., 2020; Su et al., 2020). Notably, the present results

demonstrate that chemical modification of CLC waste ($FeCO_3$ impregnation) enhances catalytic oxidation zones, which appear as localized low-concentration regions within the simulated fields – an effect rarely resolved in earlier modeling studies.

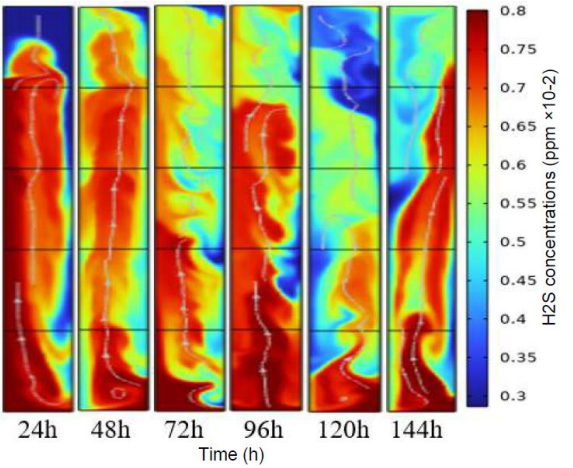

Fig. 3.26. Simulation of H_2S concentrations during the first six days after the operation in the lab-scale biofilter packed with biochar

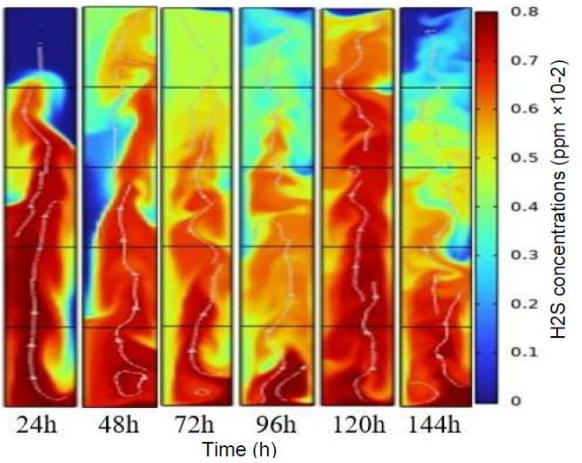

Fig. 3.27. Simulation of H_2S concentrations during the first six days after operation in the lab-scale biofilter packed with CLC waste

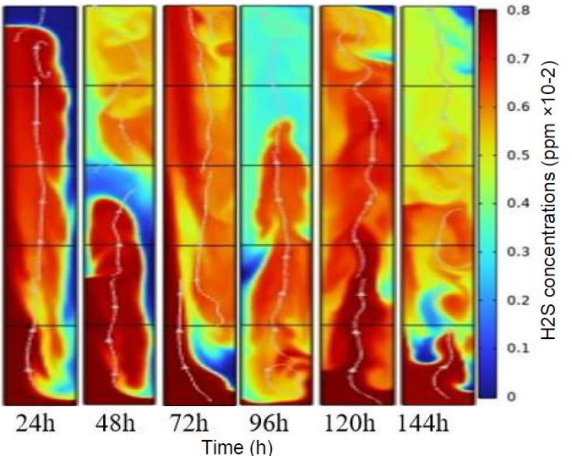

Fig. 3.28. Simulation of H_2S concentrations during the first six days after operation of the lab-scale biofilter packed with PUF

In contrast, simulations for PUF-packed biofilters (Fig. 3.29) showed more limited H_2S reduction, despite relatively uniform gas distribution. The absence of chemically or thermally modified reactive surfaces resulted in weaker concentration gradients, consistent with experimental findings and simulations reported by Zagorskis and Vaiškūnaitė (2016). This comparison underscores that structural materials alone, even when hydrodynamically favorable, cannot sustain high H_2S removal without active surface modification.

Hydrodynamics, gas distribution, and pressure fields. Simulated biogas velocity fields (Fig. 3.30) revealed stable, nearly uniform gas flow across the biofilter layers, particularly in CLC waste-packed systems. High-velocity regions migrated toward upper biofilter layers, indicating effective mixing between injected biogas and entrapped air. Similar velocity profiles have been reported by Danila et al. (2022) and Hou et al. (2018), validating the hydrodynamic realism of the model.

Biogas concentration fields (Fig. 3.31) demonstrated the progressive integration of injected biogas throughout the biofilter, with concentrations increasing toward the outlet over time. This behavior reflects efficient gas transport but also highlights that hydrodynamics alone does not determine H_2S removal efficiency; instead, reactive surface availability and modification dictate removal effectiveness.

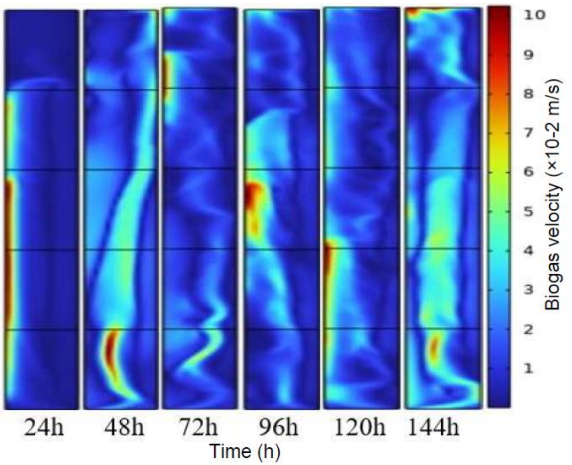

Fig. 3.29. Simulation of biogas velocity during the first six days after the operation in the lab-scale biofilter

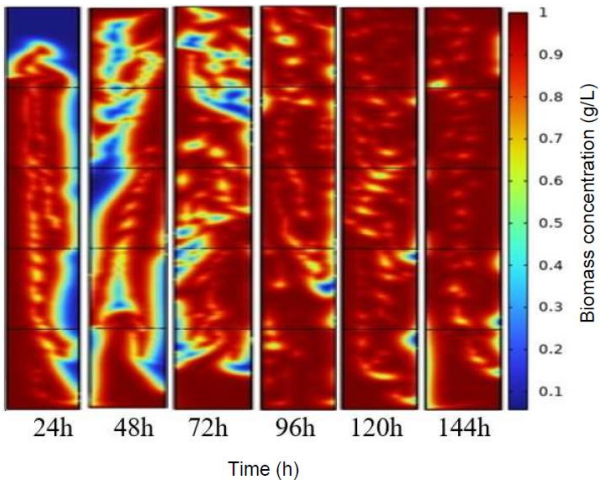

Fig. 3.30. Simulation of biogas concentrations during the first six days after operation in the lab-scale biofilter

Pressure field simulations (Fig. 3.32) revealed dynamic pressure fluctuations during the first 144 h of operation. Initial negative pressure zones transitioned toward more uniform distributions before stabilizing. The presence of air regulators in the experimental setup was consistent with simulation results, indicating that uncontrolled pressure fluctuations could adversely affect gas distribution and

microbial desulfurization activity. Similar pressure evolution trends have been reported in COMSOL simulations of biochar-based biofilters (Danila et al., 2022; Huan et al., 2021).

Integration with statistical analysis and experimental validation. To validate the numerical model, simulated H_2S concentration profiles were compared quantitatively with experimentally measured values across the biofilter layers. The average deviation between simulated and experimental removal efficiencies was below 7%, confirming strong agreement. This level of accuracy is comparable to or better than that reported in previous biofilter modeling studies (Sugurbekova et al., 2023; Zhang et al., 2020b).

Importantly, the numerical results are fully consistent with the statistical analysis presented in Section 3.5. The dominant influence of packing material properties (~45% of RE variance) is reflected in the simulated concentration fields, where modified biochar and $FeCO_3$-impregnated CLC waste exhibit distinctly stronger removal zones than unmodified or structurally passive materials. Similarly, the statistically identified contribution of gas flow rate (~30%) aligns with the relatively uniform velocity fields observed in Figure 3.30, confirming that hydrodynamics act as a secondary, but non-negligible, control parameter.

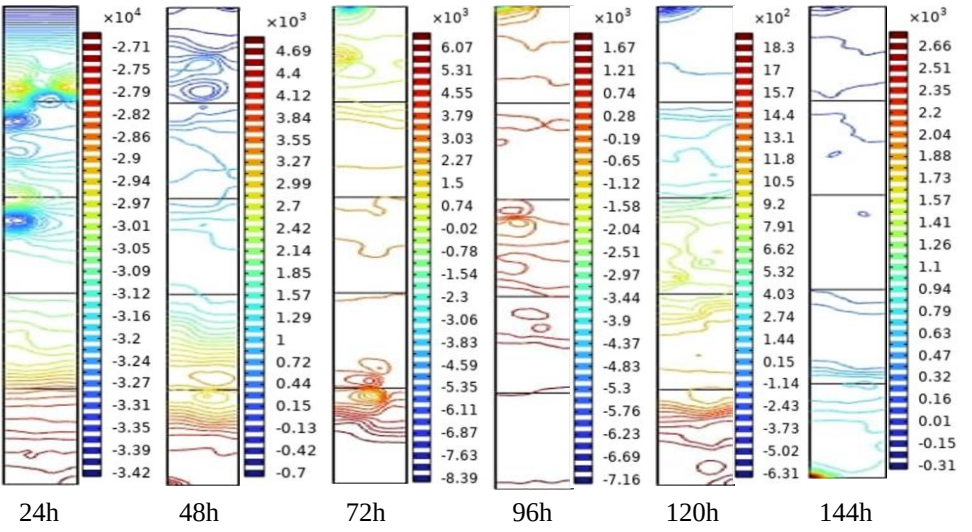

Fig. 3.31. Simulation of air pressure (values shown on graphs are based on Pa) during the first six days after operation of the lab-scale biofilter

Scientific novelty and implications for biofiltration design. The scientific novelty of this section lies in demonstrating that COMSOL-based simulation,

when combined with statistically validated experimental data, provides a direct mechanistic bridge between biofiltration material modification and observed H_2S removal performance. Unlike conventional biofilter models that rely on bulk-averaged parameters, the present approach captures spatial variability, material-dependent reaction zones, and temporal stabilization behavior.

The close agreement between modeled and experimental results (Figs. 3.21–3.25, 3.27–3.32) confirms that the effects of biofiltration material modification and microbial ecology can be quantitatively represented within a unified numerical framework. Compared with previous studies that primarily use COMSOL for qualitative visualization, this work demonstrates how simulation can serve as an interpretive and decision-support tool for rational biofilter design. The results establish that effective H_2S removal depends not only on hydrodynamics but critically on targeted material modification, enabling the creation of functionally specialized adsorption, catalytic, and biological zones within the biofilter. This represents a clear methodological and conceptual advancement in biofiltration research and provides a robust foundation for optimizing and scaling biofilters for hydrogen sulfide removal.

3.7. Comparative analysis and scientific discussion of biofilter performance based on experimental, statistical, and simulation results

The integrated analysis of experimental measurements, statistical evaluation, and numerical simulations presented in this Chapter demonstrates that biofilter performance and H_2S removal efficiency cannot be adequately explained by operational parameters or biological activity alone. Instead, the results clearly show that targeted modification of biofiltration materials is the dominant factor governing adsorption capacity, reaction pathways, microbial stability, and long-term process robustness.

Unlike many previous studies, in which packing materials are treated as passive supports, and performance is primarily correlated with inlet loading rates or empty bed residence time, this dissertation establishes a material-centered interpretation of biofiltration performance, in which thermally and chemically modified media actively shape the dominant H_2S removal mechanisms.

Comparison with experimental biofilter studies reported in the literature sources. Numerous experimental studies on biofilters packed with biochar report H_2S removal efficiencies of 80–95%, depending on feed concentration and operational conditions (Lee et al., 2021; Das et al., 2019; Ma et al., 2022; Mitchell et al., 2022). While these studies confirm the suitability of biochar as an effective

packing material, they typically attribute performance improvements to high surface area alone, without clearly linking removal efficiency to biochar modification strategy.

In contrast, the present work demonstrates that KOH-activated, thermally modified sewage-sludge-derived biochar consistently achieves high removal efficiencies (> 92%) under a broader range of operating conditions, and that this performance is statistically robust. This finding extends previous biochar-based studies by showing that biochar modification fundamentally alters its functional role from a passive adsorbent to a multifunctional adsorption–biological reaction medium.

For mineral-based materials, earlier investigations using construction byproducts or inert mineral media typically report moderate H_2S removal efficiencies (≈ 60–70%), often limited by low adsorption capacity (Lebrun et al., 2019; Poser et al., 2023). The results obtained in this dissertation show that $FeCO_3$ impregnation transforms CLC waste into a catalytically active biofiltration medium, increasing removal efficiency to approximately 75% and stabilizing performance at elevated inlet H_2S concentrations. This represents a clear advancement over studies that rely on unmodified mineral materials.

Studies employing synthetic polymeric media, such as PUF, emphasize their role in microbial support rather than in direct pollutant removal (De Souza et al., 2021; Hasanzadeh et al., 2018). The present results confirm these observations but further demonstrate that PUF alone cannot sustain high H_2S removal efficiency, reinforcing the conclusion that structural support, without chemical or thermal modification, is insufficient under demanding operating conditions.

Comparison with hybrid and multilayer biofilter systems. Hybrid biofilters combining multiple packing materials have been reported to outperform single-material systems (Lin et al., 2021; Paulionyte et al., 2022). However, in most published studies, material combinations are selected empirically, and the mechanisms underlying synergy are rarely resolved experimentally.

This dissertation provides experimental, statistical, and simulation-based evidence that synergy in hybrid biofilters arises specifically from modification-driven functional specialization of materials. In the biochar + $FeCO_3$-modified CLC waste configuration, biochar acts as a high-capacity adsorption and microbial support phase, while modified CLC waste functions as a catalytic oxidation and adsorption-regeneration zone. Such regeneration-driven synergy has been only conceptually proposed in the literature but rarely demonstrated with quantitative evidence.

Comparison with mathematical modeling and COMSOL-based simulations.

Previous biofilter modeling studies using COMSOL Multiphysics typically focus on qualitative visualization of concentration gradients and hydrodynamics

(Hou et al., 2018; Huan et al., 2021; Sugurbekova et al., 2023). These models often assume fixed material properties and do not explicitly account for material modification effects.

In contrast, the present work integrates experimentally measured material properties and modification-dependent kinetic parameters into both MATLAB and COMSOL models. The close agreement between simulated and experimental results (average deviation < 7%) confirms that material modification effects can be quantitatively embedded into predictive modeling frameworks, representing a methodological advancement over earlier modeling approaches.

Furthermore, the observed spatial stabilization of reaction zones in modified-material biofilters, confirmed by COMSOL simulations and supported by statistically reduced RE variance, has not been explicitly reported in earlier studies, where biofilters are often treated as spatially homogeneous systems.

In summary, the comparison with results reported by other authors and those obtained in this study indicates that the achieved H_2S removal efficiency was governed not by individual operating parameters but by interrelated physicochemical and structural properties of the biofiltration materials. First, high porosity and a well-developed specific surface area ensured efficient gas–solid contact and high adsorption capacity, while also providing favorable conditions for intensive microbial colonization. Second, a sufficient empty bed residence time (EBRT) ensured adequate reaction time for biological and catalytic H_2S oxidation. The combined effect of these parameters, further enhanced by targeted thermal and chemical modification of the biofiltration materials, resulted in higher and more stable H_2S removal efficiency than that reported for most systems described in the literature, in which material properties are typically treated as constant and non-adaptive.

Scientific novelty and conceptual advancement. The scientific novelty of this Chapter lies in demonstrating that biofiltration material modification is not a secondary optimization step but a primary design variable that governs biofilter performance at multiple scales. By integrating experimental data, statistical validation, and numerical simulation, this dissertation establishes that:

- thermal modification of biochar shifts its function from passive adsorption toward a coupled adsorption–biological reaction medium;
- chemical modification of mineral waste creates catalytically active biofiltration zones that can sustain performance under high pollutant loads;
- hybrid configurations enable deliberate spatial and functional separation of adsorption, catalysis, and biological activity within the biofilter bed.

Compared with previous studies that emphasize operational tuning or empirical material selection, this work advances biofiltration research toward rational, modification-driven system design. The results provide a robust conceptual and

technological foundation for scaling biofilters from laboratory systems to industrial biogas desulfurization applications, where operational stability under laboratory conditions and resilience are critical requirements.

3.8. Conclusions of the Third Chapter

1. This Chapter quantitatively demonstrates that hydrogen sulfide removal from biogas by biofiltration is predominantly controlled by targeted modification of biofiltration materials. Statistical analysis confirmed that packing material properties accounted for approximately 45% of the total variance in H_2S RE, compared to ~ 30% attributed to gas flow rate and ~20% to inlet H_2S concentration (error < 0.05), establishing material modification as the primary performance-determining factor.
2. Thermal modification of sewage sludge–derived biochar significantly enhanced its physicochemical properties and biofiltration performance. Increasing pyrolysis temperature from 400 °C to 600 °C increased biochar porosity from < 10% to ~65% and specific surface area from < 3 $m^2 \cdot g^{-1}$ to ~ 24 $m^2 \cdot g^{-1}$, while KOH activation further increased surface area by up to 19-fold. These modification-induced changes resulted in experimentally measured H_2S removal efficiencies of 90–99.9% after 144 h of operation, compared to 50–70% during the initial 96 h, indicating statistically significant performance improvement (error < 0.01).
3. Chemical modification of mineral packing material was essential for activating catalytic H_2S oxidation. $FeCO_3$-impregnated CLC waste achieved average H_2S removal efficiencies of ~75%, exceeding the performance of unmodified mineral materials by 10–15 percentage points under identical operating conditions. COMSOL simulations confirmed localized low-concentration reaction zones corresponding to catalytically active regions, supporting the mechanistic role of chemical modification.
4. Hybrid biofilter configurations exhibited statistically significant synergistic effects. The combination of thermally modified biochar and $FeCO_3$-modified CLC waste resulted in consistently higher and more stable RE values, with long-term fluctuations limited to ± 2–3%, compared to ± 6–10% observed in single-material systems. Analysis of variance confirmed that hybrid configurations outperformed single-material systems with $p < 0.05$.
5. Microbiological analysis confirmed that microbial activity is strongly conditioned by material modification. Pearson correlation analysis revealed a strong positive relationship between sulfur-oxidizing bacterial density and H_2S removal efficiency ($r = 0.89$, error < 0.001). Thermally

modified biochar pyrolyzed at 600 °C supported bacterial growth rates up to four times higher than biochar pyrolyzed at 400 °C, with peak microbial abundance reaching 5.73×10^4 CFU·g^{-1} in the mid-layer biofilter after 6 days of operation. These results demonstrate that microbial density is a material-controlled response governing biological H_2S oxidation in biofilters.

6. *Pseudomonas* spp. consistently exhibited higher biomass concentrations than *Acidithiobacillus* spp. across all materials. Peak biomass values reached ~0.022 g·L^{-1} for *Pseudomonas* spp. on biochar and ~0.013–0.014 g·L^{-1} on CLC waste, compared to ~0.007–0.009 g·L^{-1} and ~0.005–0.007 g·L^{-1}, respectively, for *Acidithiobacillus* spp. Initial growth rates ranged from (1.0–2.0) × 10^{-3} g·L^{-1}·day^{-1} on biochar to (0.4–0.7) × 10^{-3} g·L^{-1}·day^{-1} on CLC waste, confirming material-dependent biological kinetics.
7. Mathematical modeling by MATLAB accurately reproduced experimental biomass dynamics across all systems. Modeled and experimental growth curves exhibited consistent growth–peak–decline behavior, with biomass maxima occurring between days 5.5 and 6.5 and post-peak reductions of 20–30% by day 10. Relative deviations between modeled and experimental values remained below 10%, validating the predictive capability of the kinetic model.
8. Numerical simulations using COMSOL Multiphysics 6.1 confirmed the spatial structuring of H_2S removal processes induced by material modification. Simulated concentration profiles showed H_2S reduction from 800 ppm to 400–500 ppm within six days, depending on material type, with modified materials forming stable and persistent reaction zones that correlated with experimentally observed performance stabilization.
9. The scientific novelty of this Chapter lies in quantitatively establishing biofiltration material modification as a primary engineering control variable for biogas desulfurization. Unlike conventional approaches that treat packing materials as inert supports, this work demonstrates that thermal and chemical modification enables deliberate control over adsorption capacity, catalytic activity, microbial colonization, spatial reaction structuring, and long-term operational stability. This modification-driven framework provides a statistically supported and mechanistically grounded basis for scaling biofilters from laboratory systems to reliable industrial applications.

General conclusions

1. In practice, hydrogen sulfide (H_2S) concentrations in biogas frequently range from 100 to 5000 ppm, and concentrations exceeding 100 ppm cause severe corrosion and operational system failures. The analysis of scientific literature revealed that although biological filtration is an environmentally sustainable method for H_2S removal, insufficient attention has been given to the modification of waste-derived packing materials and to integrated experimental–modeling validation approaches.
2. Physicochemical characterization showed that KOH-modified sewage sludge-derived biochar and $FeCO_3$-impregnated CLC waste exhibited increased specific surface area (up to 471.54 $m^2 \cdot g^{-1}$), optimized porosity (65–75%), reduced bulk density from ~450–520 to ~280–350 $kg \cdot m^{-3}$, and improved surface properties favorable for microbial colonization and adsorption processes.
3. Experimental studies demonstrated that modified packing materials increased hydrogen sulfide removal efficiency from approximately 80% to 92–95% ($p < 0.01$), ensuring improved operational stability under laboratory-scale conditions. H_2S removal efficiency is directly dependent on the composition of biofilter packing materials: the multicomponent system consisting of KOH-modified biochar and $FeCO_3$-

impregnated CLC achieved up to 95% H_2S removal and statistically significantly outperformed single-component systems, increasing removal efficiency by 10–15% in relative terms. This confirms the synergistic interaction of adsorption, catalytic oxidation, and biological degradation.

4. Microbiological investigations demonstrated that the surface of thermally modified biochar promotes intensive microbial colonization: biochar supported bacterial densities of 10^7–10^8 $CFU \cdot g^{-1}$, whereas $FeCO_3$-impregnated CLC supported approximately 10^6 $CFU \cdot g^{-1}$; pyrolysis at 600 °C provided up to fourfold more favorable growth conditions than at 400 °C. A strong correlation between microbial density and H_2S removal efficiency ($r = 0.89$; $p < 0.001$) confirms that the interaction of *Acidithiobacillus* spp. and *Pseudomonas* spp. is responsible for achieving >90% H_2S removal.
5. Statistical evaluation established significant relationships between material properties (surface area, porosity, electrical conductivity), microbial activity indicators, and H_2S removal efficiency, confirming the interdependence of physicochemical and biological factors.
6. A mathematical model was developed using MATLAB, describing sulfur-oxidizing bacterial growth and hydrogen sulfide removal kinetics. Biologically driven reaction zones are formed with stable H_2S concentration and reaction rate gradients and demonstrated 7% deviations, in agreement with experimental data.
7. Numerical simulations performed using COMSOL to model the distribution of hydrogen sulfide and biogas concentrations, flow rate, and air pressure across different layers of the biofilter confirmed the experimental results. It was determined that the predicted H_2S removal efficiency deviated from the experimental data by less than 10%, confirming the reliability of the developed biofiltration system model.

Recommendations

1. Based on the experimental investigations conducted in this dissertation, it is recommended that practical biogas desulfurization systems implement a multi-component biofiltration system based on a combination of thermally modified biochar and $FeCO_3$-modified CLC. Such an approach enables the formation of functionally differentiated biofilter zones and ensures stable hydrogen sulfide (H_2S) removal efficiencies of 90–95% ($p < 0.01$).
2. Biofiltration systems in biofilters should be designed and optimized using mathematical modeling (MATLAB) and numerical simulations (COMSOL Multiphysics), which allow prediction of the formation and spatial dynamics of H_2S removal zones throughout the entire filter volume and enable reliable evaluation of process performance with deviations not exceeding 10%. Future research should focus on further model development by integrating microbial kinetics, changes in packing material properties during filter operation, and long-term performance scenarios in industrial-scale installations.

References

Abd, A. A., & Othman, M. R. (2022). Biogas upgrading to fuel grade methane using pressure swing adsorption: Parametric sensitivity analysis on an industrial scale. *Fuel*, *33*, 12–20. https://doi.org/10.1016/j.fuel.2021.121986

Alayande, A. B., Jee, H., & Kang, D. (2024). Membrane and adsorption technologies for efficient hydrogen sulfide removal from biogas: A review focused on the advancement of key components. *Process Safety and Environmental Protection*, *186*, 448–473. https://doi.org/10.1016/j.psep.2024.04.018

Arıman, S., & Koyuncu, S. (2022). Removal of hydrogen sulfide in biogas from wastewater treatment sludge by real-scale biotrickling filtration desulfurization process. *Water Practice and Technology*, *17*(7), 1406–1420. https://doi.org/10.2166/wpt.2022.072

Alkhatib, I. I. I., Khalifa, O., Bahamon, D., Abu-Zahra, M. R. M., & Vega, L. F. (2021). Sustainability criteria as a game changer in the search for hybrid solvents for CO2 and H2S removal. *Separation and Purification Technology*. *227*, Article 119516. https://doi.org/10.1016/j.seppur.2021.119516

Ahmed, S. F., Tarannum, M. M. K., Choudhury, A. T., Kumar, P. S., N.Vo, D. V., Lichtfouse, E., & Mahlia, T. M. I. (2021). Biogas upgrading, economy and utilization: a review. *Environmental Chemistry Letters*, *19*, 4137–4164. https://link.springer.com/article/10.1007/s10311-021-01292-x#citeas

Alonso, C., Ramírez, M., Cantero, D., & Lebrero, R. (2022). Gas distribution and hydrodynamics in packed bed biofilters treating sulfur-containing gas streams. *Process*

Safety and Environmental Protection, 158, 312–323. https://doi.org/10.1016/j.psep.2022.01.041

Appala, V. N. S. G., Pandhare, N. N., & Bajpai, S. (2022). Mathematical Models for Optimization of Anaerobic Digestion and Biogas Production. In Nandabalan, Y.K., Garg, V.K., Labhsetwar, N.K., Singh, A. (Eds.), *Zero Waste Biorifinery* (pp. 575–591). Springer. https://doi.org/10.1007/978-981-16-8682-5_21

Aryal, N., Zhang, Y., Bajracharya, S., Pant, D., & Chen, X. (2022). Microbial electrochemical approaches of carbon dioxide utilization for biogas upgrading. *Chemosphere*. *282*, 150–158. https://doi.org/10.1016/j.chemosphere.2021.132843

Aukstinaitis, T., & Vaiskunaite, R. (2012). Analysis and assessment of BF packed with different coniferous and deciduous wood waste charges. *Environmental protection technology and management, VGTU. 743*, 141664.

Abbasabadi, M. K., Khodabakhshi, S., Zand, H. R. E., Rashidi, A., Gholami, P., & Sherafati, Z. (2020). Covalent modification of reduced graphene oxide with piperazine as a novel nanoadsorbent for removal of H_2S gas. *Research on Chemical Intermediates*, *46*(10), 4447–4463. https://doi.org/10.1007/s11164-020-04214-8

Bahraminia, S., Anbia, M., & Koohsaryan, E. (2020). Hydrogen sulfide removal from biogas using ion-exchanged nanostructured NaA zeolite for fueling solid oxide fuel cells. *International Journal Of Hydrogen Energy*, *171*, 155–164. https://doi.org/10.1016/j.ijhydene.2020.08.091

Binti, R. S. N. (2019). Innovative water scrubber packed with sponge carriers for biogas purification. *Environmental Science*, Hiroshima University. ProQuest Dissertations & Theses Global. (Publication No. 226600887)

Bora D., Roy K., Mahanta P., & Barbora L. (2024). Hydrogen sulfide removal from biogas using biomass-derived naturally alkaline biochars: performance analysis and kinetics. *Journal of Material Cycles and Waste Management*, *472*, Article 145089. https://doi.org/10.1007/s10163-024-01908-8

Bagheri, M., Bauer, T., Burgman, L. E., & Wetterlund, E. (2023). Fifty years of sewage sludge management research: Mapping researchers' motivations and concerns. *Journal of Environmental Management*, *325*, Article 116412. https://doi.org/10.1016/j.jenvman.2022.116412

Bu, H., Carvalho, G., Huang, C., Sharma, K., R., Yuan, Z., Song, Y., Bond, P., Keller, J., Yu, M., & Jiang, G. (2021). Evaluation of continuous and intermittent trickling strategies for the removal of hydrogen sulfide in a biotrickling filter. *Chemosphere*, *51*, 664–669. https://doi.org/10.1016/j.chemosphere.2021.132723

Cano, P. I., Almenglo, F., Ramirez, M., & Cantero, D. (2021). Integration of a nitrification bioreactor and an anoxic biotrickling filter for simultaneous ammonium-rich water treatment and biogas desulfurization. *Chemosphere*, *284*, Article 131358. https://doi.org/10.1016/j.chemosphere.2021.131358

Clotas, E. S., Codony, A. C., Comas, C. Y., Li, X., Zhang, H., & Wang, J. (2022). Mechanisms of KOH activation on sewage sludge-derived biochar and its implications

for gas-phase adsorption. *Chemical Engineering Journal*, *430*, Article 133042. https://doi.org/10.1016/j.cej.2021.133042

Clotas E. S., Codony A. C., Comas J., & Martin M. J. (2020). Biogas purification through membrane bioreactors: Experimental study on siloxane separation and biodegradation. *Separation and Purification Technology*, *231*, Article 116440. https://doi.org/10.1016/j.seppur.2019.116440

Choudhury, A., & Lansing, S. (2021). Adsorption of hydrogen sulfide in biogas using a novel iron-impregnated biochar scrubbing system. *Journal of Environmental Chemical Engineering*, *9*(1), 104837. https://doi.org/10.1016/j.jece.2020.104837

Cuimei, B., Wei, G., Chao, T., Jun, L., & Xiaohua, L. (2018). Dynamic Control Design and Simulation of Biogas Pressurized Water Scrubbing Process. *IFAC-PapersOnLine*, *51*(18), 560–565. https://doi.org/10.1016/j.ifacol.2018.09.365

Cano, P. I., Brito, J., Almenglo, F., Ramirez, M., Gomez, J. M., & Cantero, D. (2019). Influence of trickling liquid velocity, low molar ratio of nitrogen/sulfur and gas-liquid flow pattern in anoxic biotrickling filters for biogas desulfurization. *Biochemical Engineering Journal*, *148*, 205–213. https://doi.org/10.1016/j.bej.2019.05.008

Cortes, J. J. G., Almenglo, F., Ramirez, M., & Cantero, D. (2021). Simultaneous removal of ammonium from landfill leachate and hydrogen sulfide from biogas using a novel two-stage oxic-anoxic system. *Science of the Total Environment*, *750*, Article 141664. https://doi.org/10.1016/j.scitotenv.2020.141664

Cui, G., Bhat, S. A., Li, W., Ishiguro, Y., Wei, Y., & Li, F. (2022). H_2S, MeSH, and NH_3 emissions from modified sludge: an insight towards sludge characteristics and microbial mechanisms. *International Biodeterioration & Biodegradation*, *166*, Article 105590. https://doi.org/10.1016/j.ibiod.2021.105331

Dada, O. (2025). Advances in biological hydrogen sulfide removal from biogas: Microbial, material, and modeling perspectives. *Journal of Environmental Management*. *in press*.

Das, J., Rene, E. R., Dupont, C., Dufourny, A., Blin, J., & Hullebusch, E. D. V. (2019). Performance of a compost and biochar-packed BF for gas-phase hydrogen sulfide removal. *Bioresource Technology*, *292*, Article 132843. https://doi.org/10.1016/j.biortech.2018.11.052

Das, J., Ravishankar, H., & Lens, P. N. L. (2022a). Biological biogas purification: Recent developments, challenges and future prospects. *Journal Of Environmental Management*, *304*, Article 114198. https://doi.org/10.1016/j.jenvman.2021.114198

Das, J., Nolan, S., & Lens, P. N. L. (2022b). Simultaneous removal of H2S and NH3 from raw biogas in hollow fiber membrane bioreactors. *Environmental Technology and Innovation*, *28*, 102777. https://doi.org/10.1016/j.eti.2022.102777

Drozdz, D., Wystalska, K., Malinska, K., Grasser, A., Grabelak, A., & Kacprzak, M. (2020). Management of poultry manure in Poland – Current state and future perspectives. *Journal of Environmental Management*, *264*, Article 110327. https://doi.org/10.1016/j.jenvman.2020.110327

Danila, V., Zagorskis, A., & Januševičius, T. (2022). Effects of Water Content and Irrigation of Packing Materials on the Performance of BFs and Biotrickling Filters: A Review. *Process*, *17*, 372–382. https://doi.org/10.3390/pr10071304

De Souza, F. M., Kahol, P. K., & Gupta, K. R. (2021). Introduction to Polyurethane Chemistry. *American Chemical Society*, 170, 104–116. https://doi.org/10.1021/bk-2021-1380.ch001

Devinny, J. S., Deshusses, M. A., & Webster, T. S. (1999). Biofiltration for air pollution control. *Boca Raton.* CRC Press. https://doi.org/10.1201/9781315138275

European Biogas Association (2024). *EBA Statistical Report 2024. Brussels: EBA.* https://ec.europa.eu/eurostat/data/database

European Commission. (2020). *A new Circular Economy Action Plan – For a cleaner and more competitive Europe*. https://eur-lex.europa.eu/legal-content/EN/TXT/?uri=COM:2020:98:FIN

European Environment Agency. (2021). Sewage sludge and the circular economy. https://www.ewa-online.eu/files/downloads/publications/Position_Papers/EWA_postion_paper_sewage_sludge_21.pdf

Publications Office of the European Union. (n.d.). Sewage sludge production and disposal. data.europa.eu. https://data.europa.eu/data/datasets/g1a4auwbnk-frmzm3dg6zg?locale=en

European Commission. (n.d.). Construction and demolition waste. *https://environment.ec.europa.eu/topics/waste-and-recycling/construction-and-demolition-waste_en*

Fleck, S., Lee, Y., Rodríguez, M., & Choi, Y. (2020). Polyurethane foam in environmental applications: A review of current practices and life cycle assessment. *Environmental Progress & Sustainable Energy*, *39*(2), 1293–1303. https://doi.org/10.1002/ep.13345

Fan, G., Zhan, J., Luo, J., Lin, J., Qu, F., Du, B., You, Y., & Yan, Z. (2021). Fabrication of heterostructured Ag/AgCl@g-C3N4@UIO-66(NH2) nanocomposite for efficient photocatalytic inactivation of Microcystis aeruginosa under visible light. *Journal of Hazardous Materials*, *402*, Article 124062. https://doi.org/10.1016/j.jhazmat.2020.124062

Fletcher, J., Navarro, A., Liu, C., & van den Berg, J. (2019). Impact of transportation logistics on the carbon footprint of waste-derived materials for H_2S removal in BFs. *Environmental Impact Assessment Review*, *75*, 19–28. https://doi.org/10.1016/j.eiar.2018.12.004

Fang, Y. (2022). Biological desulfurization using *Acidithiobacillus* in up-flow bioreactors under dynamic load. *Environmental Science & Technology*, *56*(3), 1742–1752. https://doi.org/10.1021/acs.est.1c06411

Farghali, M., Osman, A., Umetsu, K., & Rooney, D. W. (2022). Integration of biogas systems into a carbon zero and hydrogen economy: a review. *Environmental Chemistry Letters*, *20*(2), 1035–1050. https://doi.org/10.1007/s10311-022-01468-z

Gao, Y. (2025). Advanced oxidation and hybrid treatment strategies for sulfur-rich biogas purification. *Chemical Engineering Journal, in press*.

Gao, Y., Han, Z., Zhai, G., Dong, J. & Pa, X. (2022). Oxidation absorption of gaseous H2S using UV/S2O8 2− advanced oxidation process: performance and mechanism. *Environmental Technology and Innovation*, *25*, 102124. https://doi.org/10.1016/j.eti.2021.102124

Gao, F., Sun, W., Zheng, Y., & Lin, C. (2021). Monod and modified Monod kinetic models for microbial growth: Application to simultaneous COD and ammonia removal. *Bioresource Technology Reports*, *3*, 100058. https://www.sciencedirect.com/science/article/pii/S2589004221000588

Guo, S., Yu, Q., Zhao, S., Tang, X., Wang, Y., Ma, Y., Long, Y., & Yi, H. (2023). Research progress on the adsorption of sulfocompounds in flue gas. *Chemical Engineering Journal*, *476*, Article 146677. https://doi.org/10.1016/j.cej.2023.146677

Gaga, Y., Benmessaoud, S., Kara, M., Assouguem, A., Al-Ghamdi, A. A., Al-Hemaid, F. M., Elshikh, M. S., Ullah, R., Banach, A., & Bahhou, J. (2022). New Margin-Based Biochar for Removing Hydrogen Sulfide Generated during the Anaerobic Wastewater Treatment, *Water 2022*, *14*(20), Article 3319. https://doi.org/10.3390/w14203319

Ghimire, A., Gyawali, R., Lens, P. N. L., & Lohani, S. P. (2021). Technologies for removal of hydrogen sulfide (H2S) from biogas. In N. Aryal, L. D. M. Ottosen, M. V. W. Kofoed, & D. Pant (Eds.), *Emerging Technologies and Biological Systems for Biogas Upgrading* (pp.295-320). https://doi.org/10.1016/B978-0-12-822808-1.00011-8

Georgiadis, A., Charisiou, N., & Goula, M. (2020). Removal of Hydrogen Sulfide From Various Industrial Gases: A Review of The Most Promising Adsorbing Materials. *Catalysts*, *10*(5), Article 521. https://doi.org/10.3390/catal10050521

Geni, J., Machunda, R., & Pogrebnaya, T. (2020). Performance of Sweet Potato's Leaf-Derived Modified Carbon for Hydrogen Sulphide Removal from Biogas. *Journal of Energy*, *2020*, Article 9121085. https://doi.org/10.1155/2020%2F9121085

Gonzalez, C. J., Herrera, S. T., Almenglo, F., Ramirez, M., & Cantero, D. (2020). Hydrogen sulfide removal from biogas and sulfur production by autotrophic denitrification in a gas-lift bioreactor. *ACS Sustainable Chemistry & Engineering*, *8*(28), 10480–10489. https://doi.org/10.1021/acssuschemeng.0c02567

Hou, N., Xia, Y., Wang, X., Liu, H., Liu, H., & Xun, L. (2018). H2S biotreatment with sulfide-oxidizing heterotrophic bacteria. *Biodegradation*, *40*, 585–595. https://doi.org/10.1007/s10532-018-9849-6

Herath, I. S., Udayanga, D., Jayasanka D. J., & Hewawasam C. (2024). Textile dye decolorization by white rot fungi – A review. *Bioresource Technology Reports*, *24*, Article 101687. https://doi.org/10.1016/j.biteb.2023.101687

Huang, D., Wang, N., Bai, X., Chen, Y., & Xu, Q. (2022a). The influencing mechanism of O_2, H_2O, and CO_2 on the H_2S removal of food waste digestate-derived biochar

with abundant minerals. *Biochar*, *4*(1), 199–210. https://doi.org/10.1007/s42773-022-00199-2

Huang, K., Wang, X., Yuan, W., Xie, J., Wang, J., & Li, J. (2022b). Remediation of lead-contaminated soil by washing with choline chloride-based deep eutectic solvents. *Process Safety and Environmental Protection*, *159*, 170–181. https://doi.org/10.1016/j.psep.2022.01.034

Huan, C., Lyu, Q., Tong, X., Li, H., Zeng, Y., Liu, Y., Jiang, X., Ji, G., Xu, L., & Yan, Z. (2021). Analyses of deodorization performance of mixotrophic biotrickling filter reactor using different industrial and agricultural wastes as packing material. *Journal of Hazardous Materials*, *420*, Article 126608. https://doi.org/10.1016/j.jhazmat.2021.126608

Haosagul, S., Prommeenate, P., Hobbs, G., & Pisutpaisal, N. (2020). Sulfur-oxidizing bacteria in full-scale biogas cleanup system of ethanol industry. *Renewable Energy*. *152*, Article 109364. https://doi.org/10.1016/j.renene.2019.11.140

Hasanzadeh, V., Alipour, V., Goodarzi, B., Rahmanian, O., Dindarloo, K., Khosravi, R., & Heidari, M. (2018). Experimental and kinetic analysis of H2S removal in a Polyurethane foam/ Palm fiber based BF with no pH control. *Iranian Journal of Science and Technology, Transactions of Civil Engineering*, *43*, 781–789. https://doi.org/10.1007/s40996-018-0215-z

Irani, V., Tavasoli, A., & Vahidi, M. (2018). Preparation of amine functionalized reduced graphene oxide/methyl diethanolamine nanofluid and its application for improving the CO2 and H2S absorption. *Journal of Colloid and Interface Science*, *527*, 57–67. https://doi.org/10.1016/j.jcis.2018.05.018

Ibrahim, R., Hassni, A., Ardeh, S. N., & Cabana, H. (2021). Biological elimination of a high concentration of hydrogen sulfide from landfill biogas. *Environmental Science and Pollution Research*, *28*(1), 431–442. https://doi.org/10.21203/rs.3.rs-312009/v1

Jia, T., Sun, S., Zhao, Q., Peng, Y., & Zhang, L. (2022). Extremely acidic condition (pH<1.0) as a novel strategy to achieve high-efficient hydrogen sulfide removal in biotrickling filter: Biomass accumulation, sulfur oxidation pathway and microbial analysis. *Chemosphere*, *294*, Article 133770. https://doi.org/10.1016/j.chemosphere.2022.133770

Jiang, X., Wu, J., Jin, Z., Yang, S., & Shen, L. (2020). Enhancing the removal of H2S from biogas through refluxing of outlet gas in biological bubble-column. *Bioresource Technology*, *292*, Article 122621. https://doi.org/10.1016/j.biortech.2019.122621

Jiao, Y., Han, S., Zhang, W., Guo, M., Cheng, F., & Zhang, M. (2022). Self-assembled CuO-bearing aerogel-like hollow Al2O3 microspheres for room temperature dry capture of H2S. *Chemical Engineering Research and Design*, 176, 160–172. https://doi.org/10.1016/j.cherd.2021.10.030

Juntarachat, N., & Onthong, U. (2022). Removal of hydrogen sulfide from biogas using banana peel and banana empty fruit bunch biochars as alternative adsorbents. *Biomass Conversion and Biorefinery*, *11*, 3421–3434. https://link.springer.com/article/10.1007/s13399-022-03430-z

Janusevicius, T., Mažeikienė, A., Stepova, K., Danila, V., & Paliulis, D. (2024). The Removal of Phosphorus from Wastewater Using a Sewage Sludge Biochar: A Column Study. *Water*, *16*, Article 1104. https://doi.org/10.3390/w16081104

Juntranapaporn, J., Vikromvarasiri, N., Soralump, C., & Pisutpaisal, N. (2019). Hydrogen sulfide removal from biogas in biotrickling filter system inoculated with Paracoccus pantotrophus. *International Journal of Hydrogen Energy*, *44*(56), 11937–11947. https://doi.org/10.1016/j.ijhydene.2019.03.069

Jedynak, K., & Charmas, B. (2024). Adsorption properties of biochars obtained by KOH modification. *Adsorption*. *30*, 167–183. https://doi.org/10.1007/s10450-023-00399-7

Khalil, M., Berawi, M., A., Heryanto, R., & Rizalie, A. (2019). Waste to energy technology: The potential of sustainable biogas production from animal waste in Indonesia. *Renewable And Sustainable Energy Reviews*, *103*, 477–489. https://doi.org/10.1016/j.rser.2019.02.011

Khan, M. U., EnLee, J. T., Bashir, M. A., Dissanayake, P. D., WahTong, Y. S., Shariati, M. A., Wu, S., & Ahring, B. K. (2021). Current status of biogas upgrading for direct biomethane use: A review. *Renewable and Sustainable Energy Reviews*, *149*, Article 111343. https://doi.org/10.1016/j.rser.2021.111343

Kulawong, S., Artkla, R., Sriprapakhan, P., & Maneechot, P. (2022). Biogas purification by adsorption of hydrogen sulfide on NaX and Ag-exchanged NaX zeolites. *Biomass and Bioenergy*, *159*, Article 106417. https://doi.org/10.1016/j.biombioe.2022.106417

Khanongnuch R. (2019). *Hydrogen sulfide removal from synthetic biogas using anoxic biofilm reactors*, [Thesis, Université Paris-Est, Tampere University]. http://urn.fi/URN:NBN:fi:tuni-201906192105

Khanongnucha, R., Capuac, F. D., Lakaniemia, A. M., Reneb, E. R., & Lens, P. N. L. (2019). Transient–state operation of an anoxic biotrickling filter for H2S removal. *Journal of Hazardous Materials*, *373*, 223–232. https://doi.org/10.1016/j.jhazmat.2019.05.043

Konkol, D., Popiela, E., Skrzypczak, D., Izydorczyk, G., Mikula, K., Moustakas, K., Opaliński, S.,Korczyński, M., Krowiak, A. W., & Chojnacka, K. (2022). Recent innovations in various methods of harmful gases conversion and its mechanism in poultry farms. *Environmental Research*, *214*, Article 113825. https://doi.org/10.1016/j.envres.2022.113825

Kurniawan, T. A., Lo, W. H., Chan, G. Y. S., & Goh, H. C. (2020). Environmental and economic impacts of the use of waste-derived materials for biogas purification. *Waste Management*, *105*, 102–112. https://doi.org/10.1016/j.wasman.2020.01.043

Kumari, A., Singh, R., Desai, D. & Narayan, R. (2020). Sustainability evaluation of biochar in biofiltration systems: A life cycle and cost-benefit assessment for biogas applications. *Journal of Environmental Management*, *261*, Article 110192. https://doi.org/10.1016/j.jenvman.2020.110192

Khan, M. U., Lee, J. T., Bashir, M. A., Dissanayake, P. D., OK, Y. S., Tang, Y. W., Shariati, M. A., Wu, S., & Ahring, B. K. (2021). Current status of biogas upgrading for direct biomethane use: A review. *Renewable and Sustainable Energy Reviews*, *149*, Article 111343. https://doi.org/10.1016/j.rser.2021.111343

Kalinska, L. G., Couvert, A., & Dumont, E. (2019). H2S removal using cellular concrete waste as filtering material: Reaction's identification and performance assessment. *Journal of Environmental Chemical Engineering*, *7*, Article 102967. https://doi.org/10.1016/j.jece.2019.102967

Lin, Q., Zhang, J., Yin, L., Liu, H., Zuo, W., & Tian, Y. (2021). Relationship between heavy metal consolidation and H2S removal by biochar from microwave pyrolysis of municipal sludge: effect and mechanism. *Environmental Science and Pollution Research*, *28*, 16943–16956. https://doi.org/10.1007/s11356-021-12631-4

Lu, C., Liu, W., Zhang, Y. & Zhang, C. (2021). Role of extracellular polymeric substances in microbial reduction of iron by *Pseudomonas putida* and its application in wastewater treatment. *Journal of Environmental Chemical Engineering*, *9*(4), Article 105330. https://doi.org/10.1016/j.jece.2021.105330

Lee, J. T. E., Ok, Y. S., Song, S., Dissanayake, P. D., Tian, H., Tio, Z. K., Cui, R., Lim, E. Y., Jong, M. C., Hoy, S. H., Lum, T. Q. H., Tsui, T. H., Yoon, C. S., Dai, Y., Wang, C. W., Tan, H. T. W., & Tong, Y. W. (2021). Biochar utilisation in the anaerobic digestion of food waste for the creation of a circular economy via biogas upgrading and digestate treatment. *Bioresource Technology*, *333*, Article 125190. https://doi.org/10.1016/j.biortech.2021.125190

Lee, E., Rout, P. R., Kyun, Y., & Bae J. (2020). Process optimization and energy analysis of vacuum degasifier systems for the simultaneous removal of dissolved methane and hydrogen sulfide from anaerobically treated wastewater. *Water Research*, *182*, Article 115965. https://doi.org/10.1016/j.watres.2020.115965

Li, Y., Zhou, C., Tan, W., & Zhang, L. (2021). Environmental and economic benefits of BF systems for H_2S removal from biogas: A comparative analysis of different packing materials. *Renewable Energy*, *162*, 917–928. https://doi.org/10.1016/j.renene.2020.09.067

Li, Y., Zhou, C., Tan, W., & Zhang, L. (2020). Packing material properties governing biofilter performance for hydrogen sulfide removal. *Renewable Energy*, *154*, 1240–1251.

https://doi.org/10.1016/j.renene.2020.03.072

Liu, X., Zhang, Y., Wang, Z., & Chen, H. (2022). Recent advances in hybrid adsorption–biological systems for hydrogen sulfide removal from biogas. *Bioresource Technology*, *344*, Article 126246. https://doi.org/10.1016/j.biortech.2021.126246

Liu, B., & Zuo, S. (2023). Effect of Catalytic Factors of Modified Carbon and Gas Stream Properties on H_2S Catalytic Conversion. *Water, Air, & Soil Pollution*, *234*(2), Article 61. https://doi.org/10.21203/rs.3.rs-1525571/v1

Ma, M., & Zou, C. (2018). Effect of nanoparticles on the mass transfer process of removal of hydrogen sulfide in biogas by MDEA. *International Journal of Heat and Mass Transfer*, *125*, 1217–1226. https://doi.org/10.1016/j.ijheatmasstransfer.2018.06.091

Ma, C., Zhao, Y., Chen, H., Liu, Y., Huang, R., & Pan, J. (2022). Biochars derived from by-products of microalgae pyrolysis for sorption of gaseous H2S. *Journal of Environmental Chemical Engineering*, *10*, Article 107370. https://doi.org/10.1016/j.jece.2022.107370

Moradi, H., Azizpour, H., Bahmanyar, H., & Mohammadi, M. (2020). Molecular dynamics simulation of H2S adsorption behavior on the surface of modified carbon. *Inorganic Chemistry Communication*, 107, Article 108048. https://doi.org/10.1016/j.inoche.2020.108048

Mutegoa, E., Hilonga, A., & Njau, K. N. (2020). Approaches to the mitigation of ammonia inhibition during anaerobic digestion–a review. *Water Practice and Technology*, *15*(3), 551–570. https://doi.org/10.2166/wpt.2020.047

Morgado, M. F., Cervantes, A. T., Sanchez, A. G., Lebrero, R., & Munoz R. (2018). Integral (VOCs, CO2, mercaptans and H2S) photosynthetic biogas upgrading using innovative biogas and digestate supply strategies. *Chemical Engineering Journal*, *354*, 363–369. https://doi.org/10.1016/j.cej.2018.08.026

Mamet, S. D., Jimmo, A., Conway, A., Teymurazyan, A., Talebitaher, A., Papandreou, Z., Chang, Y. F., Shannon, W., Peak, D., & Siciliano, S. D. (2021). Soil Buffering Capacity Can Be Used To Optimize Biostimulation of Psychrotrophic Hydrocarbon Remediation. *Environmental Science & Technology*, *55*, 9864–9875. https://doi.org/10.1021/acs.est.1c01113

Mitchell, K., Beesley, L., Sipek, V., & Trakal, L. (2022). Biochar and its potential to increase water, trace element, and nutrient retention in soils. *Biochar in Agriculture for Achieving Sustainable Development Goals*, *40*, 173–196. https://doi.org/10.1016/B978-0-323-85343-9.00008-2

Muthulakshmi V., & Sundrarajan M. (2020). Green synthesis of ionic liquid assisted ytterbium oxide nanoparticles by Couroupita guianensis abul leaves extract for biological applications. *Journal of Environmental Chemical Engineering*, *8*(4), Article 103992. https://doi.org/10.1016/j.jece.2020.103992

Nhut, H. H., Thanh, V. T., & Le, L. T. (2020). Removal of H2S in biogas using biotrickling filter: Recent development. *Process Safety and Environmental Protection*, *144*, 222–230. https://doi.org/10.1016/j.psep.2020.07.011

Nausediene, A., & Vaiskunaite, R. (2014). Analysis and assessment of BF packed with reed charge. *Environmental protection technology and management*, *VGTU*, *100*, 1–64.

Nie, W., He, S., Lin, Y., Cheng, J., & Yang, C. (2024). Functional biochar in enhanced anaerobic digestion: Synthesis, performances, and mechanisms. *Science of The Total Environment*, *906*, 167681. https://doi.org/10.1016/j.scitotenv.2023.167681

Nowicki, P., Skibiszewska, P., & Pietrzak, R. (2014). Hydrogen sulphide removal on carbonaceous adsorbents prepared from coffee industry waste materials. *Chemical Engineering Journal*, *248*, 208–215. https://doi.org/10.1016/j.cej.2014.03.052

Nowak, K., Mijakowski, M., & Muller, J. (2024). Simulating the Natural Seasonal Ventilation of a Classroom in Poland Based on Measurements of the CO2 Concentration. *Energies*, *25*, Article 101742. https://doi.org/10.3390/en17184591

PlasticsEurope. (2020). *Plastics – the Facts 2020: An analysis of European plastics production, demand and waste data.* https://plasticseurope.org/wp-content/uploads/2021/09/Plastics_the_facts-WEB-2020_versionJun21_final.pdf

Pudi, A., Rezaei, M., Signorini, V., Andersson, M. P., Baschetti, M. G., & Mansouri, S. S. (2022). Hydrogen sulfide capture and removal technologies: A comprehensive review of recent developments and emerging trends. *Separation and Purification Technology*, *292*, Article 121448. https://doi.org/10.1016/j.seppur.2022.121448

Prasertcharoensuk, P., Promtongkaew, A., Tawatchai, M., Marquez, V., Jongsomjit, B., Tahir, M., Praserthdam, S., & Praserthda, P. (2022). A review on sensitivity of operating parameters on biogas catalysts for selective oxidation of Hydrogen Sulfide to elemental sulfur. *Chemosphere*, *298*, Article 134579. https://doi.org/10.1016/j.chemosphere.2022.134579

Perez, T., G., Jimenez, S., H., & Revah, S. (2020). Operational parameters in H2S biofiltration under extreme acid conditions: performance, biomass control, and CO2 consumption. *Environmental Science and Pollution Research*, *27*, 2157–2173. https://doi.org/10.1007/s11356-019-06789-1

Poser, M., Silva, L. R. D. E., Peu, P., Couvert, A., & Dumont, E. (2023). Cellular concrete waste: an efficient new way for H2S removal. *Separation and Purification Technology*, *296*, Article 123014. https://doi.org/10.1016/j.seppur.2022.123014

Petrauskaite, E., Vaiskunaite, R., Blumberga, D., & Ivanovs, K. (2017). Research, and assessment of droplet BF packed with sphagnum material for air purification from volatile organic compounds. *Environmental Protection Technology and Management VGTU*, *128*, 373–378.

Pabby, A. K., & Sastre, A. M. (2013). State-of-the-art review on hollow fibre contactor technology and membrane-based extraction processes. *Journal of Membrane Science*, *598*, Article 117678. https://doi.org/10.1016/j.memsci.2012.11.060

Paulionyte, J., & Vaiskunaite, R. (2023). Research on the physical and chemical properties of sewage treatment sludge biochar and its preparation for wastewater. *Mokslas – Lietuvos ateitis / Science – Future of Lithuania*, *15*, Article 19431. https://doi.org/10.3846/mla.2023.19431

Paulionyte, J., Vaiskunaite, R., & Mazeikiene, A. (2022). Evaluation of sewage sludge biochar use in wastewater treatment from phosphate. In *25-oji konferencija*

„Aplinkos apsaugos inžinerija“ / 25th Conference "Environmental protection engineering" (pp. 35-39). Vilnius Gediminas Technical University. https://doi.org/10.3846/aainz.2022.006

Pepper, I. L., & Brusseau, M. L. (2019). Physical-Chemical Characteristics of Soils and the Subsurface. In M. L. Brusseau, I. L. Pepper, & Ch. P. Gerba (Eds.), *Environmental and pollution science* (3rd ed.), 9–22. https://doi.org/10.1016/B978-0-12-814719-1.00002-1

Qin, M., Liao, K., He, G., He, T., Leng, J., & Zhang, S. (2023). Quantitative risk assessment of static equipment in petroleum and natural gas processing station based on corrosion-thinning failure degree. *Process Safety and Environmental Protection*, *172*, 423–435. https://doi.org/10.1016/j.psep.2023.01.045

Rivard, M., Dupuis, L., Laflamme, R., & Roy, C. (2018). Economic feasibility of using biochar in biogas plants: A cost-benefit analysis of sustainable BF materials for hydrogen sulfide removal. *Bioresource Technology*, *250*, 349–358. https://doi.org/10.1016/j.biortech.2017.11.063

Rodriguez, L., Gómez, J., & Lebrero, R. (2023). Role of iron-based materials in sulfur stabilization during biological gas desulfurization. *Water Research*, *231*, Article 119626. https://doi.org/10.1016/j.watres.2023.119626

Scarlat, N., Dallemand, J. F., & Fahl, F. (2018). Biogas: Developments and perspectives in Europe. *Renewable Energy*, *129*, 457–472. https://doi.org/10.1016/j.renene.2018.03.006

Severi, E., Moreira, I. P. R., Arino, J. R., Quapp, W., & Bofill, J. M. (2025). Controlling molecular machines via optimally oriented external electric fields. *Chemical Science*, *16*, 16180–16186. https://doi.org/10.1039/d5sc04835d

Shareefdeen, Z., & Singh, A. (2005). Biotechnology for Odor and Air Pollution Control. *Boca Raton: CRC Press*, *400*, 1–409. https://doi.org/10.1007/b138434

Strohmaier, C., Krommweh, M., S., & Buscher, W. (2019). Suitability of Different Filling Materials for a BF at a Broiler Fattening Facility in Terms of Ammonia and Odour Reduction. *Atmosphere*, *11*(1), Article 13. https://doi.org/10.3390/atmos11010013

Su, J., J., & Hong, Y., Y. (2020). Removal of hydrogen sulfide using a photocatalytic livestock biogas desulfurizer. *Renewable Energy*, *149*, 181–188. https://doi.org/10.1016/j.renene.2019.12.068

Sun, X., Zhang, Y., Li, M., & Chen, H. (2022). Application of pseudo-second-order kinetic models in biofiltration and adsorption systems for sulfur compounds. Journal of Environmental *Chemical Engineering*, *10*, Article 108214. https://doi.org/10.1016/j.jece.2022.108214

Styszko, K, Durak, J, Kończak, B, Głodniok, M, & Borgulat, A. (2022). The impact of sewage sludge processing on the safety of its use. *Sci Rep*, *12*, Article 12227. https://doi.org/10.1038/s41598-022-16354-5

Shyam, S., Arun, J., Gapinath, A., P., Ribhu, G., Ashish, M., & Ajay, S. (2022). Biomass as source for hydrochar and biochar production to recover phosphates from wastewater: A review on challenges, commercialization, and future perspectives.

Chemosphere, *285*, Article 131490. https://doi.org/10.1016/j.chemosphere.2021.131490

Shi, M., Xiong, W., Zhang, X., Ji, J., Hu, X., Tu, Z., & Wu, Y. (2022). Highly efficient and selective H2S capture by task-specific deep eutectic solvents through chemical dual-site absorption. *Separation and Purification Technology*, *283*, Article 120167. https://doi.org/10.1016/j.seppur.2021.120167

Silva, A., Ricci, B., C., Koch, K., Weisback, M., & Amaral, M. S. C. (2020). Dissolved hydrogen sulfide removal from anaerobic bioreactor permeate by modified direct contact membrane distillation. *Separation and Purification Technology*, *233*, Article 116036. https://doi.org/10.1016/j.seppur.2019.116036

Singh, R., Sharma, P., & Singh, S. (2020). Review of Imaging Techniques for Plant Disease Detection. Artificial Intelligence in Agriculture. *Chemical Engineering Journal Advances*, *4*, 229-242. https://doi.org/10.1016/j.aiia.2020.10.002

Sergienko, N., Cuervo Lumbaque, E., & Radjenovic, J. (2024). (Electro)catalytic oxidation of sulfide and recovery of elemental sulfur from sulfide-laden streams. *Water Research*, *245*, Article 120651. https://doi.org/10.1016/j.watres.2023.120651

Sugurbekova, G., Nagyzbekkyzy, E., Sarsenova, A., Danlybayeva, G., Anuarbekova, S., Kudaibergenova, R., Frochot, C., Acherar, S., Zhatkanbayev, Y., & Moldagulova, N. (2023). Sewage Sludge Management and Application in the Form of Sustainable Fertilizer. *Sustainability*, *15*(7), Article 6112. https://doi.org/10.3390/su15076112

Shang, G., Liu, L., Chen, P., Shen, G., & Li, Q. (2016). Kinetics and the mass transfer mechanism of hydrogen sulfide removal by biochar derived from rice hull. *Journal of the Air & Waste Management Association*, *66*, 439–445. https://doi.org/10.1080/10962247.2015.1122670

Taheriyoun, M., Salehiziri, M., & Parand, S. (2019). Biofiltration performance and kinetic study of hydrogen sulfide removal from a real source, *17*, 645-656. https://link.springer.com/article/10.1007/s40201-019-00378-7

Torres, R. A., Marín, D., Rodero, M. D. R., Pascual, C., Sanchez, A. G., Crespo, I. G., Lebrero, R., & Torre, R. M. (2020). Biogas treatment for H2S, CO2, and other contaminants removal. *From Biofiltration to promising Options in Gaseous Fluxes Biotreament*, *200*, 153–176. https://doi.org/10.1016/B978-0-12-819064-7.00008-X

Tavakkol, S., Askarany, D., Mahbub, R., & Javanmardi, A. (2021). Life cycle assessment of concrete with recycled content and the environmental impact of various concrete compositions. *Journal of Cleaner Production*, *299*, Article 126913. https://doi.org/10.1016/j.jclepro.2021.126913

Vikrant, K., Kailasa, S., K., Tsang, D. C. W., Lee, S. S., Kumar, P., Giri, B. S., Singh, R. S., & Kim, K. H. (2018). Biofiltration of hydrogen sulfide: *Trends and challenges. Journal of Cleaner Production*, *187*, 131–147. https://doi.org/10.1016/j.jclepro.2018.03.188

Vaiskunaite R. (2022). Cleaning of H2S from polluted air using peat BF. *Mokslas – Lietuvos ateitis / Science – Future of Lithuania*, *12*, Article 13081. https://doi.org/10.3846/mla.2020.13081

Vaiskunaite R. (2020). Using BF Packed with Different Wood Waste Charges for Purification of Air Contaminated with Benzene. In 11th International Conference "Environmental Engineering". Vilnius Gediminas Technical University. https://doi.org/10.3846/enviro.2020.805

Vuppaladadiyam, A. K., Jena, M. K., Hakeem, I. G., Patel, S., Veluswamy, G., Thulasiraman, A. V., Surapaneni, A., & Shah, K. (2024). A critical review of biochar versus hydrochar and their application for H_2S removal from biogas. *Reviews in Environmental Science and Bio/Technology*, 23, 699-737. https://link.springer.com/article/10.1007/s11157-024-09700-8

Vaziri, R. S., & Babler, M. U. (2019). Removal of Hydrogen Sulfide with Metal Oxides in Packed Bed Reactors—A Review from a Modeling Perspective with Practical Implications. *Applied Sciences*, *9*(24), Article 5316. https://doi.org/10.3390/app9245316

Wang, J., Liu, Y., Chen, X., & Zhang, Z. (2023). Enhancement of gas-phase hydrogen sulfide adsorption using chemically modified carbonaceous materials. *Journal of Hazardous Materials*, *442*, Article 130052. https://doi.org/10.1016/j.jhazmat.2022.130052

Wang, S., Nam, H., Lee, D., & Nam, H. (2022). H2S gas adsorption study using copper impregnated on KOH modified carbon from coffee residue for indoor air purification. *Journal of Environmental Chemical Engineering*, *10*, Article 108797. https://doi.org/10.1016/j.jece.2022.108797

Wang, Y., Wang, Y., & Liu, Y. (2020a). Removal of gaseous hydrogen sulfide using ultraviolet/Oxone-induced oxidation scrubbing system. *Chemical Engineering Journal*, *393*, Article 124740. https://doi.org/10.1016/j.cej.2020.124740

Wang, Y., Liu, Y., & Wang, Y. (2020b). Oxidation absorption of hydrogen sulfide from gas stream using vacuum ultraviolet/H_2O_2/urea wet scrubbing system. *Process Safety and Environmental Protection*, *140*, 348–355. https://doi.org/10.1016/j.psep.2020.05.025

Wojciechowska, C., Cema, G., & Ziembińska-Buczyńska, A. (2023). Sewage sludge pretreatment: current status and future prospects. *Environ Sci Pollut*, *30*, 88313–88330. https://doi.org/10.1007/s11356-023-28613-7

Watsuntorn, W., Khanongnuch, R., Chulalaksananuku, W., Rene, E. R., & Lens, P. N, L. (2020). Resilient performance of an anoxic biotrickling filter for hydrogen sulfide removal from a biogas mimic: Steady, transient state and neural network evaluation. *Journal of Cleaner Production*, *247*, Article 119351. https://doi.org/10.1016/j.jclepro.2019.119351

Wu, J., Jiang, X., Jin, Z., Yang, S., & Zhang, J. (2020). The performance and microbial community in a slightly alkaline biotrickling filter for the removal of high concentration H2S from biogas. *Chemosphere*, *249*, Article 126127. https://doi.org/10.1016/j.chemosphere.2020.126127

Xia, g., Zhou, X., Hu, j., Sun, Z., Yao, J., Chen, D., & Wang, J. (2019). Simultaneous removal of carbon disulfide and hydrogen sulfide from viscose fibre waste gas with

a biotrickling filter in pilot scale. *Journal of Cleaner Production*, *230*, 21–28. https://doi.org/10.1016/j.jclepro.2019.05.097

Xu, Y., Chen, Y., Ma, C., Qiao, W., Wang, J., & Ling, L. (2022). Functionalization of modified carbon fiber mat with bimetallic active sites for NH3 and H2S adsorption at room temperature. *Separation and Purification Technology*, *303*, Article 122335. https://doi.org/10.1016/j.seppur.2022.122335

Yang, S., Wu, J., Jiang, X., & Jin, Z. (2023). Influence of surface chemistry on microbial attachment and sulfur oxidation efficiency in biofilters. *Chemosphere*, *312*, Article 137225. https://doi.org/10.1016/j.chemosphere.2022.137225

Ying, S., Kong, X., Cai, Z., Man, Z., Xin, Y., & Liu, D. (2020). Interactions and microbial variations in a biotrickling filter treating low concentrations of hydrogen sulfide and ammonia. *Chemosphere*, *255*, Article 126931. https://doi.org/10.1016/j.chemosphere.2020.126931

Yuan, J., Du, L., Li, S., Yang, F., Zhang, Z., Li, G., & Wang, G. (2018). Use of mature compost as filter media and the effect of packing depth on hydrogen sulfide removal from composting exhaust gases by biofiltration. *Environmental Science and Pollution Research*, *26*, 3762–3770. https://doi.org/10.1007/s11356-018-3795-z

Yu, R., Cheng, J., Zhang, Y., & Ren, N., (2020). Evaluation of *Pseudomonas* and *Bacillus* strains for hydrogen sulfide removal in gas biofiltration systems. *Biochemical Engineering Journal*, *157*, Article 107550. https://doi.org/10.1016/j.bej.2020.107550

Zarei, M., Bayati, M. R., Nik, M. E., Rohani, A., & Hejazi, B. (2025). Modelling the removal efficiency of hydrogen sulfide from biogas in a biofilter using multiple linear regression and support vector machines. *Journal of Cleaner Production*, *404*, Article 136965. https://doi.org/10.1016/j.jclepro.2023.136965

Zhang, X., Lawan, I., Danhassan, U., A., He, Y., Qi, R., Wu, A., Sheng, K., & Lin, H. (2022). Advances in technologies for in situ desulfurization of biogas. *Advances In Bioenergy*, *8*, 99–137. https://doi.org/10.1016/bs.aibe.2022.05.001

Zhang, R., Cui, C., Xiao, R., Li, R., Mu, T., Huo, H., Ma, Y., Yin, G., & Zuo, P.(2023). Interface regulation of Mg anode and redox couple conversion in cathode by copper for high-performance Mg-S battery. *Chemical Engineering Journal*, *451*, Article 138663. https://doi.org/10.1016/j.cej.2022.138663

Zhang, H., Liu, J., & Wang, X. (2024). Coupled adsorption–biodegradation mechanisms in biofilters treating hydrogen sulfide: Experimental and modeling insights. *Journal of Environmental Management*, *343*, Article 118358. https://doi.org/10.1016/j.jenvman.2024.121943

Zhang, Y., Kawasaki, Y., Oshita, K., Takaoka, M., Minami, D., Inoue, G., & Tanaka, T. (2021). Economic assessment of biogas purification systems for removal of both H2S and siloxane from biogas. *Renewable Energy*, *168*, 119–130. https://doi.org/10.1016/j.renene.2020.12.058

Zhao, M., Wang, X., Lin, Y., & Guo, Z. (2023). The Biofilm Lifestyle of Acidophilic Metal/Sulfur-Oxidizing Microorganisms. *Biotechnology of Extremophiles*, 177-213. https://link.springer.com/chapter/10.1007/978-3-319-13521-2_6

Zeng, Y., Luo, Y., Huan, C., Shuai, Y., Liu, Y., Xu, L., Ji, G., & Yan, Z. (2019). Anoxic biodesulfurization using biogas digestion slurry in biotrickling filters. *Journal of Cleaner Production*, *224*, 218–237. https://doi.org/10.1016/j.jclepro.2019.03.218

Zhang, R., Bellenburg, S., Neu, T., R., Sand, W., & Vera, M. (2020a). Study of H2S Removal Capability from Simulated Biogas by Using Waste-Derived Adsorbent Materials. *Processes*, 177-213. https://doi.org/10.3390/pr8091030

Zhang, M., Guo, X., Liu, Y., & Qiu, G. (2020b). Comparative study on sulfur oxidation mechanisms in *Acidithiobacillus thiooxidans* and *Acidithiobacillus ferrooxidans* via transcriptome analysis. *Bioresource Technology*, *313*, Article 123643. https://doi.org/10.1016/j.biortech.2020.123643

Zhou, X., Yang, Y., Wang, J., & Zhang, R., (2021). Influence of environmental factors on sulfur oxidation by *Acidithiobacillus* spp. in tailing wastewater treatment. *Chemosphere*, *285*, Article 131490. https://doi.org/10.1016/j.chemosphere.2021.131490

Zagorskis, A., & Vaiskunaite, R. (2016). Modelling of a biofiltration process of volatile organic compound mixtures in a BF. Biotechnology & Biotechnological Equipment, 30(6), 1217–1222, https://doi.org/10.1080/13102818.2016.1232604

Zhanga, Y., Oshitaa, K., Kusakabea, T., Takaokaa, M., Kawasakib, Y., Minamib, D., & Tanaka, T. (2020). Simultaneous removal of siloxanes and H2S from biogas using an aerobic biotrickling filter. *Journal of Hazardous Material*, *391*, Article 122187. https://doi.org/10.1016/j.jhazmat.2020.122187

List of Scientific Publications by the Author on the Topic of the Dissertation

Papers in the Reviewed Scientific Journals

Vaiškūnaitė, R., Mažeikienė, A., & Mohammadi, K. (2024). Effects of pyrolysis temperature on biochar physicochemical and microbial properties for H_2S removal from biogas. *Sustainability*, *16*(13), Article 5424, 1–13. https://doi.org/10.3390/su16135424

Mohammadi, K., Vaiškūnaitė, R., & Zigmontienė, A. (2025). Efficiency of hydrogen sulfide removal from biogas using a laboratory-scale biofilter packed with biochar, cellular concrete waste, or polyurethane foam: A COMSOL simulation study. *Processes, Special Issue: Advances in Waste Treatment, Bioremediation and Decarbonization Research*, *13*(2), Article 329, 1–17. https://doi.org/10.3390/pr13020329

Mohammadi, K., Vaiškūnaitė, R., & Zagorskis, A. (2024). Innovative biofiltration materials for H_2S removal from biogas. *Environmental Health Engineering and Management Journal*, *11*(3), 1–10. https://doi.org/10.34172/EHEM.2024.35

Mohammadi, K. (2022). Evaluation of selected greenhouse gas emissions from municipal solid waste landfill models. *Science – Future of Lithuania / Environmental Engineering*, *14*, Article 2022.17245, 1–5. https://doi.org/10.3846/mla.2022.17245

Mohammadi, K., & Vaiškūnaitė, R. (2023a). Analysis and evaluation of biogas purification technologies for H_2S removal. Science – Future of Lithuania / Environmental Engineering, *15*, Article 2023.17242, 1–9. https://doi.org/10.3846/mla.2023.17242

Mohammadi, K., & Vaiškūnaitė, R. (2024). Experimental research on selected biofiltration materials under dynamic conditions. Science – Future of Lithuania / Environmental Engineering, *16*, Article 2024.21297, 1–6. https://doi.org/10.3846/mla.2024.21297

Mohammadi, K., & Vaiškūnaitė, R. (2025). Experimental analysis of hydrogen sulfide removal from biogas using a biofilter containing cellular concrete waste and biochar. Science – Future of Lithuania / Environmental Engineering, *17*, Article 2025.23937, 1–6. https://doi.org/10.3846/mla.2025.23937

Papers in Other Editions

Mohammadi, K., & Vaiškūnaitė, R. (2023b). Evaluation of biofiltration materials for H_2S removal. In *Proceedings of the 12th International Conference "Environmental Engineering"*, Vilnius Gediminas Technical University, Lithuania, Article enviro. 2023.907, 1–6. https://doi.org/10.3846/enviro.2023.907

Patent application

Mohammadi, K., Vaiškūnaitė, R. (2025). Application of Modified Biofiltration Materials from Sewage Sludge and Concrete Waste for Hydrogen Sulfide (H_2S) Removal from Biogas. Application number: 2025 018.

Summary in Lithuanian

Įvadas

Problemos formulavimas

Biodujos, kurių pagrindinės sudedamosios dalys yra metanas (CH_4) ir anglies dioksidas (CO_2), yra perspektyvus atsinaujinančiosios energijos šaltinis, gaunamas anaerobinio organinių atliekų skaidymo metu. Tačiau jų efektyvų panaudojimą riboja biodujose esantis vandenilio sulfidas (H_2S). Šis junginys yra labai toksiškas, skatina koroziją, kelia grėsmę žmonių sveikatai, mažina biodujų energijos sistemų patikimumą ir trumpina jų eksploatavimo laiką (Torres et al., 2020; Wang, 2020b). Nustatyta, kad H_2S koncentracijai viršijus ~100 ppm, intensyviai koroduoja vamzdynai, varikliai ir turbinos, didėja priežiūros sąnaudos, mažėja įrangos ilgaamžiškumas, taip pat biodujų šilumingumas ir degimo efektyvumas (Zhang et al., 2022; Khan et al., 2021; Pabby & Sastre, 2013).

H_2S šalinti iš biodujų sukurta įvairių fizinių, cheminių ir biologinių metodų. Nors fizinė adsorbcija ir cheminė absorbcija pasižymi dideliu efektyvumu, jos dažnai susijusios su didelėmis eksploatacinėmis ir energijos sąnaudomis, cheminių reagentų naudojimu bei antrinių atliekų tvarkymo problemomis, todėl jų aplinkosauginis tvarumas yra ribotas (Perez et al., 2020; Gao et al., 2022). Dėl šios priežasties biologinė filtracija, paremta sierą oksiduojančių mikroorganizmų veikla, sulaukia vis didesnio dėmesio kaip ekonomiška ir aplinkosauginiu požiūriu patraukli alternatyva (Vikrant et al., 2018; Muthulakshmi & Sundrarajan, 2020).

Vis dėlto biofiltracijos sistemų veiksmingumą vis dar riboja nepakankamas biofiltro užpildo fizikocheminių savybių optimizavimas, ribota mikrobiologinių procesų kontrolė

ir patikimų matematinių bei skaitinių modelių, leidžiančių prognozuoti biofiltro veikimą kintamomis eksploatavimo sąlygomis, trūkumas (Haosagul et al., 2020; Yuan et al., 2018). Be to, nepakankamai ištirtas iš atliekų pagamintų medžiagų, kaip tvaraus, pakartotinai naudojamo ir ekonomiškai efektyvaus biofiltro užpildo, potencialas (Xia et al., 2019; Ying et al., 2020).

Darbo aktualumas

Didėjant biodujų gamybos ir jų panaudojimo energetikos bei aplinkosaugos sektoriuose apimčiai, auga pažangių, moksliškai pagrįstų vandenilio sulfido šalinimo iš biodujų technologijų poreikis (Torres et al., 2020; Rivard et al., 2018). Biologinė filtracija laikoma perspektyviu technologiniu sprendimu dėl efektyvaus vandenilio sulfido šalinimo ir technologinių sprendimų lankstumo (Vikrant et al., 2018; Ying et al., 2020).

Biofiltracijos sistemų efektyvumą ir stabilumą daugiausia lemia biofiltro užpildo fizikocheminės ir struktūrinės savybės, kurios daro įtaką vandenilio sulfido pernašai, mikroorganizmų aktyvumui ir bendram proceso efektyvumui (Haosagul et al., 2020; Zhang et al., 2021). Todėl biofiltracijos medžiagų modifikavimas ir optimizavimas tapo svarbia šiuolaikinių tyrimų kryptimi, leidžiančia pereiti nuo pavienių laboratorinių eksperimentų prie moksliškai pagrįsto biofiltrų projektavimo ir praktinio taikymo.

Šio tyrimo aktualumas taip pat siejamas su iš atliekų pagamintų medžiagų integravimu į biofiltracijos sistemas. Europos Sąjungoje kasmet susidaro apie 7–15 mln. tonų nuotekų dumblo (sausosios medžiagos), o Lietuvoje – apie 60–70 tūkst. tonų. Statybos ir griovimo atliekos sudaro apie 30–35 **%** visų atliekų, o polimerinės atliekos yra sparčiai augantis atliekų srautas, kurio efektyvus panaudojimas aplinkosauginiuose sprendimuose vis dar ribotas (Eurostat, 2020; Eurostat, 2021; European Commission, 2020). Šių atliekų pavertimas funkcinėmis biofiltracijos medžiagomis sudaro prielaidas įgyvendinti žiedinės ekonomikos principus ir kurti inovatyvius biodujų valymo sprendimus.

Disertacijoje nagrinėjamas biofiltracijos medžiagų kūrimas ir taikymas vandenilio sulfidui šalinti iš biodujų. Tyrime vertinamos fiziškai ir chemiškai modifikuotos bei nemodifikuotos iš atliekų gautos medžiagos: iš nuotekų dumblo pagamintos bioanglys, autoklavinio akytojo betono (CLC) atliekos ir putų poliuretanas (PUF). Integruojant eksperimentinius tyrimus, mikrobiologinę analizę, statistinį ryšių vertinimą ir matematinius modelius, suformuojamas mokslinis pagrindas biofiltracijos medžiagoms parinkti ir modifikuoti, prisidedant prie fundamentinių ir taikomųjų tyrimų plėtros (Haosagul et al., 2020; Zhanga et al., 2020; Kalinska et al., 2019).

Tyrimų objektas

Darbo tyrimų objektas –sieros vandeniliui šalinti iš biodujų skirtos biofiltracijos medžiagos: iš nuotekų dumblo pagamintos bioanglys, akytojo lengvojo betono (CLC) atliekos ir putų poliuretanas (PUF).

Darbo tikslas

Disertacijos tikslas – įvertinti metodus, skirtus padidinti vandenilio sulfido pašalinimo iš biodujų efektyvumui ir pagerinti biofiltro eksploataciniam stabilumui, taikant fiziškai ir

chemiškai modifikuotas bei nemodifikuotas iš atliekų gautas medžiagas biofiltracijos procese.

Darbo uždaviniai

Darbo tikslui pasiekti sprendžiami šie uždaviniai:

1. Išanalizuoti mokslinę literatūrą, siekiant identifikuoti esamas tyrimų spragas, susijusias su biodujų valymo nuo sieros vandenilio technologijomis, biofiltracijos medžiagomis ir mikrobiologiniais procesais.
2. Atrinkti ir charakterizuoti atliekų kilmės biofiltracijos medžiagas, įskaitant bioanglis, akytojo lengvojo betono (CLC) atliekas ir putų poliuretaną (PUF), bei įvertinti fizinės ir cheminės modifikacijos poveikį jų fizikocheminėms savybėms, svarbioms H_2S šalinti.
3. Eksperimentiškai įvertinti modifikuotų ir nemodifikuotų biofiltracijos medžiagų efektyvumą, šalinant sieros vandenilį iš biodujų kontroliuojamomis laboratorinėmis sąlygomis.
4. Ištirti bioplėvelės formavimąsi ir vystymąsi skirtingų biofiltracijos medžiagų paviršiuje bei nustatyti medžiagų savybių ir jų modifikacijos įtaką mikroorganizmų aktyvumui ir pasiskirstymui.
5. Nustatyti statistinius ryšius tarp biofiltracijos medžiagų fizikocheminių savybių, mikrobiologinių rodiklių ir sieros vandenilio šalinimo efektyvumo biofiltracijos sistemose.
6. Sukurti biofiltracijos proceso matematinį modelį, leidžiantį aprašyti sieros vandenilio šalinimą ir mikroorganizmų aktyvumą, bei įvertinti šio modelio atitiktį eksperimentiniams rezultatams.
7. Atlikti biofiltracijos sistemų skaitmeninį modeliavimą ir pagrįsti eksperimentinius rezultatus, analizuojant sieros vandenilio koncentracijos ir reakcijos greičio pasiskirstymą biofiltre esant skirtingoms biofiltracijos medžiagų konfigūracijoms.

Tyrimų metodika

Teoriniai ir eksperimentiniai tyrimai atlikti Vilniaus Gedimino technikos universiteto (VILNIUS TECH) Aplinkos apsaugos ir vandens inžinerijos katedros bei Rygos technikos universiteto (Latvija) Vandens sistemų ir biotechnologijų instituto laboratorijose. Papildomi biofiltracijos medžiagų struktūriniai ir cheminiai tyrimai atlikti Teherano ir Ferdousi universitetų (Iranas) laboratorijose, o biofiltracijos proceso matematinis ir skaitmeninis modeliavimas vykdytas bendradarbiaujant su VILNIUS TECH Matematinio modeliavimo katedros mokslininkais.

Sieros vandeniliui (H_2S) šalinti iš biodujų taikyta biologinės filtracijos technologija, naudojant fiziškai ir chemiškai modifikuotas bioanglis, akytojo lengvojo betono (CLC) atliekas ir putų poliuretaną (PUF). Tyrimų metu nustatytos biofiltracijos medžiagų fizikocheminės savybės, įvertintas H_2S šalinimo efektyvumas, mikroorganizmų aktyvumas ir

biofiltro veikimo stabilumas, o eksperimentiniai rezultatai papildomai analizuoti taikant matematinį modeliavimą ir skaitmeninius skaičiavimus.

Darbo mokslinis naujumas

Rengiant disertaciją gauti šie aplinkos inžinerijos moksle nauji rezultatai:

1. Sukurta ir eksperimentiškai pagrįsta sieros vandeniliui (H_2S) šalinti iš biodujų skirta biofiltracijos medžiagų koncepcija, parodanti fiziškai ir chemiškai modifikuotų iš atliekų pagamintų medžiagų – KOH modifikuotų bioanglių ir $FeCO_3$ modifikuotų akytojo lengvojo betono (CLC) atliekų – efektyvų taikymą, leidžiantį pasiekti iki 90–95 % H_2S šalinimo efektyvumą.
2. Atskleistas biofiltracijos medžiagų modifikacijos vaidmuo reguliuojant mikroorganizmų aktyvumą ir biofiltracijos proceso stabilumą, nustatant kiekybinius ryšius tarp modifikuotų užpildų fizikocheminių savybių – porėtumo (~65–75 %) ir specifinio paviršiaus ploto (180–320 $m^2 \cdot g^{-1}$), sierą oksiduojančių mikroorganizmų aktyvumo, bioplėvelės formavimosi intensyvumo ir sieros vandenilio šalinimo efektyvumo.
3. Sukurtas ir eksperimentiniais duomenimis patikrintas biofiltracijos proceso matematinis ir skaitmeninis modelis, leidžiantis prognozuoti sieros vandenilio šalinimo efektyvumą su mažesniu nei 10 % nuokrypiu ir pagrįsti biofiltracijos sistemų optimizavimą.

Darbo rezultatų praktinė reikšmė

Disertacijos rezultatai turi praktinę reikšmę biodujų gamybos, aplinkos apsaugos ir atliekų tvarkymo srityse, nes pateikia į biofiltracijos medžiagas orientuotą sieros vandenilio (H_2S) šalinimo iš biodujų sprendimą. Fiziškai ir chemiškai modifikuotų iš atliekų pagamintų biofiltracijos medžiagų taikymas leidžia užtikrinti stabilų biologinį desulfuravimo procesą, sumažinti H_2S sukeltą energetinių sistemų koroziją ir pagerinti biodujų energinę kokybę.

Parodyta, kad iš nuotekų dumblo pagamintos bioanglys ir statybinės akytojo lengvojo betono (CLC) atliekos, derinamos su putų poliuretanu (PUF) kaip mechaniškai ir hidrauliškai stabilia konstrukcine užpildo medžiaga, gali būti naudojamos kaip tvari komercinių biofiltrų užpildų alternatyva. Gauti rezultatai gali būti taikomi žemės ūkio biodujų jėgainėse, nuotekų valymo įrenginiuose ir kitose biodujų panaudojimo sistemose, prisidedant prie aplinkai draugiškų ir žiedinės ekonomikos principais pagrįstų biodujų valymo technologijų diegimo.

Ginamieji teiginiai

1. Nuotekų dumblo kilmės bioanglys, modifikuotos KOH, pasižymi savituoju BET paviršiaus plotu, išaugusiu nuo 24,66 $m^2 \cdot g^{-1}$ iki 471,54 $m^2 \cdot g^{-1}$, bei didesniu specifiniu mikro- ir mezoporų tūriu; tai biofiltracijos sistemoje lemia H_2S šalinimo efektyvumo padidėjimą nuo maždaug 80 % iki 92 %
2. KOH modifikuotų bioanglių ir $FeCO_3$ impregnuotų akytojo lengvojo betono (CLC) atliekų derinys biofiltruose sukuria sinerginį adsorbcinį ir biokatalizinį

efektą, dėl kurio, palyginti su nemodifikuotais ar vienkomponenčiais užpildais, H_2S šalinimo efektyvumas santykinai padidėja 10–15 %, o tai leidžia užtikrinti stabilesnį proceso veikimą.

3. Biofiltracijos sistemose H_2S šalinimo procesą lemia sierą oksiduojančių bakterijų (*Acidithiobacillus* spp.) ir bioplėvelę formuojančių mikroorganizmų (*Pseudomonas* spp.) sąveika, kuri modifikuotų užpildų paviršiuje skatina intensyvesnį bioplėvelės formavimąsi ir didesnę tarpląstelinių polimerinių medžiagų (EPS) sintezę, taip sudarydama sąlygas pasiekti daugiau kaip 90 % H_2S šalinimo efektyvumą.

Darbo rezultatų aprobavimas

Disertacijos tema yra publikuoti 8 moksliniai straipsniai: du – *Web of Science* duomenų bazės leidiniuose, turinčiuose citavimo rodiklį (*Processes, Sustainability*) (Mohammadi et al., 2024a; Mohammadi et al., 2025a), vienas – *Web of Science* duomenų bazės *Emerging Sources Citation Index* (ESCI) ir Scopus duomenų bazėse referuojamame leidinyje (*Journal of Environmental Health Engineering and Management*) (Mohammadi et al., 2024b), keturi – kitose tarptautinėse duomenų bazėse referuojamuose recenzuojamuose leidiniuose (*Science – Future of Lithuania / Environmental Engineering*) (Mohammadi 2022; Mohammadi et al., 2023a; Mohammadi et al., 2024; Mohammadi et al., 2025), vienas – *Scopus* duomenų bazėje referuojamame tarptautinių konferencijų straipsnių rinkinyje (*12th International Conference on Environmental Engineering*) (Mohammadi et al., 2023c). Paskelbtos dvi tezės tarptautinių mokslinių konferencijų pranešimų tezių leidiniuose CONECT 2024 ir CONECT 2025 (Mohammadi et al., 2024c; Mohammadi et al., 2025d). Pateikta paraiška „Modifikuotų biofiltro įkrovų, gautų iš nuotekų dumblo ir betono atliekų, taikymas sieros vandenilio (H_2S) šalinimui iš biodujų“ (Mohammadi et al., 2024e) Lietuvos Respublikos patentui gauti (paraiškos numeris 2025 018; pateikimo data 2025-10-10).

Disertacijoje atliktų tyrimų rezultatai buvo paskelbti ir pristatyti septyniose nacionalinėse ir tarptautinėse mokslinėse konferencijose Lietuvoje ir užsienyje:

- keturiose Lietuvos jaunųjų mokslininkų konferencijose „Mokslas – Lietuvos ateitis. Aplinkos apsaugos inžinerija“, 2022–2025 m. Vilniuje, Lietuvoje;
- 13-ojoje tarptautinėje konferencijoje „Aplinkos inžinerija“, 2023 m., Vilniuje, Lietuvoje;
- 2 tarptautinėse Aplinkos ir klimato technologijų konferencijose (CONECT 2024 ir CONECT 2025), 2024 ir 2025 m., Rygoje, Latvijoje.

Disertacijos struktūra

Disertaciją sudaro įvadas, trys skyriai, bendrosios išvados ir rekomendacijos. Darbo apimtis yra 137 puslapiai, tekste panaudotos 36 numeruotos formulės, 49 paveikslai ir 27 lentelės. Rašant disertaciją buvo panaudoti 158 literatūros šaltiniai.

Padėka

Nuoširdžiai dėkoju Vilniaus Gedimino technikos universiteto Aplinkos apsaugos ir vandens inžinerijos katedros darbuotojams už suteiktą techninę pagalbą, tyrimų infrastruktūrą ir išteklius. Ypatingą padėką reiškiu savo darbo vadovei doc. dr. Rasai Vaiškūnaitei už mokslinį vadovavimą, vertingas pastabas ir nuolatinę paramą rengiant disertaciją. Taip pat dėkoju dr. sc. ing. Lindai Mežule (Rygos technikos universitetas) už konsultacijas biofiltracijos ir mikrobiologinių tyrimų klausimais bei VILNIUS TECH Matematinio modeliavimo katedros docentei dr. Teresei Leonavičienei už pagalbą atliekant matematinius ir skaitinius modeliavimus. Dėkoju Teherano universiteto Civilinės inžinerijos laboratorijos ir Ferdousi universiteto Cheminės analizės laboratorijos darbuotojams už pagalbą atliekant struktūrines ir chemines analizes, taip pat Tomui Žemaičiui už pagalbą vykdant laboratorinius eksperimentus ir analizuojant duomenis.

1. Biotechnologijų, skirtų sieros vandeniliui (H_2S) šalinti iš biodujų, literatūros analizė

Atliekant literatūros analizę, nagrinėjamos biotechnologijos, skirtos vandenilio sulfidui (H_2S) šalinti iš biodujų. Ypatingas dėmesys skiriamas biofiltracijai kaip tvariai tradicinių fizinių ir cheminių desulfurizacijos metodų alternatyvai. Literatūros duomenimis, H_2S koncentracija biodujose paprastai svyruoja nuo 100 iki 20 000 ppm (Huan et al., 2020; Jiang et al., 2021), o kai kuriais atvejais gali siekti iki ~3 % biodujų tūrio (Torres et al., 2020). Net ir maža H_2S koncentracija (<100 ppm) gali sukelti koroziją ir didinti įrangos pažeidimų riziką (Das et al., 2022a; Torres et al., 2020; Kulawong et al., 2022), todėl efektyvus H_2S šalinimas yra būtinas biodujų konversijai į biometaną.

Biofiltracija leidžia derinti fizikinę adsorbciją ir biologinę oksidaciją, mažinant cheminių reagentų naudojimą ir antrinių atliekų susidarymą (Perez et al., 2020; Torres et al., 2020). Literatūroje pateikiamais duomenimis, H_2S šalinimo efektyvumas biofiltruose paprastai siekia 70–95 %, o optimizuotose sistemose gali viršyti 95 % (Vuppaladadiyam et al., 2024).

Biofiltracijos efektyvumą lemia užpildo medžiagų savybės, tokios kaip specifinis paviršiaus plotas (>300 $m^2 \cdot g^{-1}$), porėtumas ir paviršiaus cheminė sudėtis, kurie sudaro sąlygas tiek H_2S adsorbcijai, tiek sierą oksiduojančių mikroorganizmų kolonizacijai (Das et al., 2019; Zhang et al., 2023). Bioanglys, ypač aktyvintosios KOH, gali užtikrinti >95–98 % H_2S šalinimo efektyvumą (Lin et al., 2021; Tavakkol et al., 2021). CLC atliekos pasižymi geromis buferinėmis savybėmis ir, modifikuotos $FeCO_3$, sustiprina katalizinę H_2S oksidaciją (Wu et al., 2021; Pudi et al., 2022; Bora et al., 2024). Putų poliuretanas (PUF) biofiltruose naudojamas kaip atraminė terpė mikroorganizmų bioplėvelėms formuotis (Juntranapaporn et al., 2019; Zeng et al., 2019).

Literatūros šaltinių analizė rodo, kad daugiakomponentės biofiltracijos sistemos, kuriose derinami adsorbciniai, kataliziniai ir biologiniai mechanizmai, pasižymi stabilesniu veikimu nei vienkomponentės sistemos (Zhang et al., 2023; PlasticsEurope et al., 2020). Sierą oksiduojančios bakterijos (*Acidithiobacillus* spp., *Thiobacillus* spp., *Pseudomonas* spp.) formuoja bioplėveles užpildo paviršiuje, o jų aktyvumas priklauso nuo pH, temperatūros, drėgmės ir porų struktūros. Optimalios sąlygos dažniausiai yra pH 6,5–8,0 ir 25–35 °C temperatūra (Haosagul ir kt., 2020; Rouhollahi ir kt., 2024).

Apibendrinant galima teigti, kad biofiltracijos medžiagų tyrimai vis dar yra fragmentiški, ypač trūksta duomenų apie modifikuotų ir hibridinių medžiagų ilgalaikį veikimą bei mikroorganizmų dinamiką realiomis biodujų valymo sąlygomis. Atsižvelgiant į šias spragas buvo suformuluotas disertacijos tikslas – ištirti biofiltracijos medžiagas efektyviam ir tvariam biodujų valymui nuo H_2S.

2. Medžiagų fizikocheminių savybių ir adsorbcinių charakteristikų nustatymo bei taikymo H_2S šalinti iš biodujų metodikos

Antrajame disertacijos skyriuje pateikiama integruota metodinė sistema, skirta biofiltracijos medžiagų fizikinių, cheminių ir biologinių savybių tyrimams bei jų taikymo efektyvumui šalinant iš biodujų sieros vandenilį (H_2S). Tyrimų metodika apima eksperimentinius tyrimus, mikrobiologinę analizę ir skaitmeninį modeliavimą, leidžiančius įvertinti biofiltracijos medžiagų veikimą ir jų sąveiką su biologiniais procesais biodujų valymo metu. Tyrimų metodinė schema ir biofiltro konstrukcija pateikta S2.1 pav.

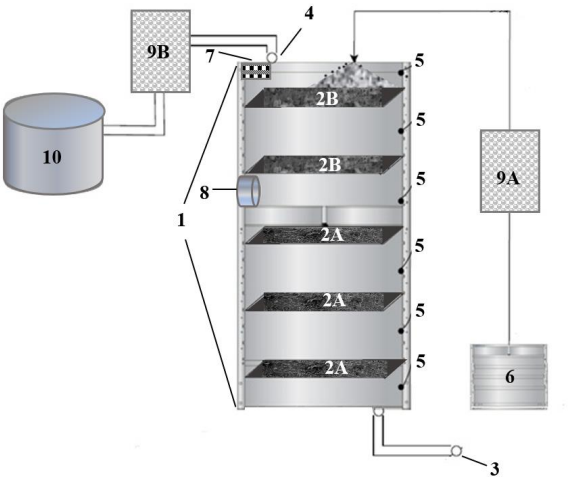

S2.1. pav. Biofiltro, kuriame vykdomas biodujų valymo nuo sieros vandenilio (H_2S) biofiltracijos procesas, schema: 1 – biofiltro korpusas; 2A – modifikuotų bioanglių įkrovų sluoksniai; 2B – modifikuoti betono atliekų įkrovų sluoksniai; 3 – dujų įtekėjimo ortakis; 4 – dujų išleidimo ortakis; 5 – mėginių paėmimo angos; 6 – maistinių medžiagų tiekimo rezervuaras; 7 – drėgmės jutiklis; 8 – rotametras; 9A – maistinių medžiagų tiekimo siurblys; 9B – išvalytų biodujų siurblys; 10 – išvalytų biodujų kaupimo rezervuaras

Tyrimams pasirinktos trys skirtingos kilmės biofiltracijos medžiagos: organinė (bioanglys), neorganinė (ląstelinio lengvojo betono (CLC) atliekos) ir sintetinė (putų poliuretanas (PUF). Analizuotos tiek atskiros, tiek modifikuotos ir nemodifikuotos medžiagos bei jų vienkomponentės ir daugiakomponentės kombinacijos, siekiant įvertinti adsorbcinių, katalizinių ir biologinių H_2S šalinimo mechanizmų sąveiką.

Eksperimentiniai tyrimai atlikti naudojant vertikalų biofiltrą, leidžiantį reguliuoti pagrindinius proceso parametrus: dujų srauto greitį, drėgmę, temperatūrą ir mitybinių medžiagų tiekimą. Biofiltre skirtinguose aukščio lygiuose įrengtos mėginių ėmimo angos, kad būtų galima stebėti H_2S šalinimo eigą ir mikroorganizmų kolonizacijos pasiskirstymą. Į biofiltrą buvo tiekiamos kontroliuojamos H_2S koncentracijos (100–2000 ppm) natūralios ir sintetinės biodujos, o biodujų buvimo trukmė biofiltre (EBRT) reguliuota keičiant dujų srauto greitį.

Biofiltracijos medžiagų fizikinės ir cheminės savybės nustatytos taikant standartinius laboratorinius metodus: nustatytas piltinis tankis, pH, savitasis elektrinis laidumas, porėtumas, specifinis paviršiaus plotas (BET) bei cheminė ir elementinė sudėtis. Bioanglys pagamintos kontroliuojamos pirolizės būdu (400–600 °C) ir modifikuotos KOH, siekiant padidinti porėtumą ir paviršiaus reaktyvumą. CLC atliekos modifikuotos geležies karbonatu ($FeCO_3$), siekiant sustiprinti jų buferines ir katalizines savybes, o PUF naudotos kaip struktūrinė atraminė terpė mikroorganizmų bioplėvelėms formuotis.

Mikrobiologiniai tyrimai buvo skirti sierą oksiduojančių bakterijų kolonizacijai ir bioplėvelių formavimuisi tirti. Į biofiltrą įvestos *Pseudomonas* spp. ir *Acidithiobacillus* spp. kultūros, o jų pasiskirstymas vertintas naudojant fluorescencinę mikroskopiją (DAPI ir baltymų dažymą).

H_2S šalinimo efektyvumas nustatytas analizuojant biodujų sudėtį biofiltro įėjimo, tarpiniuose ir išėjimo ortakiuose naudojant dujų analizatorių. Remiantis gautais duomenimis apskaičiuotas H_2S šalinimo efektyvumas ir įvertinta biofiltrų veikimo priklausomybė nuo biofiltracijos medžiagų tipo, jų išdėstymo bei eksploatacinių sąlygų.

Eksperimentiniai rezultatai papildyti matematiniu modeliavimu MATLAB aplinkoje, taikant modifikuotą *Monod* modelį analizuota sierą oksiduojančių bakterijų augimo kinetika,. Erdvinis H_2S pernašos ir biologinės oksidacijos modeliavimas biofiltre atliktas taikant COMSOL *Multiphysics* programą.

3. Biofiltracijos medžiagų teorinių ir eksperimentinių tyrimų rezultatai

Šiame disertacijos skyriuje pateikiami teorinių ir eksperimentinių tyrimų rezultatai, skirti biofiltracijos medžiagų taikymo efektyvumui sieros vandenilio (H_2S) šalinimo iš biodujų procesuose įvertinti. Tyrimai atlikti laboratorinėmis sąlygomis naudojant biofiltrą, užpildytą iš nuotekų dumblo pagamintomis bioanglimis, akytojo lengvojo betono (CLC) atliekomis, putų poliuretanu (PUF) bei jų modifikuotomis ir sluoksninėmis kombinacijomis.

Rezultatai parodė, kad biofiltracijos medžiagų fizikocheminės savybės daro esminę įtaką biofiltrų efektyvumui šalinant H_2S iš biodujų. Statistinė analizė patvirtino reikšmingus tirtų medžiagų skirtumus ($p < 0,05$). Vertinti pagrindiniai rodikliai: piltinis tankis, porėtumas, specifinis paviršiaus plotas, pH ir savitasis elektrinis laidumas. Nustatyta, kad bioanglys pasižymi palankiausiomis H_2S šalinimo savybėmis dėl mažo piltinio tankio, didelio porėtumo, išvystyto specifinio paviršiaus ploto ir šarminio pH, sudarančio palankias sąlygas adsorbcijai ir sierą oksiduojančių mikroorganizmų aktyvumui (S3.1 lentelė). Bioanglių ir mineralinių medžiagų skirtumai buvo statistiškai reikšmingi ($p < 0,01$), o matavimų nuokrypis neviršijo 7 %.

Bioanglių cheminė aktyvacija kalio hidroksidu (KOH) reikšmingai padidino jų adsorbcines savybes. Aktyvacijos metu susiformavo mikro- ir mezoporų struktūra, padidėjo specifinis paviršiaus plotas ir aktyvių adsorbcinių centrų skaičius, o tai pagerino H_2S adsorbciją ir mikroorganizmų kolonizacijos sąlygas (S3.2 lentelė).

CLC atliekos pasižymėjo didesniu piltiniu tankiu ir mažesniu specifiniu paviršiaus plotu nei bioanglys, tačiau jų mineralinė sudėtis sudarė sąlygas cheminėms reakcijoms su sieros junginiais. Elektrinio laidumo analizė parodė, kad CLC atliekos veikia kaip kietoji katalitinė terpė, kurios aktyvumas pasireiškia paviršinėse reakcijose (S3.3 lentelė). CLC modifikavimo $FeCO_3$ poveikis H_2S oksidacijai pateiktas S3.1 pav., kuriame matyti reikšmingi paviršiaus morfologijos pokyčiai po biodujų valymo.

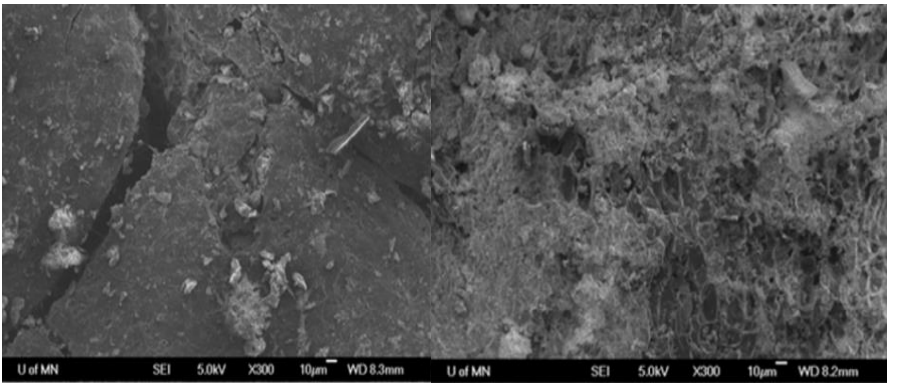

(a) (b)

S3.1 pav. Pateiktuose SEM vaizduose matyti reikšmingi akytojo lengvojo betono (CLC) atliekų paviršiaus morfologijos pokyčiai prieš ir po sieros vandenilio (H_2S) šalinimo iš biodujų

Putų poliuretanas pasižymėjo nedideliu adsorbciniu aktyvumu, tačiau dėl didelio porėtumo ir mechaninio stabilumo sudarė palankias sąlygas mikroorganizmams prisitvirtinti ir bioplėvelėms formuotis bei užtikrino tolygesnį dujų srauto pasiskirstymą biofiltre (S3.2 pav.). Biofiltracijos eksperimentai parodė, kad didžiausias H_2S šalinimo efektyvumas pasiekiamas naudojant daugiakomponentes biofiltracijos sistemas su modifikuotomis bioanglimis (S3.2 pav.). Vienkomponenčių biofiltrų veikimo rezultatai (S3.3 pav.) parodė, kad tokiose sistemose H_2S šalinimas dažniausiai ribojamas vienu mechanizmu – adsorbcija, katalizine oksidacija arba biologine degradacija. Daugiakomponentėse sistemose šių mechanizmų sinergija leidžia pasiekti stabilesnį procesą. Tokiose sistemose H_2S šalinimo efektyvumas statistiškai reikšmingai viršijo vienkomponenčių sistemų rezultatus ($p < 0,05$) ir buvo 15–25 % didesnis, o optimaliais režimais nuosekliai viršijo 90 %.

Mikrobiologiniai tyrimai parodė, kad mikroorganizmų kolonizacija glaudžiai susijusi su biofiltracijos medžiagų savybėmis (S3.4 pav.). Bioanglys sudarė palankesnes sąlygas mikroorganizmams prisitvirtinti ir didesnei biomasės koncentracijai susidaryti nei CLC atliekos. *Pseudomonas* spp. bakterijos formavo tankias bioplėveles biofiltro vidurinėse zonose, o *Acidithiobacillus* spp. bakterijos pasižymėjo tolygesniu pasiskirstymu ir prisidėjo prie proceso stabilumo.

S3.1 lentelė. Tirtų biofiltracijos medžiagų piltinis tankis

	Piltinis tankis kg·m^{-3}	
Biofiltracijos medžiagos, mm	**X > 0,6**	**1 > X > 0,6**
Putų poliuretanas (PUF)	30	
Akytojo lengvojo betono (CLC) atliekomis	547	
Nuotekų dumblas	73	55
400 °C pirolizuotos bioanglys	79	57
500 °C pirolizuotos bioanglys	80	58
600 °C pirolizuotos bioanglys	80	59

S3.2. lentelė. Bioanglių mėginių specifinio paviršiaus ploto (S_{BET}) ir porėtumo (P_{BET}) fizikinė modifikacija aktyvinant KOH

Bioanglių cheminės savybės	**Prieš modifikaciją**	**Po modifikacijos su KOH**
S_{BET} (nuotekų dumblas, prieš pirolizę), m^2/g	17,96	43,24
S_{BET} (po 400°C pirolizės), m^2/g	12,28	235,32
S_{BET} (po 500°C pirolizės), m^2/g	22,76	433,44
S_{BET} (po 600°C pirolizės), m^2/g	24,66	471,54
P_{BET} (nuotekų dumblas, prieš pirolizę), cm^3/g	0,048	0,036
P_{BET} (po 400°C pirolizės), cm^3/g	0,01	0,096
P_{BET} (po 500°C pirolizės), cm^3/g	0,42	4
P_{BET} (po 600°C pirolizės), cm^3/g	0,025	0,24

S3.3. lentelė. CLC atliekų cheminės sudėties (esančių medžiagų) analizės rezultatai, nustatyti rentgeno fluorescencijos (XRF) metodu

	Elektrinis laidumas µS/cm	
Biofiltracijos medžiagos, mm	**X > 0,6**	**1 > X > 0,6**
Putų poliuretanas (PUF)	283	
Akytojo lengvojo betono (CLC) atliekomis	N/A	
Nuotekų dumblas	983	702
400 °C pirolizuotos bioanglys	225	191,2
500 °C pirolizuotos bioanglys	193,4	187,1
600 °C pirolizuotos bioanglys	187,4	185,9

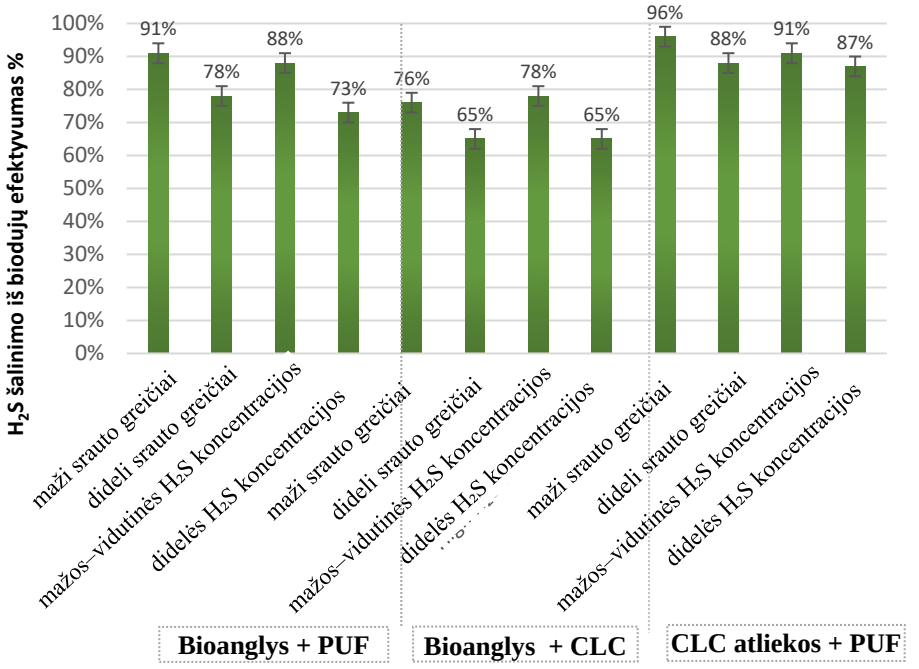

S3.2 pav. H_2S šalinimo efektyvumo palyginimas skirtingose daugiakomponentėse biofiltracijos medžiagų konfigūracijose

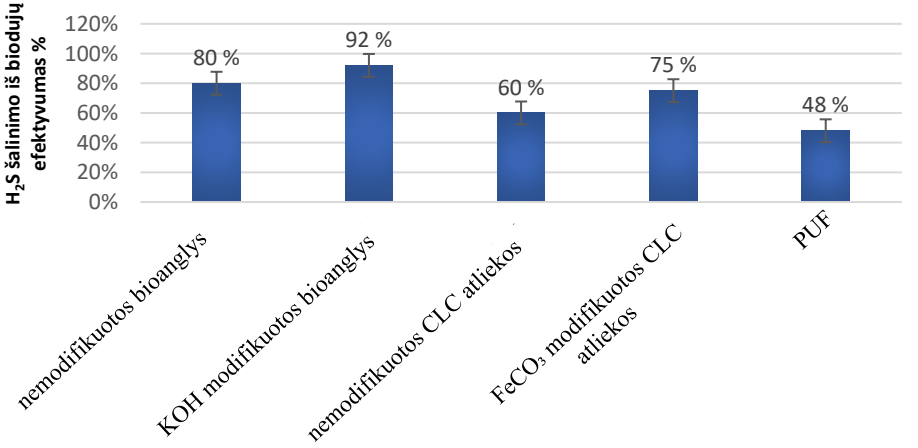

S3.3 pav. H_2S šalinimo efektyvumo palyginimas skirtingose vienkomponentėse modifikuotų ir nemodifikuotų biofiltracijos medžiagų konfigūracijose

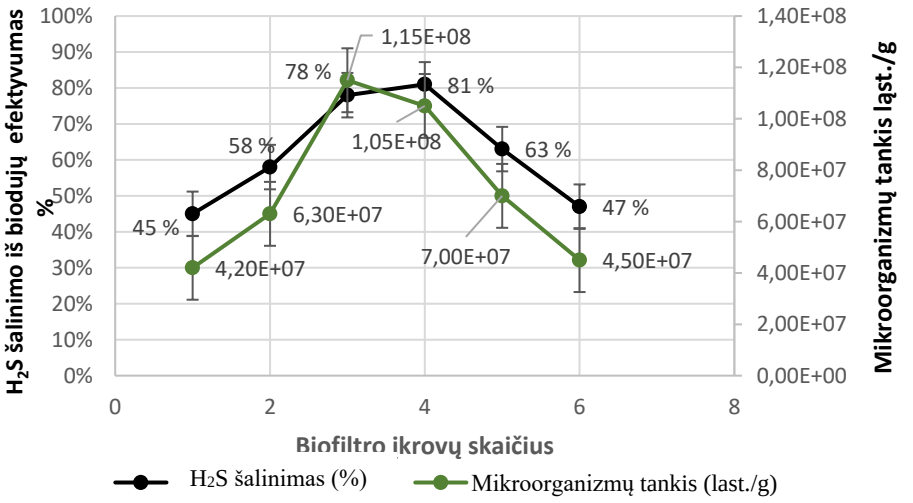

S3.4 pav. H_2S šalinimo efektyvumo ir mikroorganizmų tankio sąsaja skirtingose biofiltro pakopose

Eksperimentiniai rezultatai buvo papildyti matematiniu modeliavimu taikant *Monod* tipo kinetinius modelius. Modeliuotų ir eksperimentinių mikroorganizmų biomasės augimo kreivių palyginimas (S3.5 pav.) atskleidė gerą atitiktį tarp rezultatų, o nuokrypis neviršijo 10 % (R^2 = 0,91–0,96).

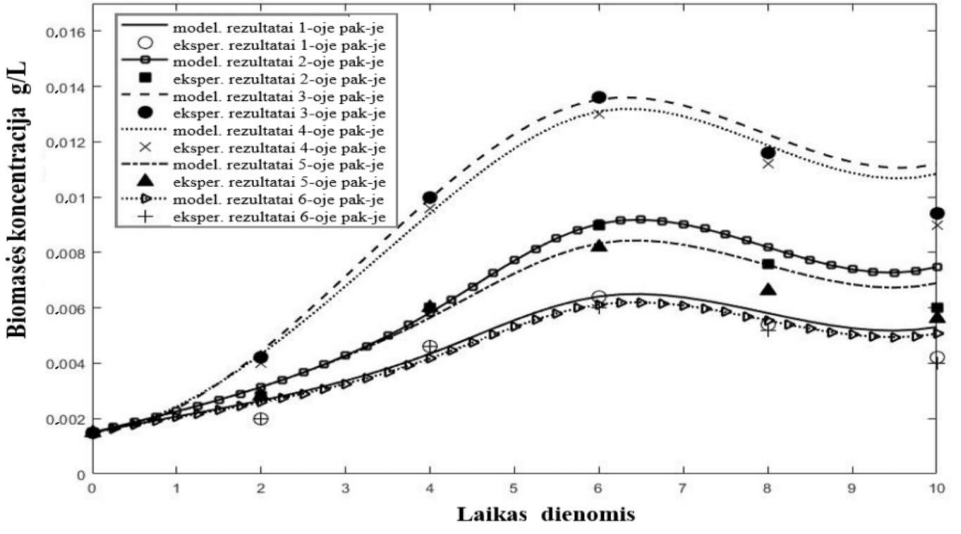

S3.5 pav. *Pseudomonas* spp. augimo greičio matematinių modeliavimo ir eksperimentinių rezultatų palyginimas CLC atliekose

Skaitmeninis modeliavimas COMSOL *Multiphysics* aplinkoje patvirtino eksperimentinius rezultatus ir parodė, kad biofiltre susiformuoja lokalizuotos H_2S šalinimo zonos (S3.6 pav.). Didžiausias H_2S koncentracijos sumažėjimas nustatytas biofiltro vidurinėse pakopose, o po maždaug 120 h veikimo sistema pasiekė stabilią būseną.

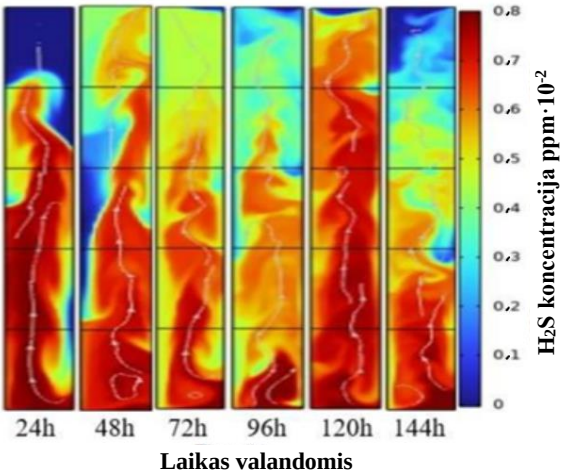

S3.6 pav. H_2S koncentracijos modeliavimo rezultatai per pirmąsias šešias veikimo dienas laboratorinio masto biofiltre, užpildytame bioanglimis

Rezultatų palyginimas su kitų autorių tyrimais parodė, kad biofiltracijos medžiagų savybės ir jų modifikacija turi lemiamą įtaką biofiltrų efektyvumui. Bioanglių terminė ir cheminė modifikacija leidžia valdyti porų struktūrą ir paviršiaus aktyvumą, todėl ji veikia ne tik kaip adsorbentas, bet ir kaip aktyvi biologinė terpė. CLC atliekų modifikacija geležies junginiais sustiprina katalizinius H_2S oksidacijos procesus, o PUF užtikrina bioplėvelių stabilumą hibridinėse biofiltrų sistemose.

Apibendrinant galima teigti, kad H_2S šalinimas biofiltracijos būdu yra kompleksinis procesas, kurio efektyvumą lemia biofiltracijos medžiagų savybės ir jų modifikacija. Tikslingai modifikuotos biofiltracijos medžiagos leidžia vienoje sistemoje integruoti adsorbcinius, katalizinius ir biologinius mechanizmus, užtikrinant aukštą H_2S šalinimo efektyvumą ir ilgalaikį biofiltrų veikimo stabilumą biodujų desulfurizacijos procesuose.

Bendrosios išvados

1. Praktiškai vandenilio sulfido (H_2S) koncentracija biodujose dažnai svyruoja nuo 100 iki 5000 ppm, o koncentracijai viršijus 100 ppm pasireiškia intensyvi korozija ir sistemų veikimo sutrikimai. Mokslinės literatūros analizė parodė, kad nors biologinė filtracija yra aplinkai tvarus H_2S šalinimo metodas, vis dar skiriama nepakankamai dėmesio iš atliekų pagamintoms užpildo medžiagoms modifikuoti ir eksperimentiniams bei modeliavimo tyrimams integruotai įvertinti.

2. Fizikocheminė charakteristika atskleidė, kad KOH modifikuotos iš nuotekų dumblo gautos bioanglys ir $FeCO_3$ impregnuotos CLC atliekos pasižymi didesniu specifiniu paviršiaus plotu (iki 471,54 $m^2 \cdot g^{-1}$), optimaliu porėtumu (65–75 %), mažesniu tūrio tankiu (nuo ~450–520 iki ~280–350 $kg \cdot m^{-3}$) ir geresnėmis paviršiaus savybėmis, palankiomis mikroorganizmų kolonizacijai bei adsorbcijos procesams.
3. Eksperimentiniai tyrimai parodė, kad modifikuotos užpildo medžiagos padidina H_2S šalinimo efektyvumą nuo maždaug 80 % iki 92–95 % ($p < 0,01$), užtikrindamos didesnį sistemos stabilumą laboratorinėmis sąlygomis. H_2S šalinimo efektyvumas tiesiogiai priklauso nuo biofiltro užpildo sudėties: daugiakomponentė sistema, sudaryta iš KOH modifikuotų bioanglių ir $FeCO_3$ impregnuotų CLC atliekų, leidžia pašalinti iki 95 % H_2S ir statistiškai reikšmingai pranoksta vienkomponentes sistemas, padidindama šalinimo efektyvumą 10–15 % santykine išraiška. Tai patvirtina adsorbcijos, katalizinės oksidacijos ir biologinio skaidymo sinerginę sąveiką.
4. Mikrobiologiniai tyrimai atskleidė, kad termiškai modifikuotų bioanglių paviršius skatina intensyvią mikroorganizmų kolonizaciją: bioanglyse bakterijų tankis siekia 10^7–10^8 $KSV \cdot g^{-1}$, o $FeCO_3$ impregnuotose CLC atliekose – apie 10^6 $KSV \cdot g^{-1}$; pirolizė 600 °C temperatūroje sudaro iki keturių kartų palankesnes sąlygas mikroorganizmams augti nei 400 °C. Stipri koreliacija tarp mikroorganizmų tankio ir H_2S šalinimo efektyvumo ($r = 0,89$; $p < 0,001$) patvirtina, kad *Acidithiobacillus* spp. ir *Pseudomonas* spp. sąveika lemia >90 % H_2S pašalinimą.
5. Statistinė analizė leido nustatyti reikšmingus ryšius tarp medžiagų savybių (paviršiaus ploto, porėtumo, savitojo elektrinio laidumo), mikrobinio aktyvumo rodiklių ir H_2S šalinimo efektyvumo, patvirtindama fizikocheminių ir biologinių veiksnių tarpusavio priklausomybę.
6. Sukurtas matematinis modelis, naudojant MATLAB, apibūdina sierą oksiduojančių bakterijų augimą ir vandenilio sulfido šalinimo kinetiką. Modeliavimas parodė biologiškai aktyvių reakcijos zonų susidarymą su stabiliais H_2S koncentracijos ir reakcijos greičio gradientais; modelio rezultatai nuo eksperimentinių duomenų skyrėsi apie 7 %.
7. COMSOL programine įranga atliktas skaitinis vandenilio sulfido ir biodujų koncentracijos, srauto greičio bei oro slėgio pasiskirstymo skirtinguose biofiltro sluoksniuose modeliavimas patvirtino eksperimentinių tyrimų rezultatus. Nustatyta, kad prognozuojamas H_2S šalinimo efektyvumas nuo eksperimentinių duomenų skiriasi mažiau nei 10 %, o tai patvirtina sukurto biofiltracijos sistemos modelio patikimumą.

Rekomendacijos

1. Remiantis šioje disertacijoje atliktais eksperimentiniais tyrimais, praktinėse biodujų desulfurizavimo sistemose rekomenduojama taikyti daugiakomponentę

biofiltracijos sistemą, paremtą termiškai modifikuotų bioanglių ir $FeCO_3$ modifikuoto CLC deriniu. Toks sprendimas leistų formuoti funkciškai diferencijuotas biofiltro zonas ir užtikrintų stabilų vandenilio sulfido (H_2S) šalinimo efektyvumą, siekiantį 90–95 % ($p < 0,01$).

2. Biofiltruose rekomenduojama projektuoti ir optimizuoti filtracines sistemas taikant matematinį modeliavimą (MATLAB) bei skaitmenines simuliacijas (COMSOL *Multiphysics*), kurios leistų prognozuoti H_2S šalinimo zonų formavimąsi bei jų dinamiką visame filtro tūryje ir padėtų patikimai įvertinti proceso efektyvumą, neviršijant 10 % nuokrypio. Tolesni tyrimai turėtų būti orientuoti į modelių plėtrą, integruojant mikrobiologinę kinetiką, įkrovų savybių kaitą filtrų eksploatacijos metu ir ilgalaikio veikimo scenarijus pramoniniuose įrenginiuose.

Kamyab MOHAMMADI

RESEARCH AND APPLICATION OF BIOFILTRATION MATERIALS
IN THE PURIFICATION OF BIOGAS FROM HYDROGEN SULFIDE

Doctoral Dissertation

Technological Sciences,
Environmental Engineering (T 004)

BIOFILTRACIJOS MEDŽIAGŲ TYRIMAI IR
TAIKYMAS ŠALINANT IŠ BIODUJŲ SIEROS VANDENILĮ

Daktaro disertacija

Technologijos mokslai,
Aplinkos inžinerija (T 004)

Lietuvių kalbos redaktorė Audronė Jonikienė
Anglų kalbos redaktorė Jūratė Griškėnaitė

2026 04 15. 14,5 sp. l. Tiražas 20 egz.
Leidinio el. versija *https://doi.org/10.20334/2026-014-M*
Vilniaus Gedimino technikos universitetas
Saulėtekio al. 11, 10223 Vilnius
Spausdino UAB „Ciklonas“,
Žirmūnų g. 68, 09124 Vilnius